NASA/CR—2002-211320

ARL–CR–0485
1L18211–FR–01001

Development of Face Gear Technology for Industrial and Aerospace Power Transmission

Gregory F. Heath, Robert R. Filler, and Jie Tan
The Boeing Company, Mesa, Arizona

May 2002

The NASA STI Program Office . . . in Profile

Since its founding, NASA has been dedicated to the advancement of aeronautics and space science. The NASA Scientific and Technical Information (STI) Program Office plays a key part in helping NASA maintain this important role.

The NASA STI Program Office is operated by Langley Research Center, the Lead Center for NASA's scientific and technical information. The NASA STI Program Office provides access to the NASA STI Database, the largest collection of aeronautical and space science STI in the world. The Program Office is also NASA's institutional mechanism for disseminating the results of its research and development activities. These results are published by NASA in the NASA STI Report Series, which includes the following report types:

- TECHNICAL PUBLICATION. Reports of completed research or a major significant phase of research that present the results of NASA programs and include extensive data or theoretical analysis. Includes compilations of significant scientific and technical data and information deemed to be of continuing reference value. NASA's counterpart of peer-reviewed formal professional papers but has less stringent limitations on manuscript length and extent of graphic presentations.

- TECHNICAL MEMORANDUM. Scientific and technical findings that are preliminary or of specialized interest, e.g., quick release reports, working papers, and bibliographies that contain minimal annotation. Does not contain extensive analysis.

- CONTRACTOR REPORT. Scientific and technical findings by NASA-sponsored contractors and grantees.

- CONFERENCE PUBLICATION. Collected papers from scientific and technical conferences, symposia, seminars, or other meetings sponsored or cosponsored by NASA.

- SPECIAL PUBLICATION. Scientific, technical, or historical information from NASA programs, projects, and missions, often concerned with subjects having substantial public interest.

- TECHNICAL TRANSLATION. English-language translations of foreign scientific and technical material pertinent to NASA's mission.

Specialized services that complement the STI Program Office's diverse offerings include creating custom thesauri, building customized data bases, organizing and publishing research results . . . even providing videos.

For more information about the NASA STI Program Office, see the following:

- Access the NASA STI Program Home Page at ***http://www.sti.nasa.gov***

- E-mail your question via the Internet to help@sti.nasa.gov

- Fax your question to the NASA Access Help Desk at 301–621–0134

- Telephone the NASA Access Help Desk at 301–621–0390

- Write to:
  NASA Access Help Desk
  NASA Center for AeroSpace Information
  7121 Standard Drive
  Hanover, MD 21076

NASA/CR—2002-211320

ARL–CR–0485
1L18211–FR–01001

Development of Face Gear Technology for Industrial and Aerospace Power Transmission

Gregory F. Heath, Robert R. Filler, and Jie Tan
The Boeing Company, Mesa, Arizona

Prepared under Cooperative Agreement NCC3–356

National Aeronautics and
Space Administration

Glenn Research Center

May 2002

The Aerospace Propulsion and Power Program at
NASA Glenn Research Center sponsored this work.

Available from

NASA Center for Aerospace Information
7121 Standard Drive
Hanover, MD 21076

National Technical Information Service
5285 Port Royal Road
Springfield, VA 22100

Available electronically at http://gltrs.grc.nasa.gov/GLTRS

SUMMARY

Tests of a 250 horsepower proof-of-concept (POC) split torque face gear transmission were completed by The Boeing Company in Mesa, Arizona, while working under a Defense Advanced Research Projects Agency (DARPA) Technology Reinvestment Program (TRP). This report provides a summary of these cooperative tests, which were jointly funded by Boeing and DARPA. Design, manufacture and testing of the scaled-power TRP split torque gearbox followed preliminary evaluations of the concept performed early in the program. The testing demonstrated the theory of operation for the concentric, tapered face gear assembly. The results showed that the use of floating pinions in a concentric face gear arrangement produces a nearly even torque split. The POC split torque tests determined that, with some improvements, face gears can be applied effectively in a split torque configuration which yields significant weight, cost and reliability improvements over conventional designs.

An input torque of 1767 in-lbs was applied to each pinion shaft during the split torque tests. The tests were run by slow rolling the input pinions while in mesh with two face gears. Resistance was applied at the output face gear, to create the required loading conditions in the gear teeth. A system of weights, pulleys and cables were used in the test rig to supply the input torque and output resistance torque specified for the design. Strain gages applied in the tooth roots provided strain indication of the torque splitting conditions existing in the gear teeth. The overall torque split for the full-up two pinion-two idler configuration was calculated to be 48% upper face gear mesh and 52% lower face gear mesh for the input pinions. The idlers appeared to share the load at a rate of 57% for Idler 3 and 43% for Idler 4. This significant difference is due to the fact that the Idler 4 backlash was set based on upper face gear (UFG) strain indications. Subsequent test data indicated that used directly, the UFG strain was not a reliable indicator of idler load split. With the torque calibration information and additional test time, idler backlash could have been adjusted to make the load sharing even better.

Relatively high tooth root bending strains were noted. For some of the idler-face gear meshes, load appears to be concentrated near the end of the face gear teeth, contributing to the higher idler strains measured. Minimal tooth crowning was added during manufacture of the POC gears, which may have influenced the above. This will be corrected in future configuration studies.

For future testing of this type, a more robust method for torque split determination - one that is less sensitive to changes in tooth load distribution during tests - is needed. Additional recommendations for future testing include the addition of more gages across the face width of all gears, if possible, and that tooth root strain gages need not be calibrated.

New methods have been developed for face gear grinding, grinding wheel dressing and coordinate measurement as part of the TRP Program. Under related work, a face gear grinding machine was custom-built and operated by Derlan Aerospace Canada and has demonstrated the capabilities of finishing face gears to required case hardness, profile accuracy and surface finish for aerospace applications.

Face gear technology offers promise for power density improvement and lower cost when applied in helicopter gearboxes. The ability of face gears to provide high ratios of gear reduction and achieve self adjusting-torque splitting allows the replacement of multiple reduction stage gearboxes with units requiring fewer stages. This yields a better power to weight ratio, reduction in parts relative to multiple-stage designs and reduction in volume. The split torque face gear design offers improved reliability and reduction in O & S cost over existing conventional gearing designs used in large horsepower applications.

TABLE OF CONTENTS

I. INTRODUCTION

Drive system engineers continuously strive to develop improvements in gear, shaft and bearing configurations, as well as investigating new materials and processes, modular design methods and improved technology components. The TRP program and the follow-on 2800 Horsepower Demonstrator Transmission program, both jointly-funded by DARPA and Boeing [1], were initiated to develop and refine transmission technologies which will provide increased power density, increased reliability and reduced costs. The results of this work will provide initial information to allow these improvements to be designed into future transmissions.

The contracting agency for the TRP program was the NASA Glenn Research Center, working in conjunction with the U.S. Army Research Laboratory in Cleveland, Ohio. These two agencies also provided engineering and facilities support in the face gear durability tests [2-5] during the TRP and earlier ART I Programs.

This report documents the test objectives, specimens, fixture, procedure, data acquisition and reduction, results and final conclusions and recommendations made from the TRP slow roll split torque tests. A proof-of-concept (POC) gearbox using face gears was designed and built as part of the program for the tests. Face gears can be used in aerospace applications similar to those of spiral bevel gears, when reduction ratios are greater than approximately 3.5 to 1. The geometry of face gears provides an inherent capability to handle larger reduction ratios than bevel gears. In the POC split torque stage, face gears are located one directly over the other, resulting in a compact shape and reduced volume for this stage. Part sizes are decreased due to torque being divided in half at the input pinion meshes, which allows use of a larger face gear reduction ratio and results in significant weight reduction. For these reasons, a high-ratio concentric split torque face gear stage can replace two stages of a conventional transmission.

The TRP test gearbox is comprised of a reduced-size, scaled-power (250 HP) split torque face gear stage. It was completed in late 1998, and is configured with two face gears located face-to-face one over the other in the gearbox. Two input pinions and two idler gears are also used in this torque splitting arrangement. The pinion shafts utilize a cantilevered bearing mount arrangement that allows the pinions to float between the two face gear meshes in finding a center of force equilibrium. It was anticipated that the division of torque to the two face gear meshes at this point of equilibrium would be approximately equal. The two idler gears are employed as a means of recombining the torque that is fed to the lower face gear back to the upper face gear. Similar to the two pinions, the idlers mesh with both face gears from a location in between them. During the TRP tests, steady torsional loading was applied to slowly roll the test gears through mesh. Single pinion loading was used during half of the tests, and dual pinion loading was used during the other half. Strain gages bonded to the roots of selected test gear teeth provided readout of the tooth strain experienced by the gears as they rolled through mesh under representative loading conditions. The tests were performed in a fixture built at Boeing Mesa.

The three main objectives of the tests covered in this report were first, to determine the relative torque split percentages obtained between the pinion meshes with the upper and lower face gear test articles. Second, to determine the load recombination percentages obtained between the two idlers during dual idler testing (when two pinions are used also). Third, to investigate tooth bending stresses obtained from the tooth strain measurements during tests. This includes making comparisons to predicted spur and face gear stresses, to static and fatigue allowables and checking for indications of tooth end loading.

The face gears, pinions and idlers used in the POC tests were precision ground to AGMA class 12 quality at Derlan Aerospace Canada in Milton, Ontario. Derlan built a face gear grinding machine from the base up, as found required to create the machine configuration and operating capabilities needed to precision grind face gears. Prior to this, face gear grinding development work was performed by Derlan Aerospace, Boeing and the University of Illinois at Chicago [6-7]. To date, the method developed has been used to produce 2800 Hp test gear sets, as well as the POC test gears. This work is based on mathematical principles of face gear geometry, tooth contact, grinding, grinding wheel dressing and coordinate measurement.

Prior to the split torque testing summarized in this report, experimental durability tests performed at NASA Glenn Research Center indicated strong potential for the use of face gears in aerospace applications. The tests were performed on AISI 9310 steel face gears in support of the DARPA TRP Program, to enhance face gear technology. The tests were conducted in the NASA Glenn spiral-bevel-gear/face-gear test facility. Tests were run at 2300 rpm face gear speed and at loads of 64, 76, 88, 100, and 112-percent of the design torque of 377 N-m (3340 in-lb). The carburized and ground face gears demonstrated the required durability when run for ten-million cycles at each of the applied loads. Other than wear lines caused by isolated situations, the spur pinions and face gears had no significant wear problems or failure modes. Proper installation was critical for the successful operation of the spur pinions and face gears. A large amount of backlash produced tooth contact patterns that approached the inner-diameter edge of the face-gear tooth. Low backlash produced tooth contact patterns that approached the outer-diameter edge of the face-gear tooth. Measured backlashes in the range of 0.178 to 0.254 mm (0.007 to 0.010 in) produced acceptable tooth contact patterns during the durability tests.

II. TEST GEARBOX DESCRIPTION

The face gear proof-of-concept test gearbox assembly (P/N FGRR01) was used for the TRP split torque tests. A cross section of the assembly, shown in Figure 1, indicates the basic configuration of the gearbox. The configuration involves an input tapered pinion driving two face gears simultaneously, one located directly above the other. The upper face gear teeth are directed downward and the lower face gear teeth are directed upward. The pinion (part number FGRR008) is arranged to pivot about a face to face ball bearing set located at the rear of the pinion shaft. The pinion then is allowed to float between the two face gear meshes in finding a center of force equilibrium to facilitate torque splitting. Two of these pinions drive the face gears, from either side of the gearbox. Two tapered idler gears (part number FGRR17) are also employed in this configuration as a means of recombining the torque that is fed to the lower face gear (part number FGRR19) back to the upper face gear (part number

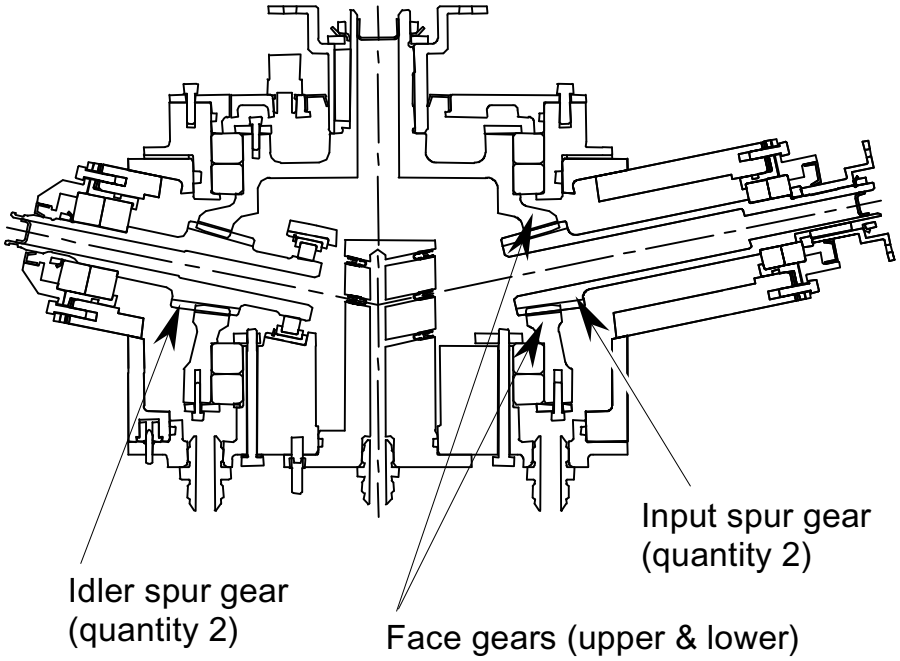

Figure 1. Cross Section of Test Gearbox Assembly

FGRR11). Similar to the two pinions, the idlers mesh with both face gears from a location in between them. Each idler is located around the circumference of the face gears, arranged evenly between the two pinions in an alternating manner. One half of the slow roll tests used just one pinion and one idler (and then the other pinion and idler) with the two face gears, while the other half of tests used two pinions and two idler gears with the face gears. A light coating of Mobil SHC626 transmission oil was brushed onto the gear teeth after backlash and pattern adjustments, prior to the slow roll tests.

Drive hubs with keyway connections are used on the input and output shafts. All bearings, seals, locknuts, retaining rings, o-rings and fasteners for the test gearbox were purchased off-the-shelf per applicable quality standards. The gearbox housing weldment assembly was made from 6061 aluminum, T42 condition. The bottom cover was made from 6061 aluminum, T6 condition. The input, output and idler covers and sleeves were machined from 4340 steel.

1. Face Gear Manufacturing Method

Face gears have been found in literature [8-9] and in non-critical applications for more than half a century, but were not considered for high power applications until recent years [5]. Limited use of face gears for power transmission can be attributed partly to insufficient understanding of the complex 3D geometry of the gear tooth and its meshing properties, and more to the lack of manufacturing processes to produce face gears that can meet the tough

requirements of high-power applications. This includes requirements for, among others, gear tooth case hardness, profile accuracy and surface finish. One of the main objectives of this project was to develop face gear grinding and coordinate measuring methods to form a closed-loop face gear manufacturing system.

i. Face Gear Grinding

Grinding is a gear finishing operation commonly used in aerospace industry. It is capable of producing gears with superior quality. One of the key factors in using face gears for aerospace applications is to develop face gear grinding methods that can be effectively applied in production. In their efforts to promote face gear application, Boeing and Dr. F.L. Litvin of the University of Illinois at Chicago have made important progress in this area.

One major development is described in the U.S. patent application given in [10]. The grinding method used is based on the principle of continuous generation. A continuous generating grinding method is well developed for spur and helical gears, consistently producing gears with better tooth-to-tooth accuracy and at higher production rates. Figure 2 is a schematic showing a face gear grinding method where an imaginary pinion, a face gear and a grinding wheel are shown in their meshing positions. Installation of the grinding wheel on the face gear should account for the lead angle λ_{ws} of the thread on the wheel body, which is given by

$$\sin \lambda_{ws} = \frac{N_w}{N_p} \bullet \frac{d_p}{d_w} \qquad (1)$$

where

N_p = number of teeth on the pinion,
d_p = pitch diameter of the pinion,
N_w = number of threads on the grinding wheel,
d_w = diameter of the reference circle passing through the pitch point on the grinding wheel.

The grinding wheel has thread geometry that, in synchronous rotation with the face gear, will emulate the generating action of the pinion in rotation. Face gears ground with this method will have tooth surfaces which are truly conjugate to the mating pinion. While the generating motion is relatively simple, obtaining the correct form of the grinding wheel is the key and the biggest challenge in the development. One method to dress the grinding wheel is described in [10], which utilizes a tool conforming to the tooth space of the pinion.

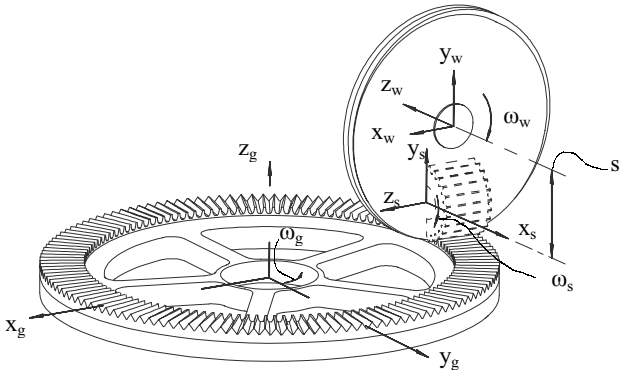

Figure 2. Face Gear Grinding Configuration

Another major development is given in [11]. An improved method of dressing (or truing, to be more technically accurate) the grinding wheel has been developed that offers numerous unique features and advantages. Figure 3 shows all mating members, i.e., the pinion, the face gear, the grinding wheel and the dressing tool conceptually superimposed onto each other. The dressing tool is a disk with a flat surface (mathematically a plane) as the generating feature. The extremely simple geometry of a flat surface makes the dressing tool very easy to prepare to high accuracy. A flat surface also has inherent advantages in absorbing installation and motion errors in that any error components in the direction of the plane have no effect on the generating action, and positional errors of constant amount along the normal of the plane (often the case with installation errors) will produce deviations in the generated surface that are of constant magnitude along the surface normals. Surface deviations of constant magnitude along surface normals have significantly alleviated damaging effects because the relative errors are substantially reduced.

A second feature of the dressing method is its true conjugate action. Referring to Figure 3, installation and motion of the dressing tool relative to the grinding wheel can be specified by referencing to the involute pinion (imaginary). The dressing tool is positioned such that it is always in tangency with the pinion tooth surface. The positioning can be represented in term of parameters α and s, where α is the angle between the dressing surface and a line representing the shortest distance from the grinding wheel axis of rotation to the pinion axis of rotation, while s is the distance from the dressing surface to the pinion axis. With the pinion being a regular spur involute gear, parameters α and s can be related to the rotation of the pinion by:

$$\alpha = \varphi_p + \theta \qquad (2)$$

and

$$s = \theta \; r_b \qquad (3)$$

where in equations (1) and (2), φ_p is the angle of rotation of the pinion, θ is the roll angle on the pinion involute profile where the dressing surface is in tangency with the pinion, and r_b is the base radius of the pinion.

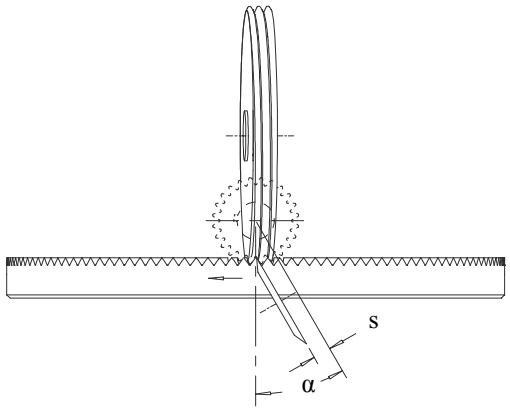

Figure 3. Dressing Configuration, with
Pinion and Gear as References

Considering the face gear meshing with the pinion, rotations of the two members are governed by

$$\frac{\omega_p}{\omega_g} = \frac{N_g}{N_p} \qquad (4)$$

where ω_p = angular velocity of the pinion,
ω_g,= angular velocity of the face gear,
N_p = the number of teeth on the pinion,
N_g = the number of teeth on the gear

which determines the transmission ratio of the gear drive. In the process of grinding, rotation of the grinding wheel is related to rotation of the face gear by

$$\frac{\omega_w}{\omega_g} = \frac{N_g}{N_w} \qquad (5)$$

where ω_w = angular velocity of the threaded wheel,
ω_g,= angular velocity of the face gear,
N_w = the number of threads on the wheel,
N_g = the number of teeth on the gear

Simultaneous consideration of equations (1)—(5) leads to the relation of the dressing tool and the grinding wheel in terms of their positioning parameters:

$$s = r_b \bullet (\alpha \pm \varphi_w \frac{N_w}{N_p}) \qquad (6)$$

where the "+" sign corresponds to dressing the left side of a right-handed thread, or the right side of a left-handed thread, and the "-" sign corresponds to dressing the left side of a left-handed thread, or the right side of a right-handed thread. Given any angular position of the grinding wheel, there is infinite number of pairs of parameters (α, s) that satisfy equation (6), corresponding to the dressing tool in tangency condition with different points on the grinding wheel thread.

Assuming constant angular velocity of the grinding wheel, the corresponding velocity of the dressing tool can be obtained by differentiating equation (6):

$$v_d = \dot{s} = r_b \bullet (\dot{\alpha} \pm \omega_w \frac{N_w}{N_p}) \quad (7)$$

where v_d represents the velocity of the dressing tool along the normal to its flat surface.

As the grinding wheel is rotating, the instantaneous position and orientation of the dressing tool and its motion is specified with two parameters (α, s). These two parameters can be independently varied while still satisfying conditions of meshing. All dressing tool positions corresponding to different combinations of parameters (α, s) that satisfy equations (6) constitute a family of generating planes on the grinding wheel. The final form of the grinding wheel is generated as the envelope of the family of these planar surfaces. Such a generating process is called two-parameter enveloping in gearing theory. Practical application of a two-parameter enveloping process usually involves introduction of specially designated relationships between the two theoretically independent parameters to make the implementation realistically feasible. As for the dressing process discussed here, the motion of the dressing tool is specified to be along the normal of the flat surface while holding the variation of angle α. Equation (7) then becomes a simple equation involving only pure translation of the dressing tool:

$$v_d = r_b \omega_w \frac{N_w}{N_p} \qquad (8)$$

It is seen that, the magnitude of the velocity is constant for any value of a fixed α angle. The dressing tool in pure translation makes it possible to avoid running into sensitive areas in the grinding wheel where undercutting may occur. This is one of the advantages of this planar surface dressing tool over one with an involute profile.

Another important characteristic of two-parameter enveloping is the point contact condition at any instant between the generating and the generated surfaces. This contact condition combined with advanced CNC (computer numerical control) technology allows us to topologically control, or modify, the profile of the grinding wheel. Modifications to the grinding wheel will be transferred to the face gear in the process of grinding. One-to-one

correspondence has been established between the position of the dressing tool, a point on the grinding wheel, a point on the face gear tooth and a point on the pinion. Desired meshing properties between the pinion and the gear can be translated to specifications in tooth modifications to the face gear, which will eventually be translated into motion control in the dressing process through CNC software and parameters. Topological control of the face gear tooth has important practical applications:

- To correct face gear profile deviations that are caused by inevitable set-up errors in machining. This is a powerful tool in the development stage.

- To introduce specially designed modifications to the face gear so that the contact pattern with the mating pinion can be localized and the shift of the contact pattern under load can be controlled in size, location and orientation. This is especially important for high load applications where a relatively large amount of deflection is expected.

- To introduce specially designed modifications to the face gear to provide prescribed shapes of transmission error functions that produces lower levels of noise than alternative types and absorb more damaging transmission error shapes caused by manufacturing errors and structural deflections. This is often an important consideration in high speed applications.

Figure 4 and Figure 5 show photos of the dressing and grinding operations.

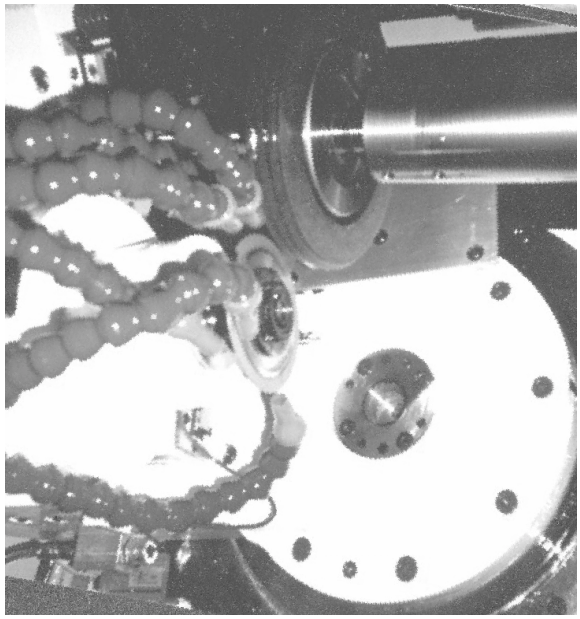

Figure 4. Worm Wheel Dressing Operation

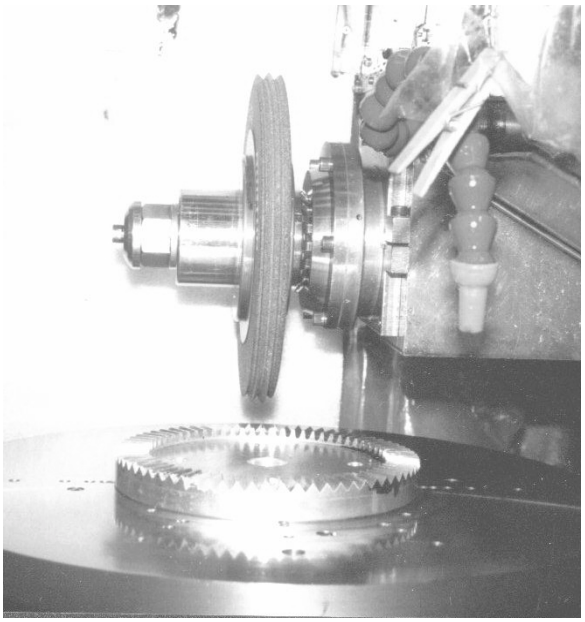

Figure 5. Face Gear Grinding Operation

ii. Face Gear Coordinate Measurement

Coordinate measurement of gear tooth surfaces provides useful information for the development of tooth contact patterns and is an essential component in the closed-loop of manufacturing process control. It has been one of the objectives of this project to develop the CMM process for face gears. The development can be explained from the following aspects:

a. Geometrical Modeling of the face gear. The coordinates of a typical point and its surface normal on the gear tooth are determined mathematically and serve as the theoretical reference for coordinate measurement.

$$ {}^{g}\{r\} = \begin{Bmatrix} {}^{g}x \\ {}^{g}y \\ {}^{g}z \\ 1 \end{Bmatrix} \quad {}^{g}\{n\} = \begin{Bmatrix} {}^{g}n_x \\ {}^{g}n_y \\ {}^{g}n_z \\ 0 \end{Bmatrix} \qquad (9) $$

A grid-net of 9 sections by 7 depths has been constructed, totaling 63 well-located points that cover the main bearing area on the face gear tooth, as shown in Figure 6.

b. Coordinate measuring machine and kinematics. The CMM machine has a multi-axis design and is equipped with a CNC controller. Commonly used in modern gear shops are stand alone dedicated gear CMM machines that are designed, built and loaded with software for inspecting gears of different tooth geometry. On the other hand, advanced CNC gear grinding machines often come with the essential features required for coordinate

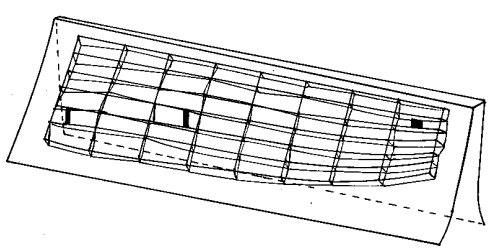

Figure 6. CMM Grid Points, Theoretical and Measured Results

measurement: a controller to process NC programs and command multi-axis machine movements, precision linear and rotary glass scales for high precision measurement of machine movements, feed-back systems for closed-loop control and built-in probes for locating the workpiece and the grinding wheel. With all these features, the machine is potentially capable of performing the task of coordinate measurement on the gears before, during and after the grinding operation, all on the same machine. If effectively employed, this technology offers the following advantages:

- It reduces the need for frequent use of a stand-alone dedicated CMM machine.
- It eliminates mounting, dismounting and transferring of the gear between the grinding machine and the CMM machine, thus maintaining common and accurate references between the two operations.
- It allows for constant monitoring, easy information feedback and immediate error corrections based on the processing of measuring results.

Obviously, these benefits are more significant for gears of larger size and lower quantities. Production of helicopter transmissions usually falls into this category.

Kinematic analysis of a multi-axis CNC machine yields equations that relate machine movements to the position of the probe stylus and the gear on the machine:

$$ {}^{m}r_p = {}^{m}r_p(\theta) = \begin{Bmatrix} {}^{m}x_p \\ {}^{m}y_p \\ {}^{m}z_p \\ 1 \end{Bmatrix} \qquad (10) $$

$$ {}^{m}r_g = {}^{m}r_g(\theta) = \begin{Bmatrix} {}^{m}x_g \\ {}^{m}y_g \\ {}^{m}z_g \\ 1 \end{Bmatrix} \qquad (11) $$

$$^{m}n_g = {}^{m}n_g(\theta) \qquad (12)$$

where θ = (X, Y, Z, A, B, C) are the machine movements of respective axes.

c. Probing System. There are two types of probes: analog probe and touch-trigger probe. Analog probes are commonly used on gear CMM machines in which surface deviation is the direct output of the probe. Touch-trigger probes are more often used on grinding machines where information about the location of the workpiece on the machine is needed for machining operations. Resulting directly from touch-trigger probing are the coordinates of machine movement recorded by the CNC controller at the instant when the probe trips. For touch-trigger probes to measure gear tooth deviations, coordinates of machine movement must then be converted into actual coordinates (locations) of the measured point in the machine-attached coordinate system according to machine kinematics (equations (11)—(12)). Gear surface deviations will be obtained as the results of calculating the difference of actual and theoretical coordinates, projected to the surface normal, i.e.:

$$\delta = ({}^{m}r_p - \rho\,{}^{m}n_g - {}^{m}r_g) \bullet {}^{m}n_g \quad (13)$$

where ρ is the effective radius of the probe in the direction along the surface normal $^{m}n_g$, and must be obtained through careful calibration. Accuracies are improved by

- commanding the probe to approach the surface along the normal,
- properly orienting the gear so that approaching along the normal can be realized with minimum number of axes of machine movement.

Geometric modeling of the gear and kinematic analysis of the machine provides solutions to these requirements. Implementation of the developed method was tested on a 5-axis tool grinding machine. The configuration of the gear and the touch-trigger probe is shown in Figure 7. Measured results are shown superimposed on the theoretical grid points in Figure 6.

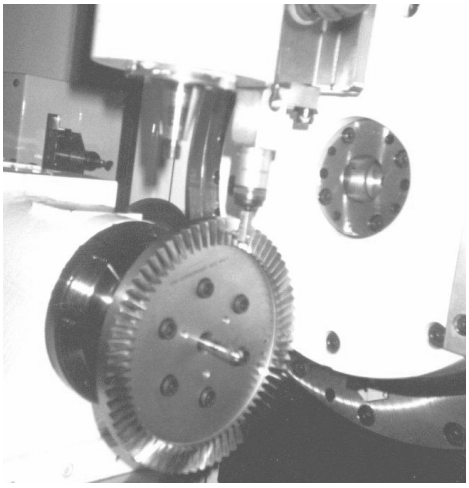

Figure 7. Face Gear CMM Operation

Even with a CMM method available, pattern rolling is still an indispensable inspection method in shop floor practice, and pattern development is an important operation. Advancements in theories of gearing and computer technology make it possible to predict contact patterns (ref. Figure 8) by Tooth Contact Analysis, which was later confirmed by pattern rolling (ref. Figure 9). Although an old mechanical machine was used to test the new grinding method, pattern development has been an easy task and a pleasant experience. Little effort was needed in light-load pattern development. Loaded pattern development went through only one iteration. In testing the ground face gear sets on NASA's test rig [2], it was observed that loaded patterns shifted to the toe area of the face gear, causing edge contact. Additional amounts of end relief in the said area solved the problem. It is believed that pattern development is relatively easy mainly because of the nature of true conjugate surfaces, as compared to the pseudo-conjugate surfaces of a spiral bevel gear set. There are well defined, theoretically correct tooth surfaces which provide full tooth contact and true conjugate action (zero transmission error). Profile modifications are specified by referencing to the correct surfaces, so that actual contact pattern and transmission error functions are well under control.

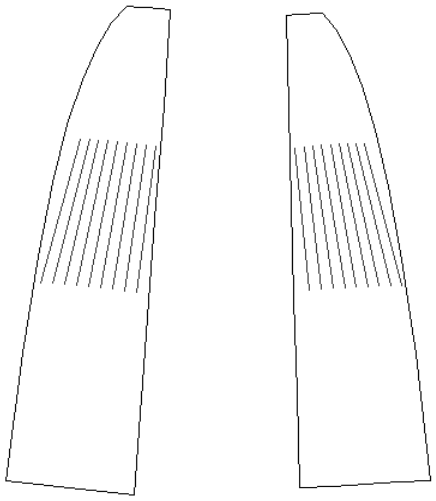

Figure 8. TCA Contact Pattern

With the promising results emerging from design studies, manufacturing developments, durability tests and now the split torque tests, efforts are being made to build prototype helicopter transmissions of appreciable horsepower. A 2828 HP split torque face gear demonstrator transmission has been produced and is currently being assembled. To support the efforts, a custom-built CNC face gear grinding machine was developed at Derlan Aerospace in Milton, Ontario. The machine is capable of grinding face gears of large and small sizes, with different face angles and to aerospace quality. To date, the machine has produced AGMA class 12 face gears and pinions ranging in size from 7.8 inch to 20 inch outside diameter. Figure 10 shows a close-up of the worm wheel and face gear workpiece.

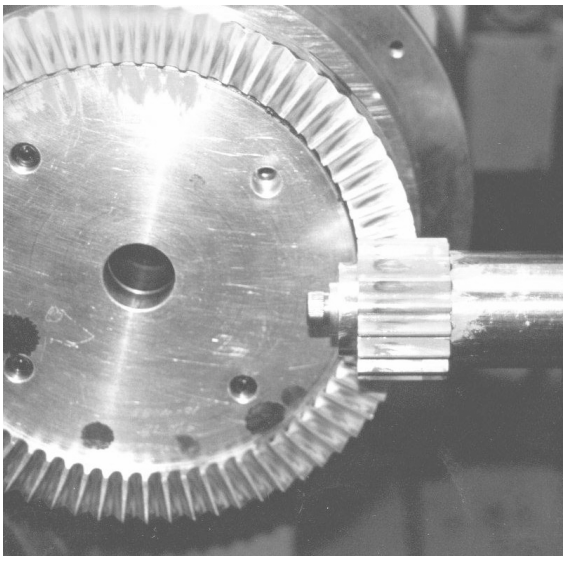

Figure 9. Rolling Contact Pattern

Figure 10. Worm Wheel and Face Gear Workpiece

III. DESIGN CRITERIA

For the POC gearbox design, the 100% input shaft torque for tests was 1767 inch-lbs. The 100% design torque level for each upper and lower pinion mesh with the face gears is 883.5 inch-lbs. This torque value assumed a 50%-50% torque split from each pinion to the face gears for design sizing purposes. The 100% design torque level for each face gear at each of its two pinion and two idler meshes is 3570.8 inch-lbs. The lower face gear transfers torque (divided out to it from the lower pinion meshes) to the upper face gear through the idler gears. The upper face gear combines the torque from its four meshes, to provide 14,283.3 inch-lbs. at the output shaft. A complete production transmission using the face gear configuration would include an output planetary being driven from the upper face gear, an arrangement similar to the intended aircraft configuration.

The gear material for the POC face gears, pinions and idlers is 9310 steel per AMS6265. The test gears for slow roll tests were as-heat treated, quenched and tempered, with a hardness of Rc 34-38. Since gear tooth elasticity depends little on surface hardness, it was found appropriate to use allowables similar to those for high quality hardened gears when making actual bending stress comparisons based on slow roll test strain data (ref. Section IX). The POC gears are 12.5 diametral pitch, with the pinions and idlers having 24 teeth and the face gears having 97 teeth in the design. The gears are of AGMA Class 11-12 quality. The input shaft angle is 78° with the upper face gear and 102° with the lower face gear. The pressure angle for the gear teeth is 25°. Tooth backlash is within a design range of .006 to .010 inch (.008 inch nominal) for the set. Surface roughness of the active tooth profiles was measured at an average of 16 micro-inches during inspection.

IV. TEST DESCRIPTION

1. Test Objectives

The first objective of the TRP face gear split torque tests was to determine the relative torque split percentages obtained between the input pinion meshes with the upper and lower face gear test articles. These pinion torque split percentages were determined for both single input pinion tests and dual input pinion tests. During single pinion tests, one pinion and one idler were run with the face gears. The other pinion was then run with the other idler to obtain additional strain data. During dual pinion tests, two pinions and two idlers were run with the face gears.

The second objective of the tests was to determine the relative percentages of load recombined from the lower face gear to the upper face gear through each of the two idlers used during dual pinion tests.

The third objective of the tests was to investigate tooth bending stresses obtained from the tooth strain measurements during tests. This includes comparing these to predicted spur and face gear stresses, to static and fatigue allowable stresses and checking for indications of tooth end loading.

2. Test Fixture

The test stand fixture for the TRP proof-of-concept gearbox test was designed and built at Boeing Mesa in 1999. Shown in Figures 11 and 12, the fixture used weights, pulleys and cables to provide appropriate loading within the gearbox. The test gearbox was installed with the output shaft horizontal and the input shafts nearly horizontal off of each side, to provide good orientation of the pulleys which were attached to the shaft ends. For the fixture design, weight values and pulley radii were selected which would yield the required input torque values at the pinions and output resistance torque at the upper face gear, specified as part of the POC gearbox design criteria. The pulley widths were designed so that the cable did not double-up on the pulley surface, since the cable radius was used as part of the overall radius for torque calculation. The pulleys were counterbalanced, with equal weight suspended off of each side of them. This assured that the input and output shafts were loaded in pure torsion, as well as increasing safety levels during tests. The weights and shaft pulleys were custom machined for the tests. Intermediate pulleys directed three of the six cables over the side of the fixture, so as to provide appropriate spacing of the weights and load cell wiring. The mounting structure for these pulleys could be adjusted to align them with the gearbox input and output shaft pulleys. The test fixture height was designed to provide the required travel distance for the weights, accommodating the number of gear rotations (specified as four pinion turns for each test in the test plan), pulley radii and length of weights. Spools were also attached to the input and output shafts to allow non-binding wind up and feed of the strain gage wire bundles during tests. The wire bundle for the lower face gear was fed out of a one-inch hole in the gearbox, and a small weight was attached to it to provide tensioning during wind up and feed. Wire junction boards were mounted on the upper level of the fixture near the gearbox. The boards simplified connection and disconnection of gage feed wires, as well as providing good wire identification for setting gage zeros and performing circuit checks.

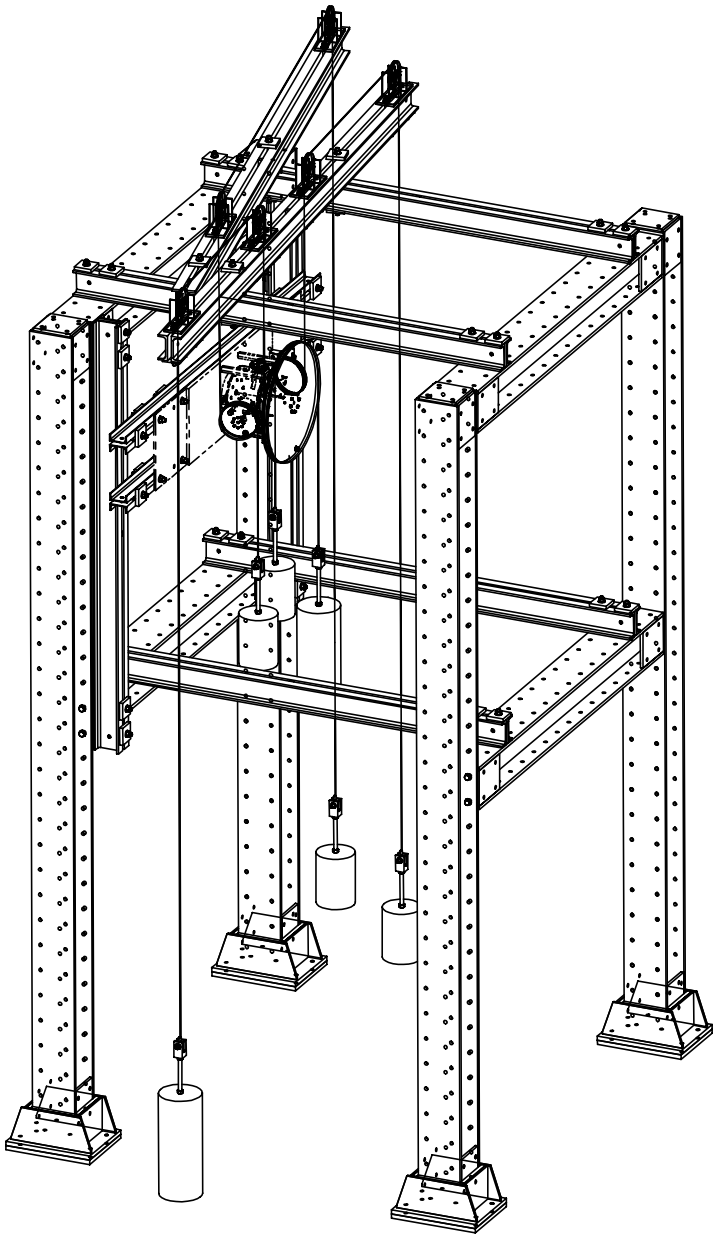

Figure 11. Isometric of POC Gearbox Test Fixture

Figure 12. POC Gearbox Test Fixture

3. Strain Gage and Test Instrumentation

Strain gages were applied along the roots of selected gear teeth (on all gears) to measure strain of the loaded teeth during slow roll tests. An optical encoder was installed on the end of one pinion shaft (and on the end of one idler shaft during torque calibration procedure described in Section VII) during tests to determine angular position of the gears as they rolled through mesh. This allowed strain vs. position data to be plotted for all gears after each slow roll test run. Locations where the strain gages were bonded to the roots along the gear teeth are shown in Figures 13 through 16. Table 1 summarizes the number of gages bonded to the root areas of the different teeth for two test shipsets. The self-compensating gages (all identical) have .015 inch grid length and integral solder tabs. Wires running from

connectors to the strain gages were routed along the inside bores of the gear shafts and then to the tooth roots through small holes drilled in the shaft walls. Retention clamps and strain relief clamps were utilized on the wire bundles at one or more locations along the routing, depending on which gear. Interface solder tabs were bonded to the gear shafts near the gear teeth. The lead wires terminated at these tabs, and the strain gage wires were bonded to the shafts between the interface tabs and the strain gage solder tabs.

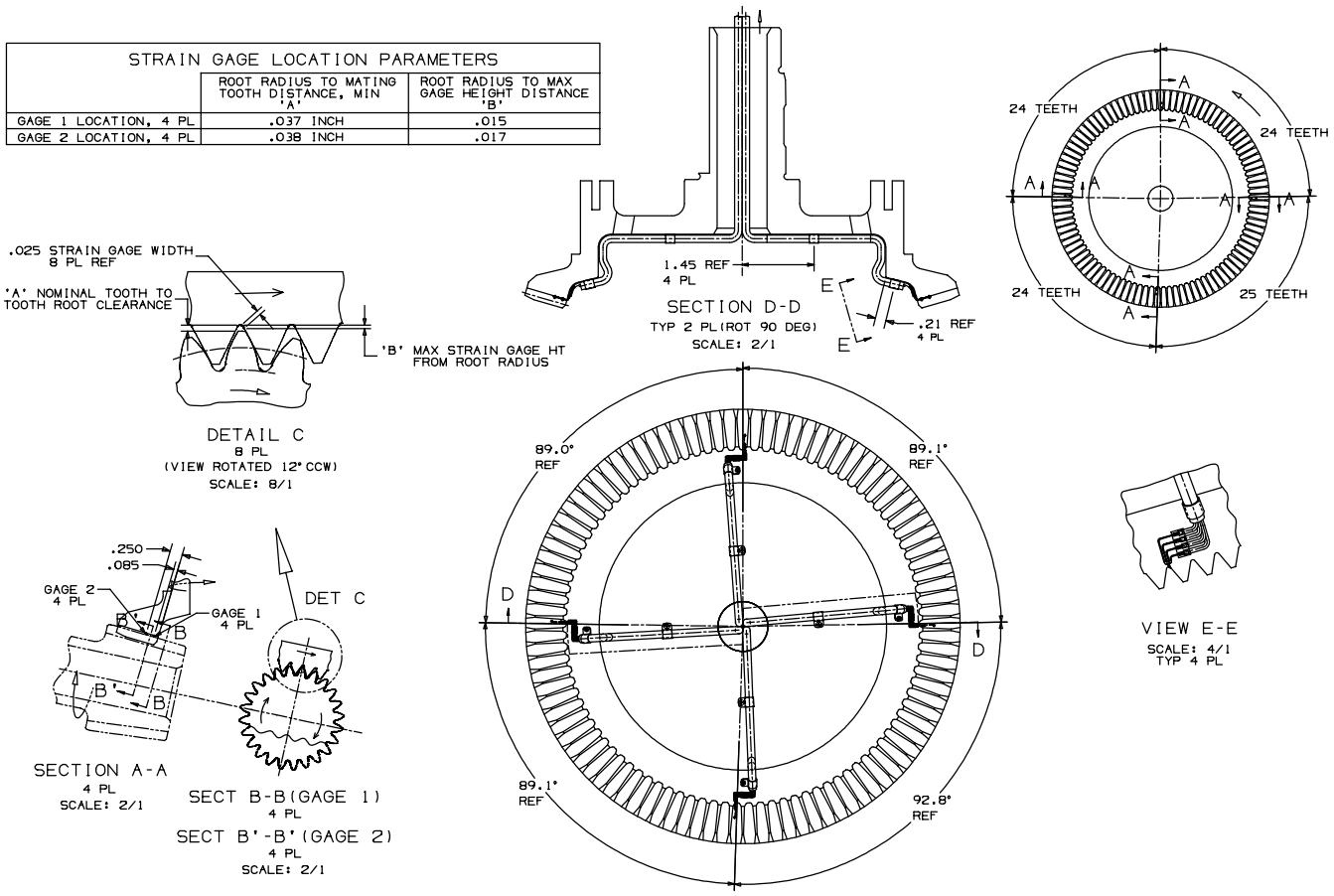

UPPER FACE GEAR STRAIN GAGE AND WIRE INSTALLATION
(REF P/N FGRR11)

Figure 13. Strain Gage Wiring Diagram for Upper Face Gear

In addition to the strain gages, load cells were installed in-line along each of the weighted cables loading the two pinion shafts and the upper face gear shaft. The load cells were used to verify correct input and output torque levels prior to each test. A total of one hundred seventy two channels were employed, one hundred sixty for the eighty strain gages and twelve for the six load cells. A master measurement list was used for tests to describe the strain gage locations, gage type and number, gage factor and wire ID's for signal conditioner / amplifier and MUX cards. For strain gages, the description column of the list gives the gear the gages are attached to, gage position along tooth, the gear being meshed with, starting

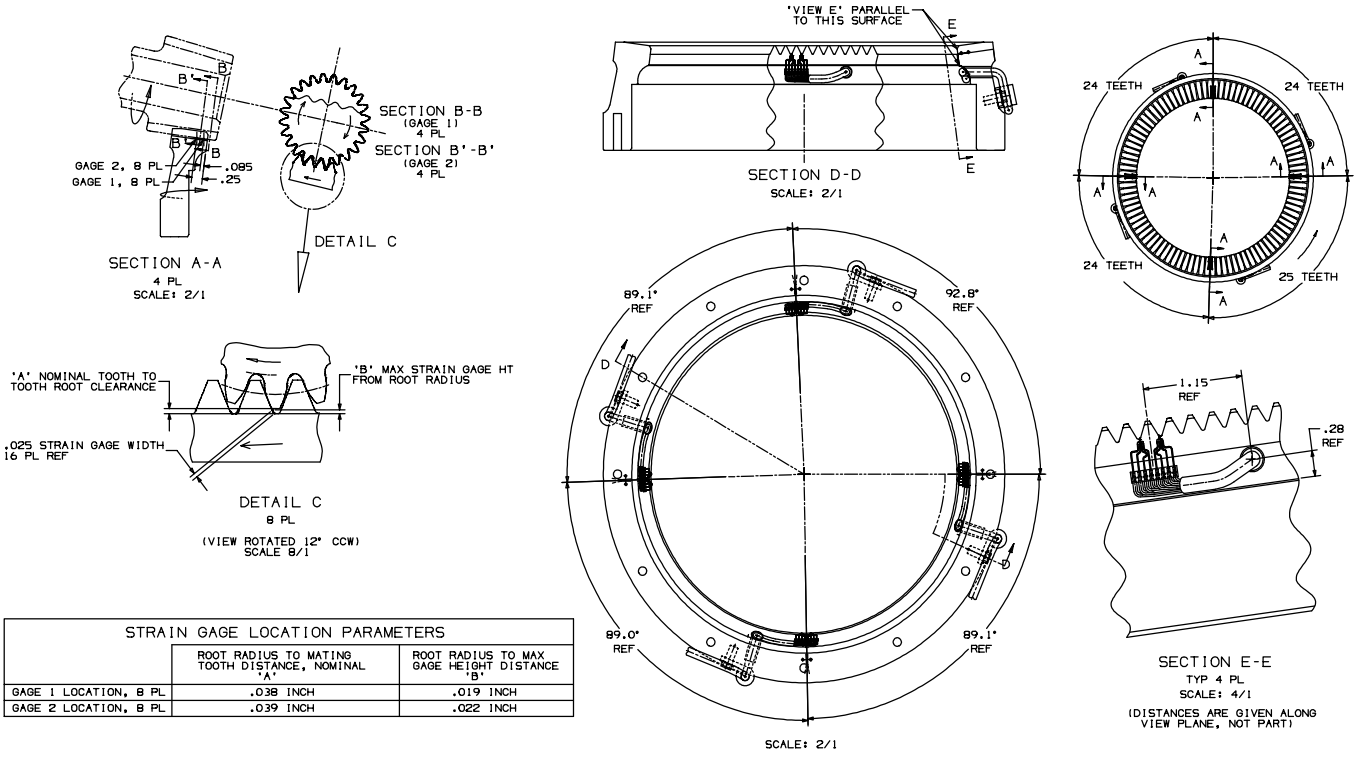

STRAIN GAGE LOCATION PARAMETERS		
	ROOT RADIUS TO MATING TOOTH DISTANCE, NOMINAL 'A'	ROOT RADIUS TO MAX GAGE HEIGHT DISTANCE 'B'
GAGE 1 LOCATION, 8 PL	.038 INCH	.019 INCH
GAGE 2 LOCATION, 8 PL	.039 INCH	.022 INCH

LOWER FACE GEAR STRAIN GAGE AND WIRE INSTALLATION
(REF P/N FGRR19)

Figure 14. Strain Gage Wiring Diagram for Lower Face Gear

position of instrumented tooth, and whether the gage is on the drive or coast side of the tooth (starting side for idlers). The number of channels utilized varied with the number of gears used for each test (or torque calibration).

For the load cells, the description column of the measurement list indicates whether the cell is measuring a left input, right input or output load and which side of each pulley the weight is located on (shafts were loaded in pure torsion, with a weight on each side of pulley). Related instrumentation included the signal conditioning amplifiers, multi-channel recording equipment, power supplies, MUX cards, A/D converter boards and computer.

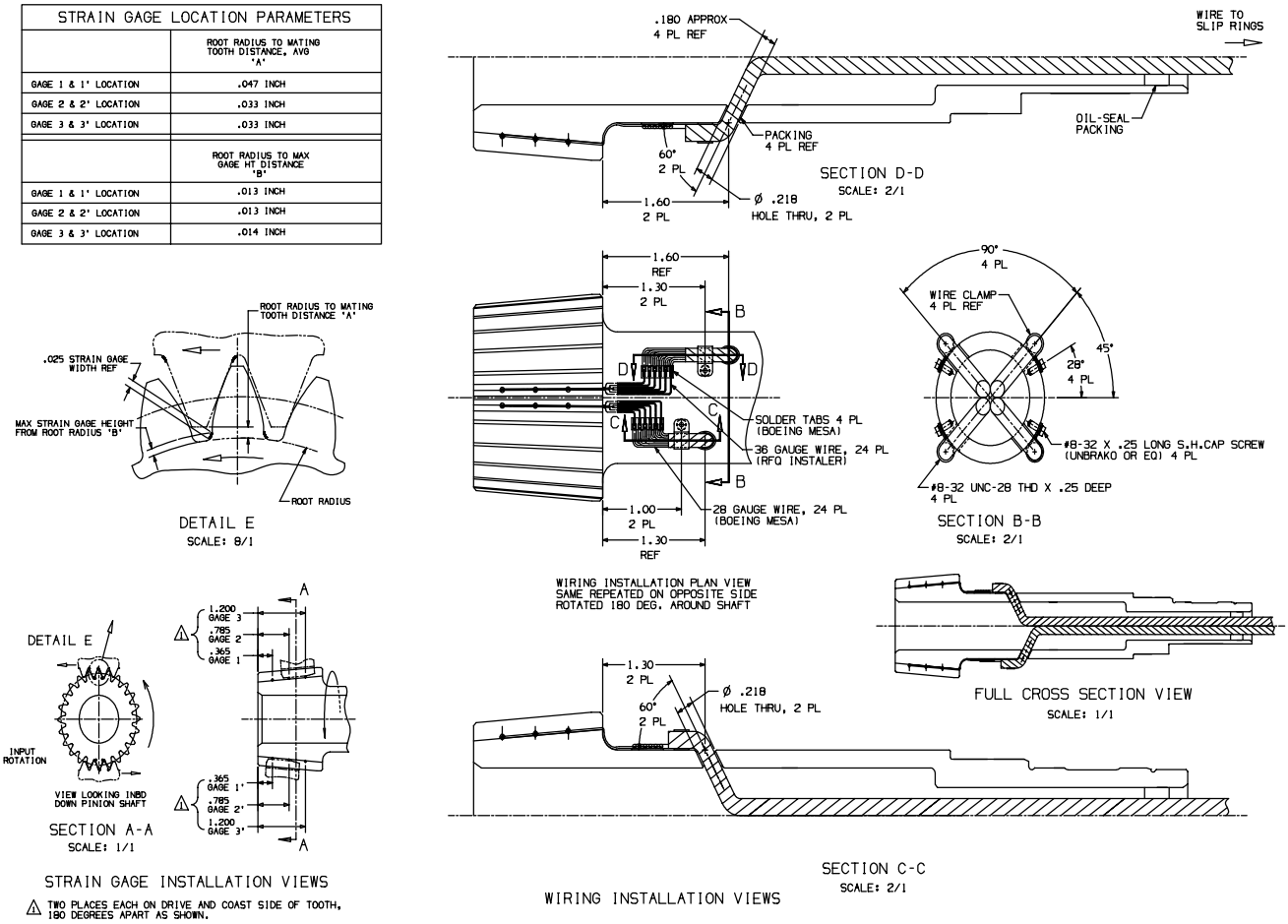

INPUT PINION STRAIN GAGE AND WIRE INSTALLATION
(REF P/N FGRR08)

Figure 15. Strain Gage Wiring Diagram for Pinion

4. Test Procedure

The proof of concept slow roll tests were conducted in the Boeing Advanced Development Center to indicate static torque splitting percentages and stresses for the face gear sets tested. Both face gears were used during all tests. Pinion and idler counts varied with the type of test performed below, but whenever they were used, each gear's serial number stayed with the one housing bore to which it was originally assigned. The one exception to this was when the two idlers were swapped temporarily during one of the initial tests, to verify a housing bore problem (ref. Section VI). All tests were performed at the 100% load level of

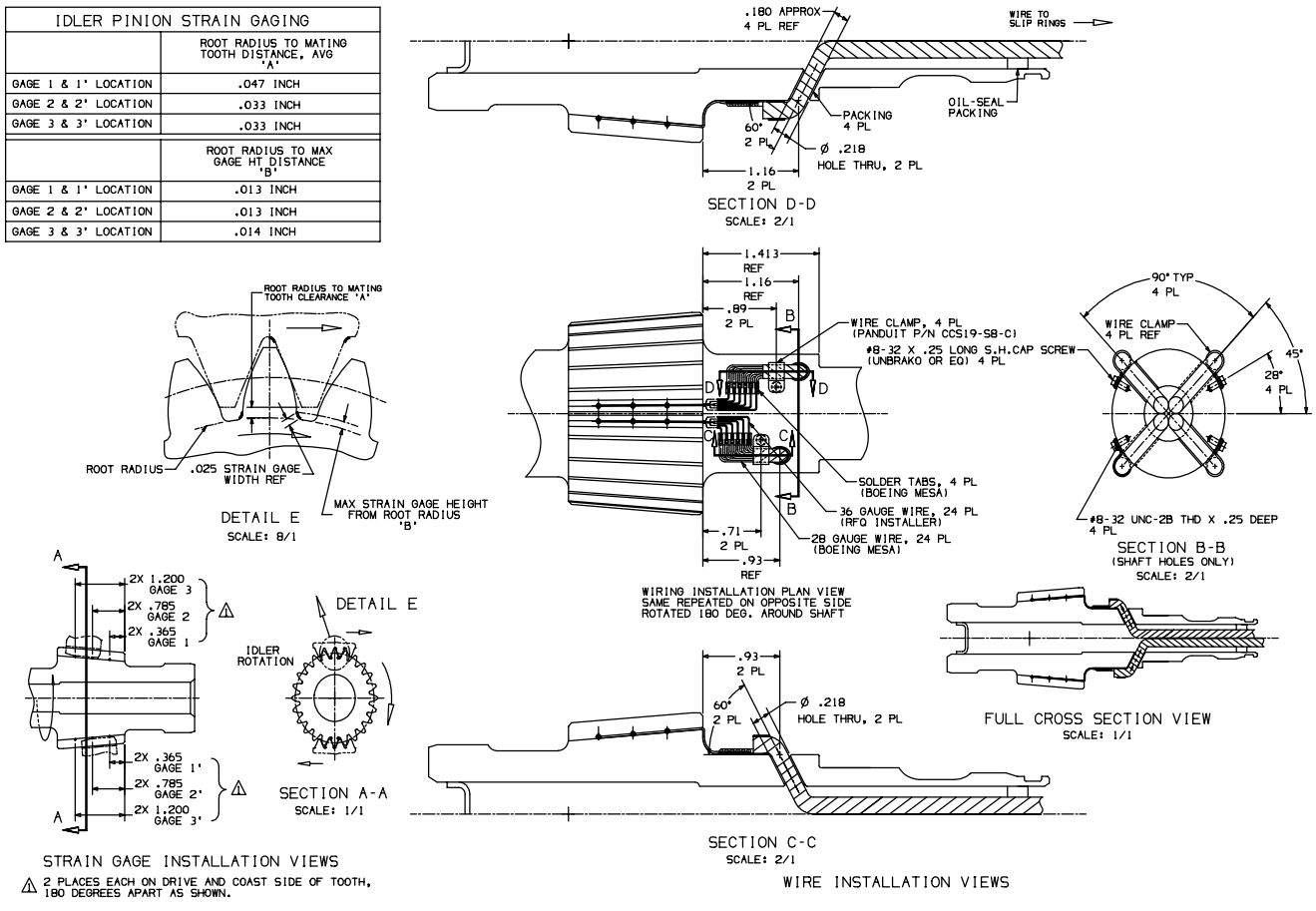

IDLER GEAR STRAIN GAGE AND WIRING INSTALLATION
(REF P/N FGRR17)

Figure 16. Strain Gage Wiring Diagram for Idler

Table 1. POC Test Gear Strain Gage Quantities

Test Gear	Number of Teeth Gaged per Gear	Number of Sides of Tooth Gaged	Number of Gages per Side	Total Gages Slow Roll Test
FGRR08 *(Qty4) Input Pinion	2	2	3	48 gages (12 gages on each of 4 gears)
FGRR17 *(Qty4) Idler Gear	2	2	3	48 gages (12 gages on each of 4 gears)
FGRR19*(Qty 2) Lower Face Gear	4	2	2	32 gages (16 gages on each of 2 gears)
FGRR11*(Qty 2) Upper Face Gear	4	2	2	32 gages (16 gages on each of 2 gears)

Total 160 gages + spares as required

*Two 'shipsets' of gears were produced. Each shipset consists of 2 pinions, 2 idlers, 1 upper face gear and 1 lower face gear.

Load cells (total of 6 located in-line on pulley cables) were used to determine input and output torque values.

1767 in-lbs (ref. Section III), as seen at each pinion shaft before torque split. Data was gathered for applicable strain gages on the teeth described for each subset of tests. For each strain gage location, tooth root strain was determined as the instrumented pinion and idler gear teeth were rolled through eight full meshes (four full pinion and idler turns), four with the upper face gear teeth and four with the lower face gear. Data was actually taken during about 3½ of these pinion and idler turns, or approximately 313° of face gear rotation, over a total of 1800 readings available with the instrumentation. Measurements were therefore taken at about each .17° of face gear roll angle increment, as triggered by an optical encoder attached to the end of a pinion shaft. This yielded 512 increments per pinion revolution, for about each .70° increment of pinion roll angle. Strain readings taken at each roll angle increment were displayed for each gage, along with mV/V output voltage readouts. Because the tooth thickness and tooth geometry changes along the length of each gear's teeth and between teeth of different gears, only the readings between gages located in identical positions (along the tooth length) on the teeth of similar gears were compared directly. Indirect comparisons included strain curve characteristics for the different gears and load distribution trends along the different gear teeth. The set-ups below were used to obtain separate sets of strain data within the slow roll tests. A graphical display of the gage output voltage (mV output / V excitation) versus angular position was viewable during tests, as part of the HP equipment set-up used.

i. Dual Input Pinion Loading Tests

Two instrumented input pinions and two instrumented idlers were installed for the dual input pinion tests. The mounting distances obtained from pre-test setup work (ref. Section IV.5) were used initially. During tests, the input pinions were rolled four full turns

counterclockwise (as viewed from behind). The test fixture was designed so that the weights would touch the floor and stop before pinion rotation could continue much beyond four turns. Strain values were obtained at all gages of the teeth involved in the four meshes (two pinions and two idlers) with the upper face gear and four meshes with the lower face gear. The pinions were then rolled back four turns (clockwise) to return face gears (and all wiring) to the initial starting position. The above slow roll test was performed two more times to verify output data repeatability. Test data and strain vs. position curves were then reviewed. Starting with the idlers, backlash changes were made as required to facilitate near-equalization of strain levels for similar gears. Achieving strain values of nearly the same magnitude between the two idlers and between the two pinions was perceived as the best going-in position for performing torque calibrations later. The torque calibrations (ref. Section VIII) characterized tooth strain levels (developed ratios of tangential load to strain) for each mesh by relating them to a known input torque value, and this information was then used for the purpose of torque split determination. By the end of tests (following torque calibration), it was found that close matching of strain magnitudes through backlash adjustments wasn't required before running torque calibrations. Some adjustments made to improve the balance of strain levels (for gages at same tooth locations on same gear types) would be sufficient prior to torque calibration. This is because while characterizing the meshes, torque calibrations also served to quantify unique characteristics of the different shaft bores (bore centerline angles and offsets, housing flange squareness, etc.) as these related to torque split values, and these other factors could not be accounted for until torque calibration was performed. Sections X and XI give some conclusions and recommendations regarding the above as consideration for future programs. For the two pinions, strain magnitudes tracked closely during dual pinion tests, so no adjustments (beyond original backlash and pattern adjustments) were made for these. All data from the above tests was documented and filed for additional study.

ii. Single Input Pinion Loading Tests

One instrumented input pinion and one instrumented idler were installed for the first single input pinion test. The other instrumented pinion and idler were paired for the second single pinion test. Each idler was selected as the one located downstream of the pinion being tested, in the direction of lower face gear rotation. The backlash values obtained from the final dual pinion tests were used for the single pinion tests. Similar to previous tests, the input pinion was rolled four full turns counterclockwise (as viewed from behind). Strain values were obtained at all gages of the teeth involved in the two meshes (one pinion and one idler) with the upper face gear and two meshes with the lower face gear. The pinion was then rolled back four turns (clockwise) to return face gears (and all wiring) to the initial starting position. The slow roll test was performed two more times to verify output data repeatability. Test data and strain vs. position curves were then reviewed. The full test sequence above was repeated for the other pinion and idler. Similar to the dual idler tests, torque split determinations were not made for these tests until after the torque calibrations (ref. Section VIII) were performed. All data from the above tests was again documented and filed for further study.

5. Tooth Backlash and Contact Pattern Adjustment

Prior to initial tests, gear tooth backlash and contact pattern adjustment was carried out for the first shipset of strain gage instrumented test gears. Following re-bore operations performed on the POC housing (ref. Section VI) for the idler shaft subassemblies prior to formal tests, identical procedures were used to re-adjust tooth backlash and contact patterns (for the same first instrumented shipset) to accommodate the housing modifications.

For both test builds, the two face gears were installed at their manufactured mounting distances (scribed on the gears by Derlan). It was decided to adjust backlash and contact patterns by adjusting pinion and idler positions, as long as good backlash and pattern correlations were observed early with the two face gears installed at their specified mounting distances. This decision was made because further adjustments made to either face gear location would impact backlash and contact for all four pinions and idlers at once (plus the other face gear), resulting in the potential need for backlash adjustments for most or all of the other gears. Ultimately, the upper and lower face gear mounting locations remained the same for both initial and formal tests, since intermediate housing rework did not require any adjustments.

i. Idler and Pinion Adjustment for Backlash and Pattern:

For the initial and formal test build, tooth backlash for all gears was adjusted to fall within the design backlash range prior to first contact pattern checks. To measure tooth backlash in the setups below, a bar was first attached to the end of the pinion or idler shaft involved (ref. Figure 17). The bar extended normal to the shaft centerline a few inches in either direction from it. The bar was stiff enough that it wouldn't deflect while it was being used to rock the gear being measured. A dial indicator was placed normal to the bar at a distance three inches from the shaft centerline and its base was magnetically locked to a large plate resting on the inspection table. The pinion or idler gear being checked was rocked back and forth to allow the range of travel to be noted from the indicator. This travel distance was converted to a backlash value by first rationing it down (using bar and pitch radii) to travel at the pitch radius and then using geometry to convert it to travel normal to the tooth. The equations used are given below.

Tangential Pinion Travel at Pitch Point = Pinion Pitch Radius x (Bar Reference Point Travel / Bar Reference Point Radius)

Tooth Backlash = Tangential Pinion Travel at Pitch Point x Cos (Tapered Pinion Helix Angle) x Cos (Pressure Angle)

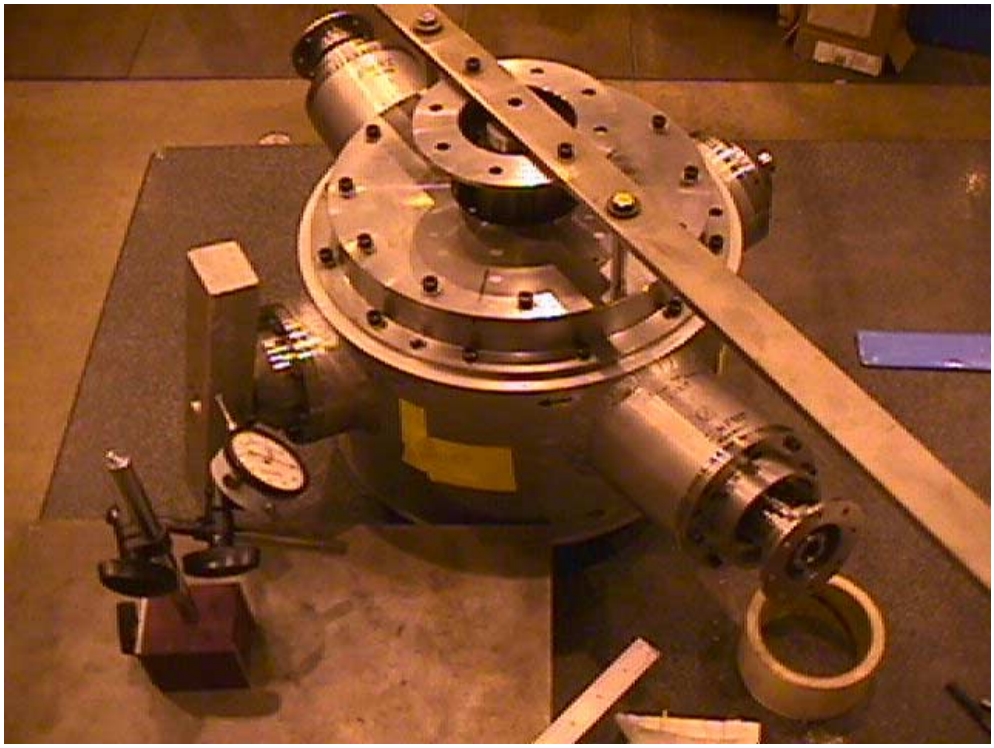

Figure 17. POC Gear Tooth Backlash Measurement

An exception to the above approach was pinion and idler backlash checks with the lower face gear (teeth were accessible with top cover removed), for which the dial indicator was physically placed normal to the (idler or pinion) tooth near the pitch point and magnetically secured for backlash measurement. The serial number of each pinion and idler was assigned to and stayed with one housing shaft bore for the duration of backlash and pattern adjustments, as well as tests.

Idler gear locations were adjusted to obtain a nominal backlash value (within .006 to .010 inch design range for POC gears) with only the lower face gear installed and then separately with the upper face gear installed, before a final location was arrived at for pattern checks. During idler backlash adjustments with the lower face gear, both pinions were installed, rotated in opposite directions against the lower gear, and locked. This kept the lower face gear from rotating during idler backlash measurements. The backlash of each idler was then determined and adjusted. The lower face gear itself was not locked (instead) because this was difficult to do. For idler backlash adjustments with the upper face gear, the upper face gear was locked at its hub, and backlash of the two idlers was determined and adjusted one at a time.

The pinion positions were adjusted to obtain nominal backlash values using a procedure similar to the above for idlers. Pinion backlash settings were adjusted for the lower and upper face gears separately, before a final pinion location was calculated and maintained for pattern checks. Idler gears were used to lock the lower face gear during pinion backlash adjustments, again similar to the approach for idler adjustments.

Once backlash values were adjusted within the intended design range, tooth contact patterns were checked. Marking compound was applied evenly to the gear teeth (two opposite sectors of five teeth on the pinions and idlers and four quadrant sectors of five teeth on the face gears), and all gears were indexed to a position a few teeth upstream of initial meshing. To check patterns, the pinions (and idlers) were rolled 150 degrees under full load to cover the range of one full mesh only. Rotation beyond that point would have resulted in mixing of upper and lower face gear contact patterns (which are offset, with significant overlapping present) on the pinions. The gearbox was then disassembled and contact patterns inspected and photographed. A couple of adjustments were made to shift contact patterns towards central locations on the gear teeth during low load checks. The POC face gear backlash vs. pattern trends were found to be similar to those for face gears from durability tests performed at NASA Glenn [2], as well as those for spiral gears. Figures 18 through 20 show a few of the final low load contact patterns for pinion, lower face gear and upper face gear teeth (prior to full load pattern checks). The patterns were obtained by hand using loading bars on the assembly table.

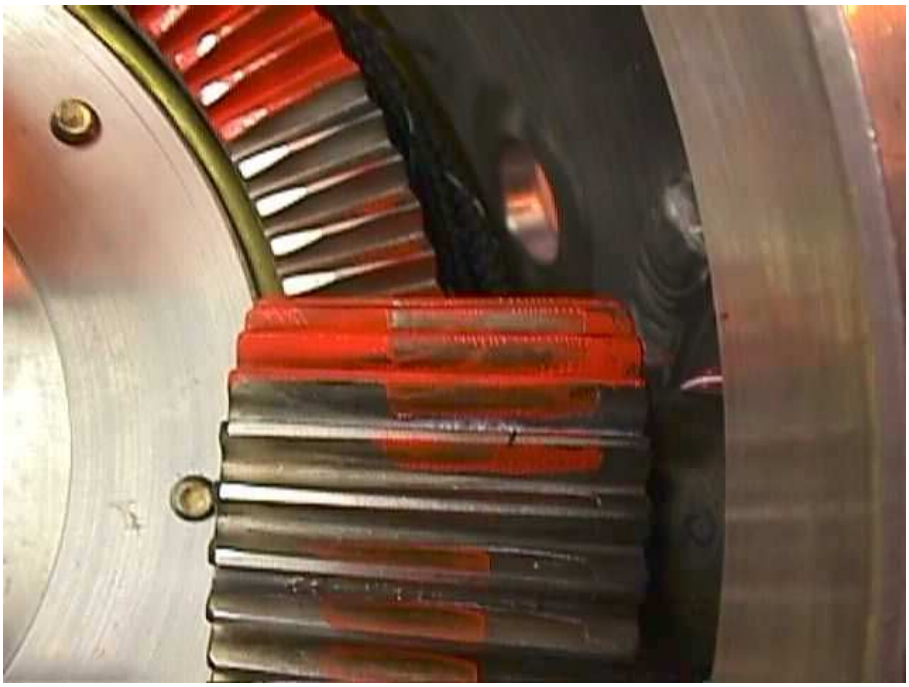

Figure 18. Pinion 1 Low Load Contact Patterns with Upper Face Gear

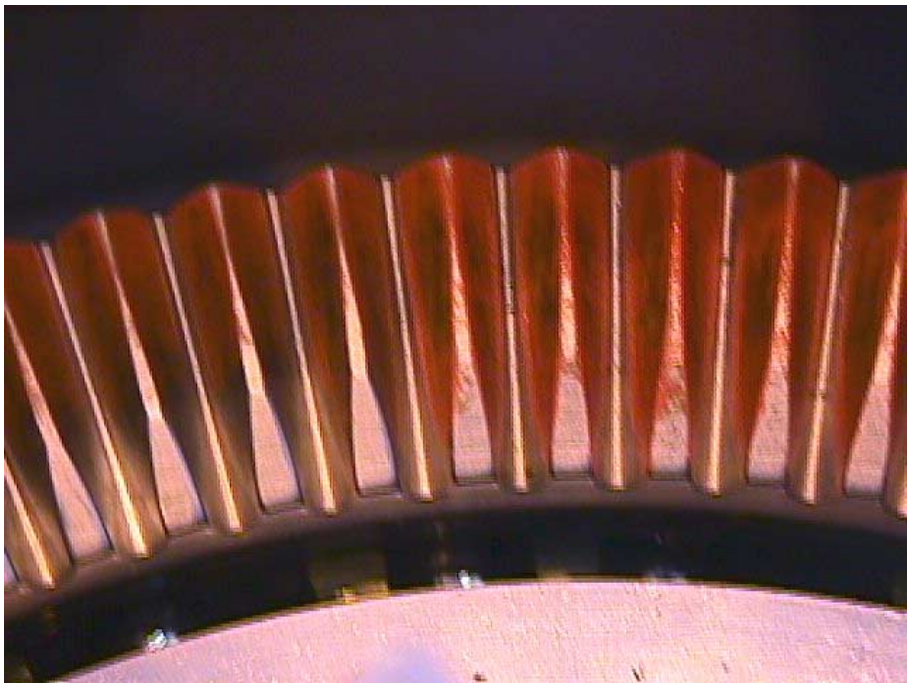

Figure 19. Lower Face Gear Low Load Contact Patterns

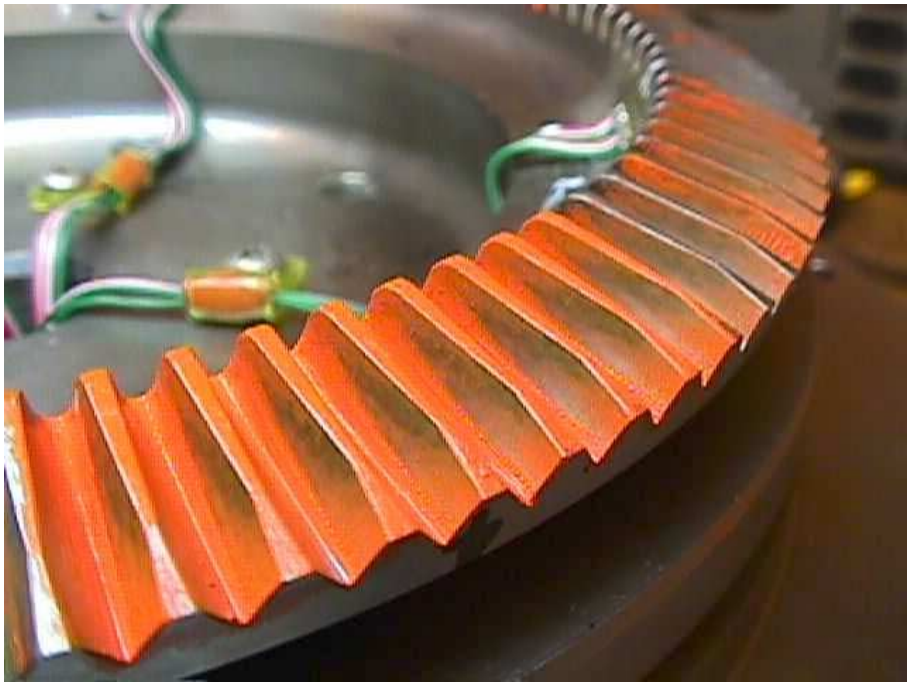

Figure 20. Upper Face Gear Low Load Contact Patterns with Idler 4

ii. Full Load Tooth Contact Pattern Checks:

Using final gear mounting distances obtained from the adjustments above, full load contact patterns were obtained next. Preliminary steps were similar to those for low load pattern checks. Prior to final assembly of the gearbox, marking compound was applied evenly to the gear teeth (two sectors of five teeth on the pinions and idlers and four sectors of five teeth on the face gears), and all gears were indexed to a position a few teeth upstream of initial meshing. The pinions were lock-wired to prevent gear rotation until after the gearbox was installed in the test fixture and ready for the full load slow roll pattern checks. The gearbox was then installed in the test rig (ref. Figure 21), and the weight, pulley and cable system was rigged to it. To check patterns, the pinions (and idlers) were rolled 150 degrees under full load to cover the range of one full mesh only. Rotation beyond that point would have resulted in mixing of upper and lower face gear contact patterns (which are offset, with significant overlapping present) on the pinions. Rolling motion was verified to be smooth with neither the gears nor the pulleys binding during rotation. The pinions (and idlers) were rolled back and forth four times through the same single mesh to set contact patterns. Before removal of the gearbox, the pinions were lock-wired again to prevent rotation and changes to the contact patterns. The gearbox was then removed, disassembled and contact patterns inspected and photographed. No patterns required modification based on full load inspections made prior to tests. Figures 22 though 25 show pre-test full load contact patterns for pinion, idler and upper face gear teeth. Root areas were also checked to see how far down the contact had progressed and to verify that no strain gage interference areas existed. A strain gage life check was also performed to assure continued operation of all gages after full load pattern runs, before actual tests.

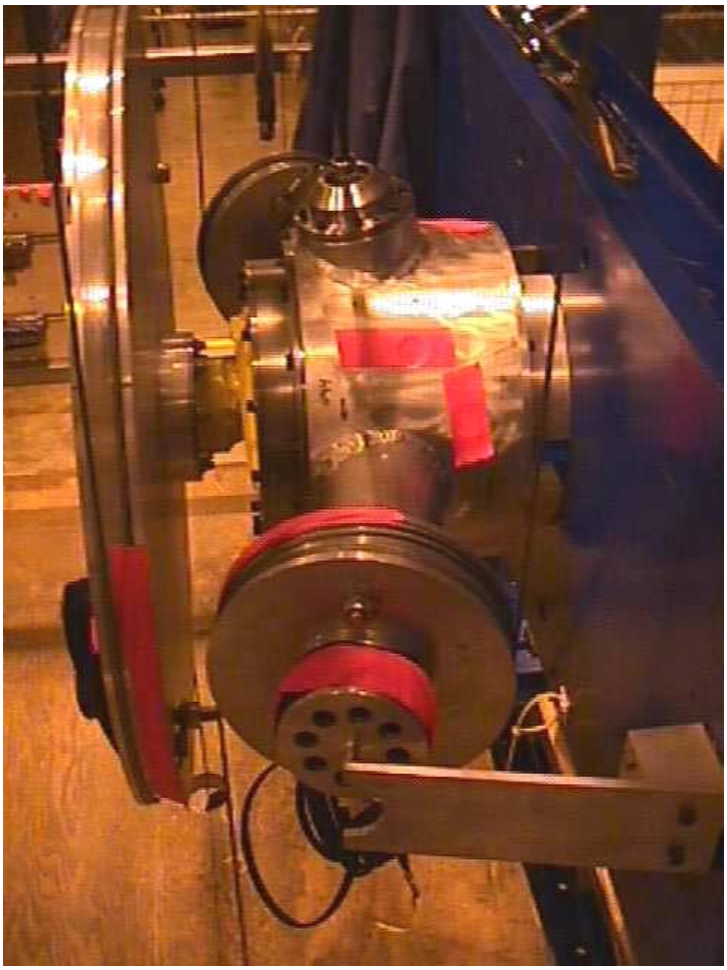

Figure 21. Full load Contact Pattern Checks
(Same as test set-up, but no instrumentation connected.)

During dual pinion tests, backlash adjustments were made to idler 4 to equalize strain levels for the two recombining idlers. Idler 4 backlash was increased to reduce its strain and increase strain for idler 3. Patterns shifted towards the toe (as anticipated) during that strain investigation (ref. contact patterns shown in Figs. 59-61 for run 141 of Table 2). Torque calibrations performed later (ref. Section VIII) indicated that idler 4 backlash could have remained close to the original settings, and that higher strain values did not equate to excessive load carried by idler 4. This is probably due to some unexpected characteristics of housing bore 4 (still existing to some extent after the housing rework was performed, ref. Sections VI and VII), which were verified by the torque calibration procedure (used in torque split determination).

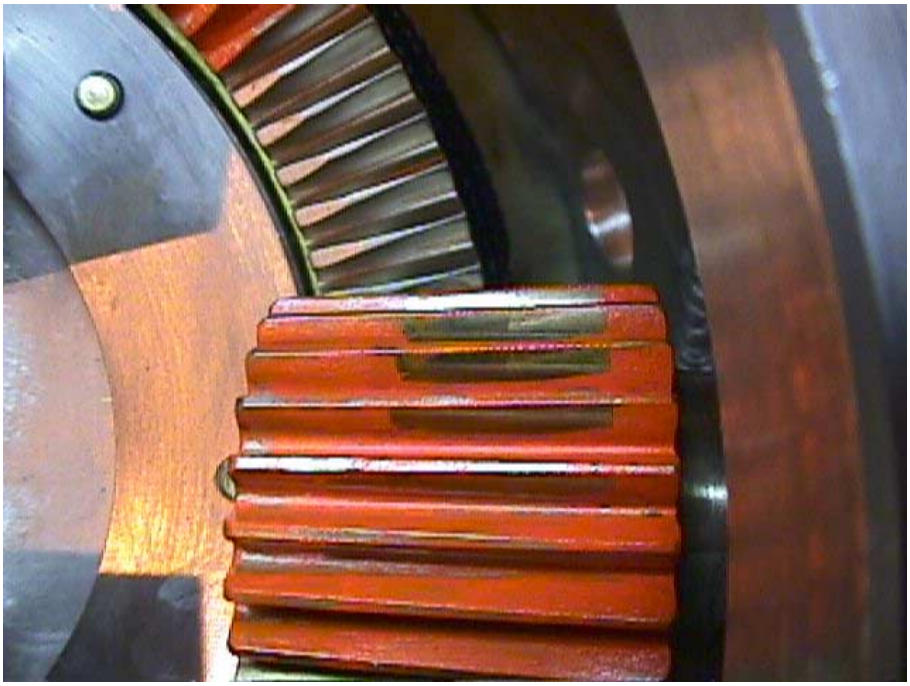

Figure 22. Pinion 2 Upper Mesh Contact Patterns
Full Load Contact Pattern Inspection

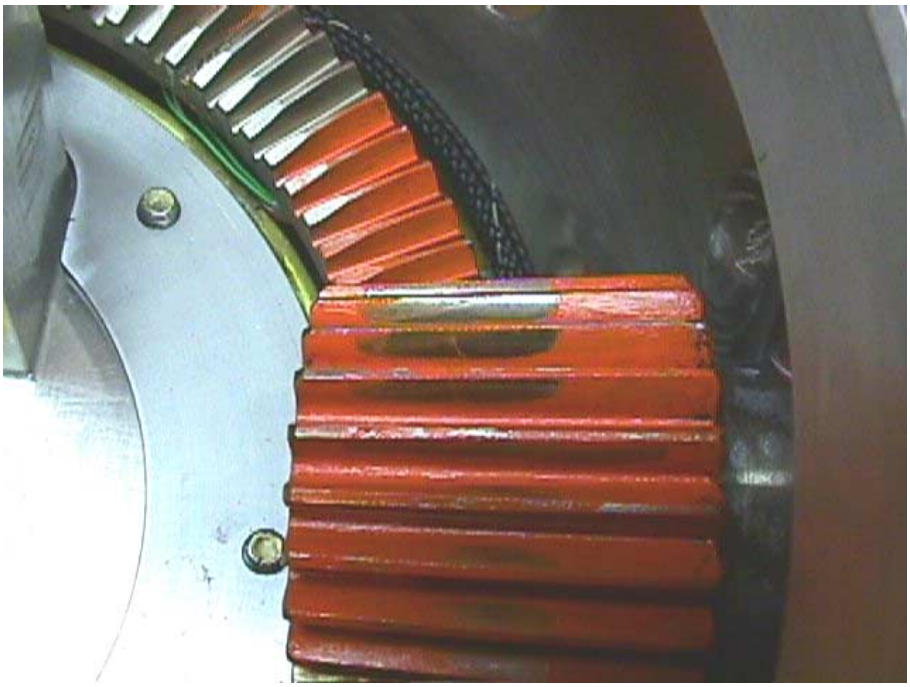

Figure 23. Pinion 1 Lower Mesh Contact Patterns
Full Load Contact Pattern Inspection

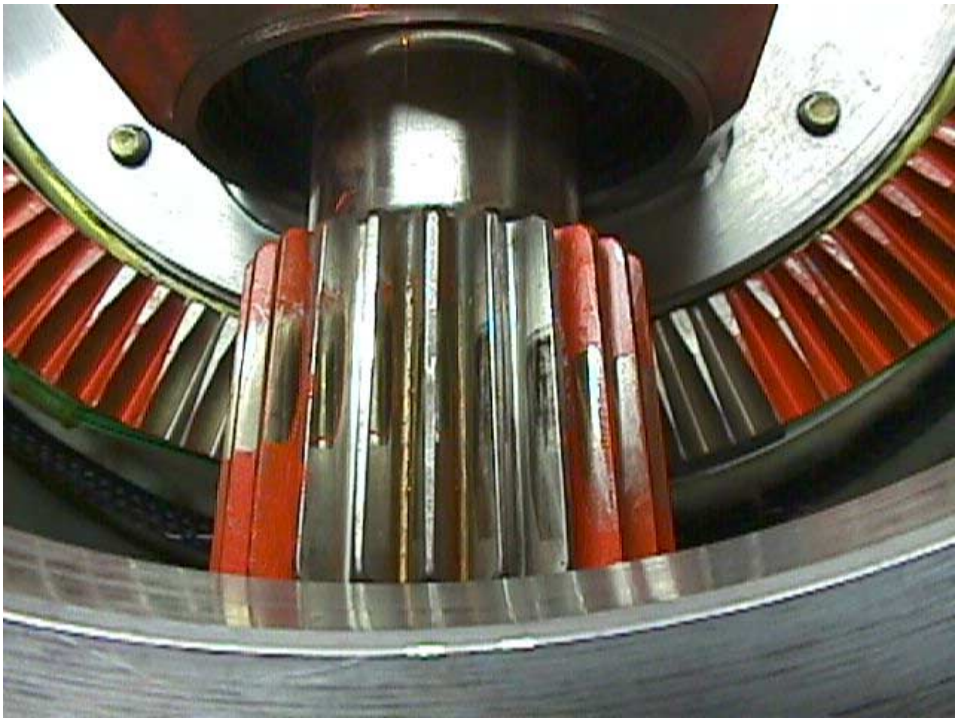

Figure 24. Idler 4 Contact Patterns with Upper and Lower Face Gears
Full Load Contact Pattern Inspection

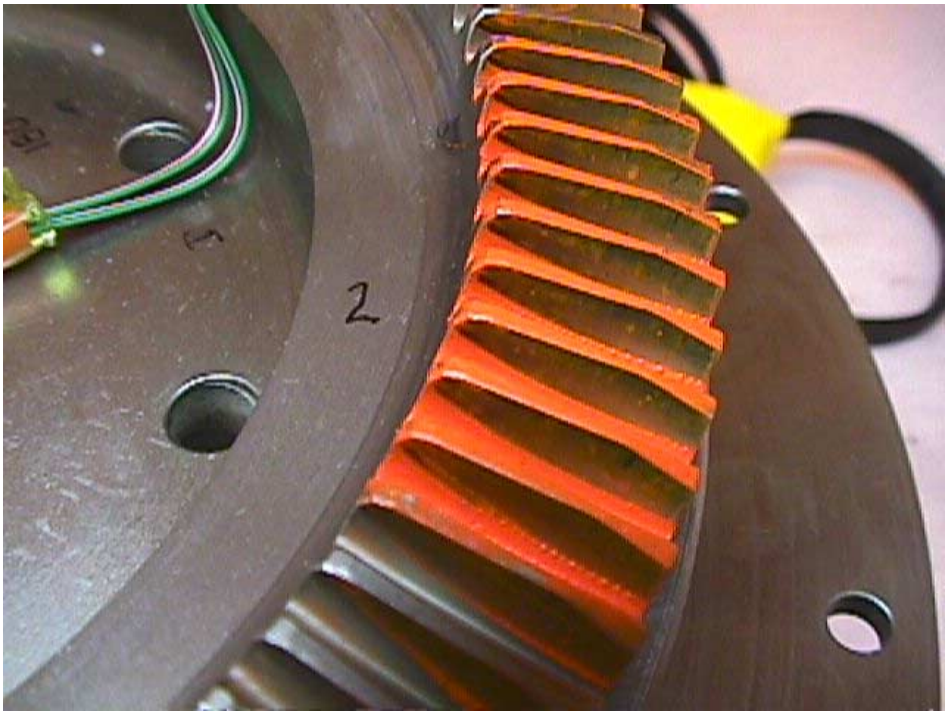

Figure 25. Upper Face Gear Contact with Pinion 2
Full Load Contact Pattern Inspection

V. STRAIN GAGE CALIBRATION

For this Proof-of Concept (POC) slow roll test, a total of 80 strain gages were applied to the face gear, pinion and idler teeth. All gages were applied at the tooth root to measure strain due to bending and compression. For the pinions and idlers, three gages across the tooth length were applied to both the drive and coast sides of two diametrically opposed teeth for a total of 12 gages per pinion or idler. For the face gears, two gages across the tooth length were applied to both drive and coast sides of 4 teeth spaced approximately every 90 degrees about the face gear azimuth for a total of 16 gages per face gear. Figure 26 shows a top view of the strain gage locations for the lower face gear – upper face gear strain gages are located similarly. Figure 27, a section view of the pinion in mesh with the upper and lower face gears, shows the location along the tooth length of the pinion and upper and lower face gear strain gages. Strain gage installation locations are defined in detail in the engineering test request (ETR) [12].

As described in Section 7.3 of [12], all 80 strain gages were calibrated. Although not a calibration in the truest sense, the gage calibration performed involved the application of load perpendicular to the pitch surface of each gear via a 0.1378 inch diameter ball placed between adjacent gear teeth. For the calibration of a given gage, the ball, which was actually soldered or bonded (both methods were used) to a steel post, was positioned directly over the gage location. This was accomplished using various calibration fixtures to maintain the proper position of the gear being calibrated and the load application ball/post assembly. The pinion idler calibration fixture is shown in Figure 28. A cross-section through the pinion (or idler) teeth at the three gage locations with the calibration ball in place is shown in Figure 29. The strain gage calibration procedure was intended to provide a means to compensate for possible differences in gage placement between gage installations at the same location on different gears. The intended result of the calibration procedure was correction factors that could be applied to each gage such that, when corrected, strain differences due to installation would be eliminated.

The ETR originally called for a relatively high calibration load that would produce the same tangential load on the gear tooth as would be experienced by the tooth during test torque loading. Subsequent analysis showed that this would produce unacceptably high compressive stresses due to the localized nature of the ball loading. Calculations showed that 25 lbs could be safely applied without the risk of compressive yielding of the surface material, i.e., dimpling. A side test was conducted on an uninstrumented upper face gear to determine, starting with 25 lbs, the maximum calibration load that could be applied without sustaining dimpling. Results showed dimpling occurred well below 100 lbs, however, 100 lbs was chosen as the final calibration load in order to produce strain gage output levels of reasonable magnitude. Based on visual examination, the amount of dimpling detected at 100 lbs was small and considered acceptable.

Calibrations were performed for all 80 gages. At the beginning of the calibration process, it was immediately obvious that there was significant hysteresis. The relationship between gage output and calibration load was fairly linear for increasing calibration load, but very non-linear for the decreasing load calibration steps. It was thought that this might be related to the dimpling at high load and a “sticking” phenomenon with the ball. Nevertheless, initial results

for the upper face gear strain gages looked very reasonable leaving no reason to believe the calibration procedure was inaccurate. Subsequent calibrations of the pinions and idlers showed large variation in sensitivity between gages in the same location on different teeth. Test lab personnel repeated calibrations for some gages with the most non-linear results and noted that the calibration slope was not repeatable. The calibration procedure was scrutinized and the surface of the calibrated teeth were examined using a microscope. In addition to dimpling, surface damage, which appeared to be a "track" left by the calibration ball, was noted on some teeth. It is probable that, particularly for the pinions and idlers, the calibration was done with the ball slightly misaligned relative to the tooth space. The calibration procedure included an initial manual alignment of the calibration ball in the tooth space, and then a tightening of the hardware that suspended and centered the pinion or idler within the fixture. During the tightening step, it is possible that the gear was rotated slightly. Furthermore, the tightened assembly provided frictional restraint against rotation by the calibration ball attempting to become aligned with the tooth space.

Other findings of the investigation were that the calibration ball used for the pinions and idlers, upon close examination, was out-of-round and had areas of poor surface finish. Based on these findings, an improved calibration procedure was tested. A new calibration ball, with proper roundness and surface finish characteristics was obtained. The pinion/idler gear was installed in the fixture only tight enough to eliminate significant radial or axial play. Copious grease lubrication was applied to the faying surfaces of the calibration fixture and pinion/idler, as well as to the calibration ball. Various amounts of preload were applied to the ball/post assembly prior to conducting the actual calibration. Gage 1009 was one of those for which data was recorded in the "consistency" test. It was also the gage used to assess the best preload value to use. Figure 30 shows results of the various calibrations for Gage 1009. The "special" calibration was conducted after the "original" one due to the obviously non-linear nature of the original calibration. Note the improvement in repeatability attained by use of the revised calibration procedure. A preload value of 40 lbs was decided on, although Figure 30 shows little effect due to the amount of preload used. Most of the improvement is attributed to the use of a better ball and lubrication.

All four pinions and idlers were re-calibrated using the improved procedure. Due to schedule constraints and the fact that the face gear calibrations appeared to be much more linear and reasonable, face gear gage calibrations were not repeated. Data from the re-calibration was examined and 12 pinion/idler gages for which the slope deviated the most from the average value for a given location were calibrated a final time. These final calibrations included several repeat runs in an effort to obtain a consistent slope. The slope used for each of these 12 gages was an average of the slopes for the various iterations from the final calibration. The final calibration slope results are shown in Figures 31-33. In Figures 31-33, in addition to the slopes, correction factors are listed for each gage. These factors are the end result the calibration effort was intended to provide. The correction factor for a given gage was calculated by dividing the average calibration slope for all gages of a given type, e.g., all pinion and idler toe gages, by the calibration slope for that gage. This factor was then to be used to multiply all strain output for that gage to eliminate any effects on the strain results due to gage placement.

Several findings surfaced as a result of the calibration effort. A review of Figures 31-33 shows that the gage calibration slopes are quite consistent for a given location. In fact, for the improved gage calibration procedure for the pinions and idlers, the variation in calibration slopes generally decreased. This indicates a gage installation of high quality and consistency. There have also been no instances of gage failure to date (there have been instances of wiring failure that were repairable). From Figure 31, for the pinion and idler gages, there also appears to be some correlation between magnitude of gage output and variation of calibration slopes. This is likely due to the fact that as the magnitude of the gage output decreases, the effects of any sources of inaccuracy in the calibration become magnified.

Significant effort and expense, both in terms of fixture hardware design and manufacture, and development and execution of the procedure, was invested in the calibration of the POC gear strain gages. Due to the apparent accuracy of the installations, for future tests, the need for such a calibration should be re-evaluated. For most of the test objectives that have been envisioned, the strain need only be measured with reasonable accuracy. Torque split as approximated by the upper face gear gages is independent of gage accuracy. If this type of gage calibration is used again in the future, the method should be improved such that first time quality is achieved. More attention should be given to reducing friction in the calibration setup to a minimum.

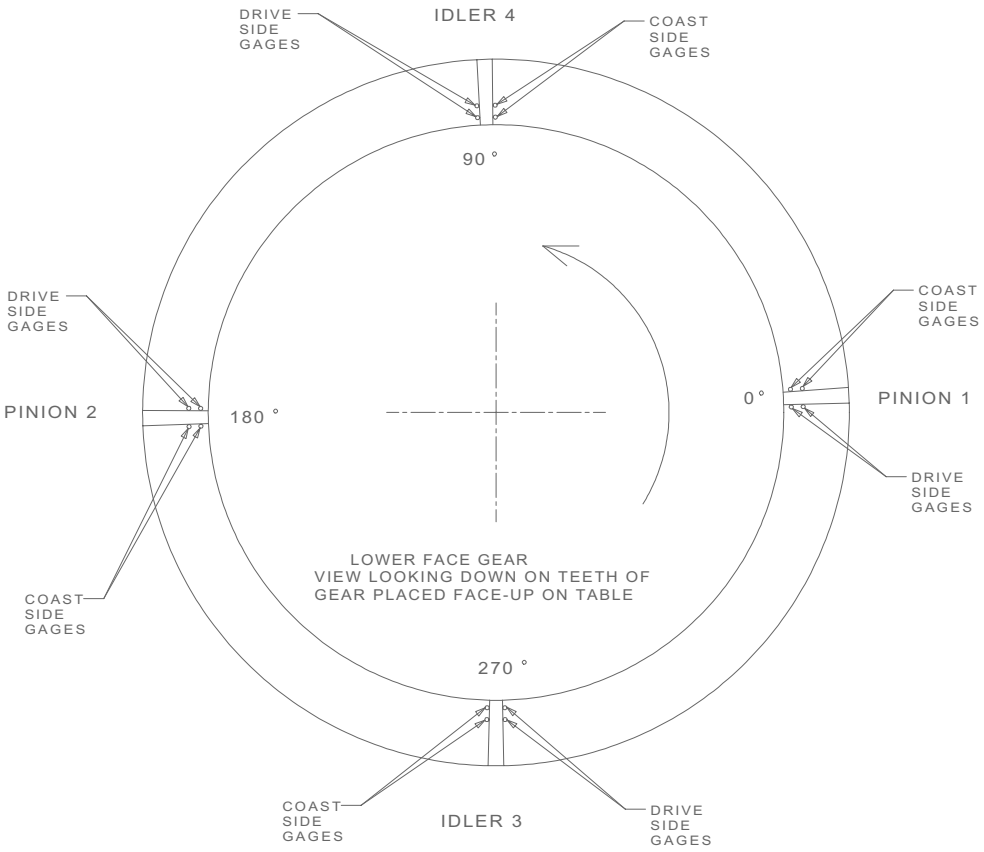

Figure 26. Designation of pinions and idlers.

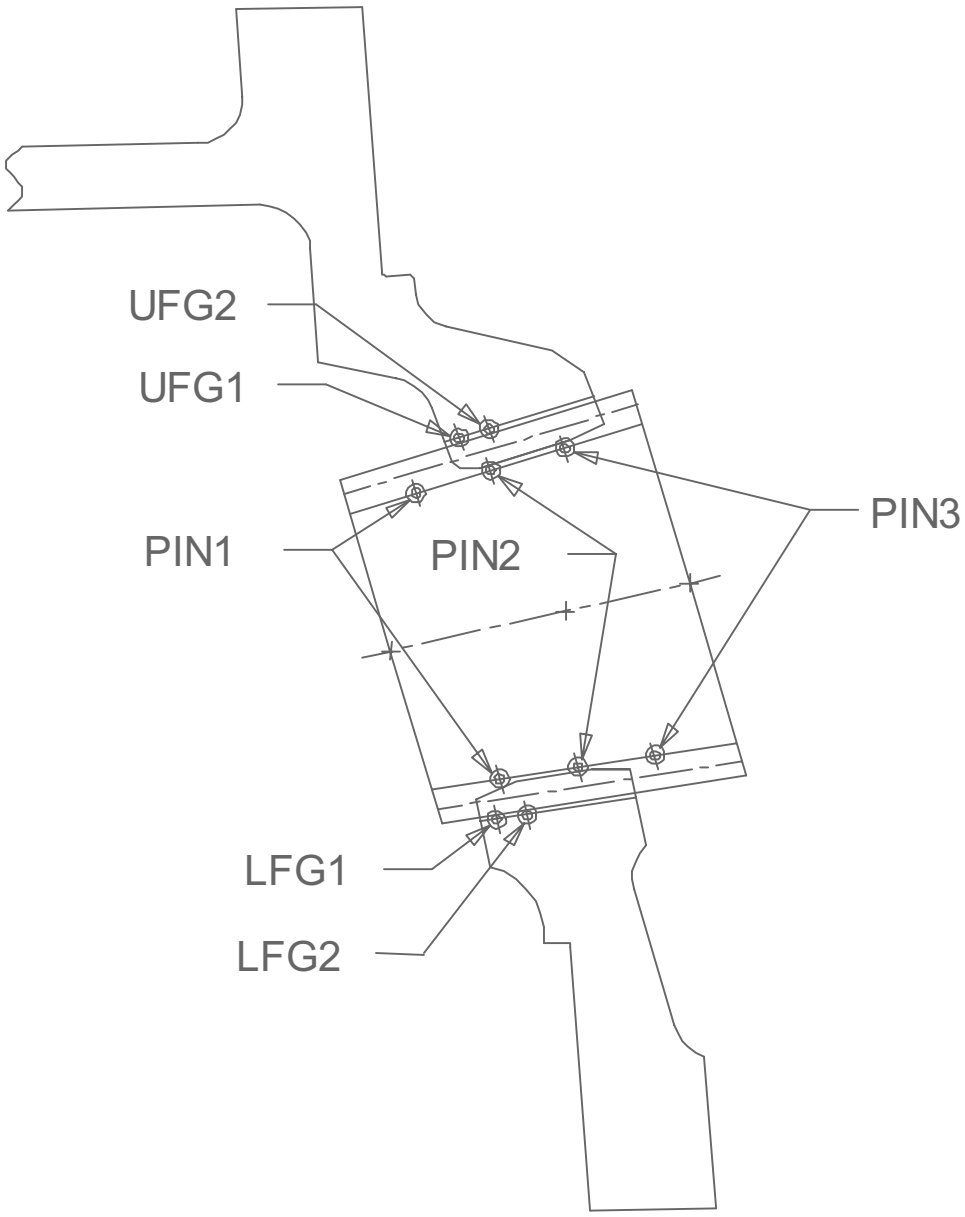

Figure 27. Strain gage locations.

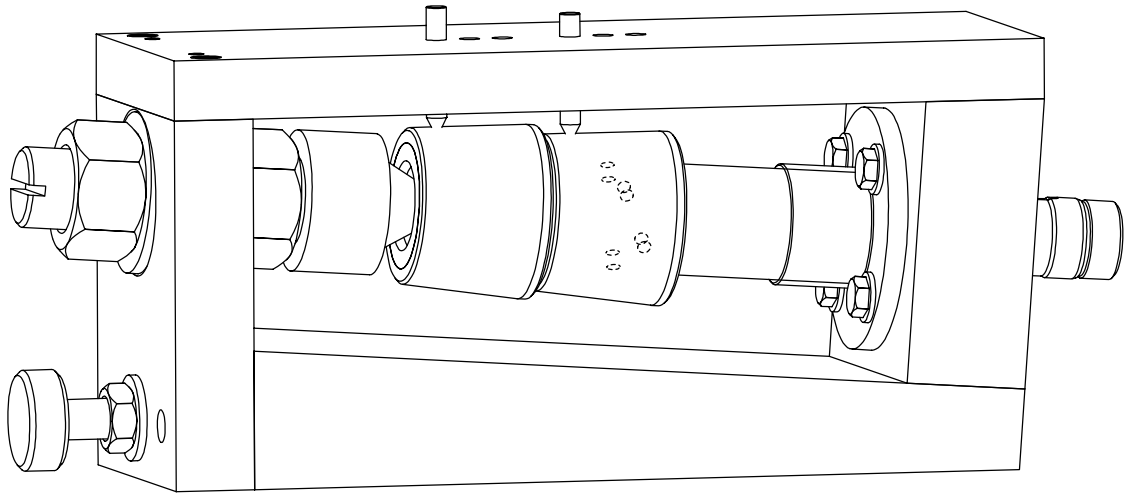

Figure 28. Pinion and idler strain gage calibration fixture.

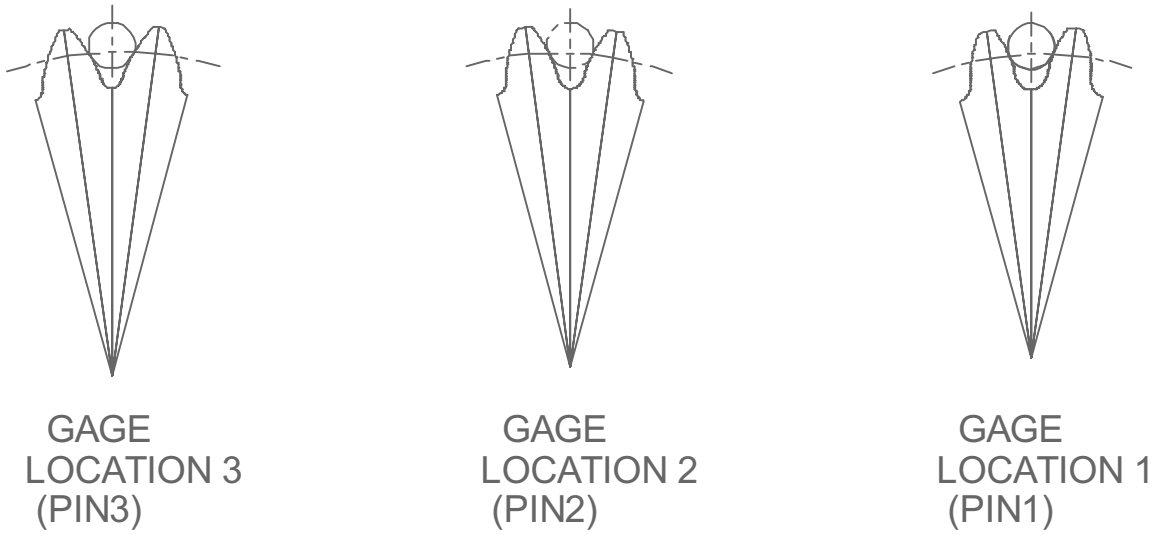

Figure 29. Sections through pinion teeth at gage locations.

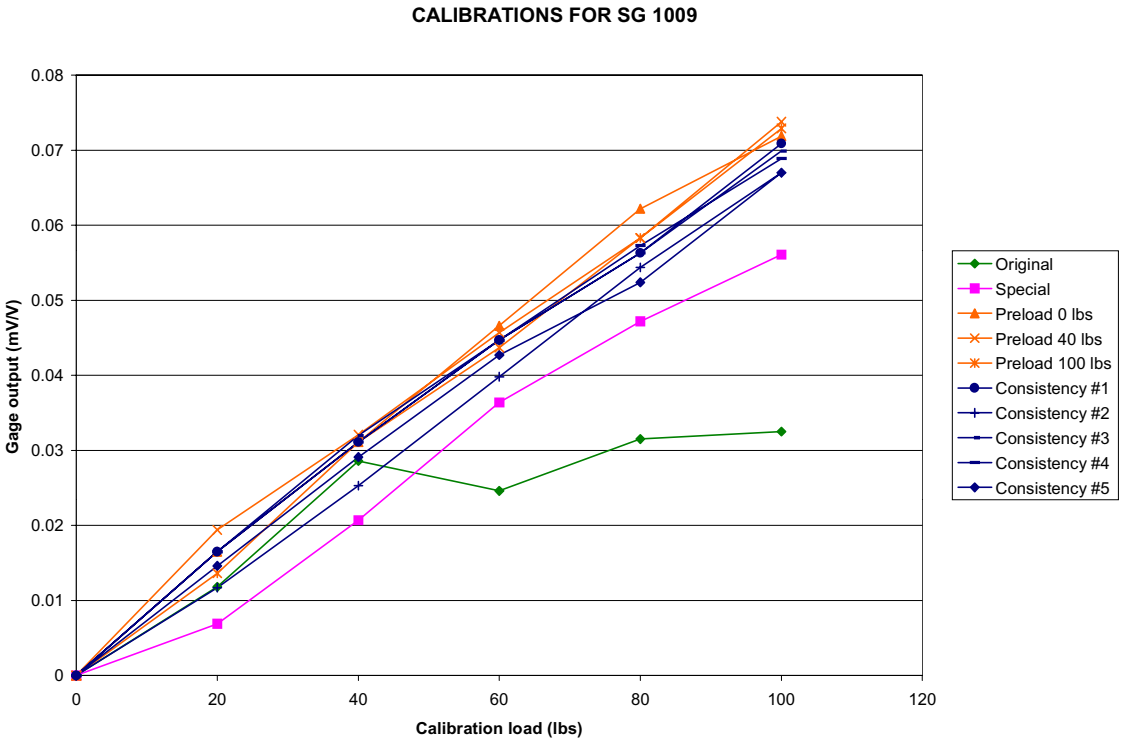

Figure 30. Calibration results for Gage 1009.

Units of Slope are mV/V / lb.

Conversion factor between engineering units and millivolts/volt:
1960.8 (μin/in) / (mV/V)

TOE (No.1) GAGES

Gage No.	Slope	Correction Factor
1001R	0.001687	0.9385
1004R	0.001534	1.0325
1007R	**0.001635**	**0.9687**
1010R	0.001636	0.9676
1013R	0.001621	0.9768
1016R	0.001675	0.9454
1019R	0.001619	0.9783
1022R	0.001584	0.9995
1025R	0.001611	0.9826
1028R	0.001449	1.0927
1031R	**0.001550**	**1.0219**
1034R	0.001602	0.9885
1037R	0.001571	1.0077
1040R	0.001500	1.0556
1043R	0.001524	1.0393
1046R	0.001538	1.0296
Average	0.001583	1.001589
Std Dev	0.000065	
CoV	4.08%	
avg μin/in at 100 lbs =		310

MIDDLE (No.2) GAGES

Gage No.	Slope	Correction Factor
1002R	**0.001337**	**0.7793**
1005R	0.001031	1.0110
1008R	0.001081	0.9641
1011R	**0.001024**	**1.0172**
1014R	0.001098	0.9490
1017R	0.001036	1.0061
1020R	0.001104	0.9442
1023R	0.001061	0.9820
1026R	0.000949	1.0975
1029R	0.001002	1.0403
1032R	**0.001073**	**0.9711**
1035R	**0.001038**	**1.0036**
1038R	**0.000846**	**1.2314**
1041R	0.000975	1.0688
1044R	0.001036	1.0056
1047R	0.000981	1.0621
Average	0.001042	1.008332
Std Dev	0.000101	
CoV	9.73%	
avg μin/in at 100 lbs =		204

HEEL (No.3) GAGES

Gage No.	Slope	Correction Factor
1003R	0.000819	0.9495
1006R	0.000981	0.7931
1009R	0.000660	1.1780
1012R	**0.000952**	**0.8173**
1015R	**0.000668**	**1.1639**
1018R	0.001001	0.7770
1021R	0.000969	0.8029
1024R	0.000923	0.8427
1027R	**0.000611**	**1.2726**
1030R	0.000880	0.8836
1033R	**0.000635**	**1.2247**
1036R	0.000816	0.9529
1039R	0.000622	1.2506
1042R	**0.000580**	**1.3406**
1045R	0.000637	1.2208
1048R	0.000690	1.1275
Average	0.000778	1.037353
Std Dev	0.000154	
CoV	19.84%	
avg μin/in at 100 lbs =		152

Figure 31. Correction factors for pinion/idler strain gages.

Units of Slope are mV/V / lb.

Conversion factor between engineering units and millivolts/volt:
1960.8 (μin/in) / (mV/V)

TOE (No.1) GAGES

Gage No.	Slope	Correction Factor
1049	0.002435	1.0632
1051	0.002580	1.0031
1053	0.002171	1.1924
1055	0.002578	1.0039
1057	0.002390	1.0830
1059	0.002585	1.0015
1061	0.002788	0.9285
1063	0.003181	0.8136
Average	0.002588	1.011174
Std Dev	0.000300	
Cov	11.58%	
avg μin/in at 100 lbs =		508

MIDDLE (No.2) GAGES

Gage No.	Slope	Correction Factor
1050	0.001136	1.0477
1052	0.001127	1.0565
1054	0.000963	1.2363
1056	0.001165	1.0217
1058	0.001220	0.9759
1060	0.001264	0.9418
1062	0.001212	0.9825
1064	0.001437	0.8285
Average	0.001190	1.011356
Std Dev	0.000135	
Cov	11.31%	
avg μin/in at 100 lbs =		233

Figure 32. Correction factors for upper face gear strain gages.

Units of Slope are mV/V / lb.

Conversion factor between engineering units and millivolts/volt:
1960.8 (μin/in) / (mV/V)

TOE (No.1) GAGES

Gage No.	Slope	Correction Factor
1065	0.002290	0.9939
1067	0.002701	0.8427
1069	0.002120	1.0734
1071	0.002132	1.0678
1073	0.002430	0.9368
1075	0.002532	0.8990
1077	0.002099	1.0844
1079	0.001905	1.1945
Average	0.002276	1.011575
Std Dev	0.000263	
Cov	11.55%	
avg μin/in at 100 lbs =		446

MIDDLE (No.2) GAGES

Gage No.	Slope	Correction Factor
1066	0.000973	0.8561
1068	0.000855	0.9748
1070	0.000816	1.0212
1072	0.001028	0.8104
1074	0.000568	1.4677
1076	0.000951	0.8755
1078	0.000620	1.3442
1080	0.000854	0.9751
Average	0.000833	1.040637
Std Dev	0.000164	
Cov	19.71%	
avg μin/in at 100 lbs =		163

Figure 33. Correction factors for lower face gear strain gages.

VI. INITIAL TESTING

Prior to the formal start of the test, the complete POC gearbox assembly with Pinions 1 and 2 and Idlers 3 and 4 was installed and slow roll tested. This was intended as an initial look to verify correct operation of the entire system and to checkout the instrumentation and test procedure. As stated in the test procedure section, each slow roll test run consisted of 3½ pinion/idler rotations and approximately 313 degrees of face gear rotation (relative rotations proportional to tooth ratio – 24 pinion and idler teeth, 97 face gear teeth). During each run, strain gage data was recorded at 1800 evenly spaced roll angle intervals (512 readings per pinion revolution). An effective means to view the resulting strain output is using plots of strain versus sample no. (roll angle). Strain traces for all gages on a single tooth flank are displayed on the same plot (gage locations shown in Figure 27 – idler gage locations are the same as those for the pinion). This gives some indication of how the tooth is loaded along its length. Various strain data was plotted and reviewed to include the upper face gear strain data shown in Figure 34 (Run No. 3).

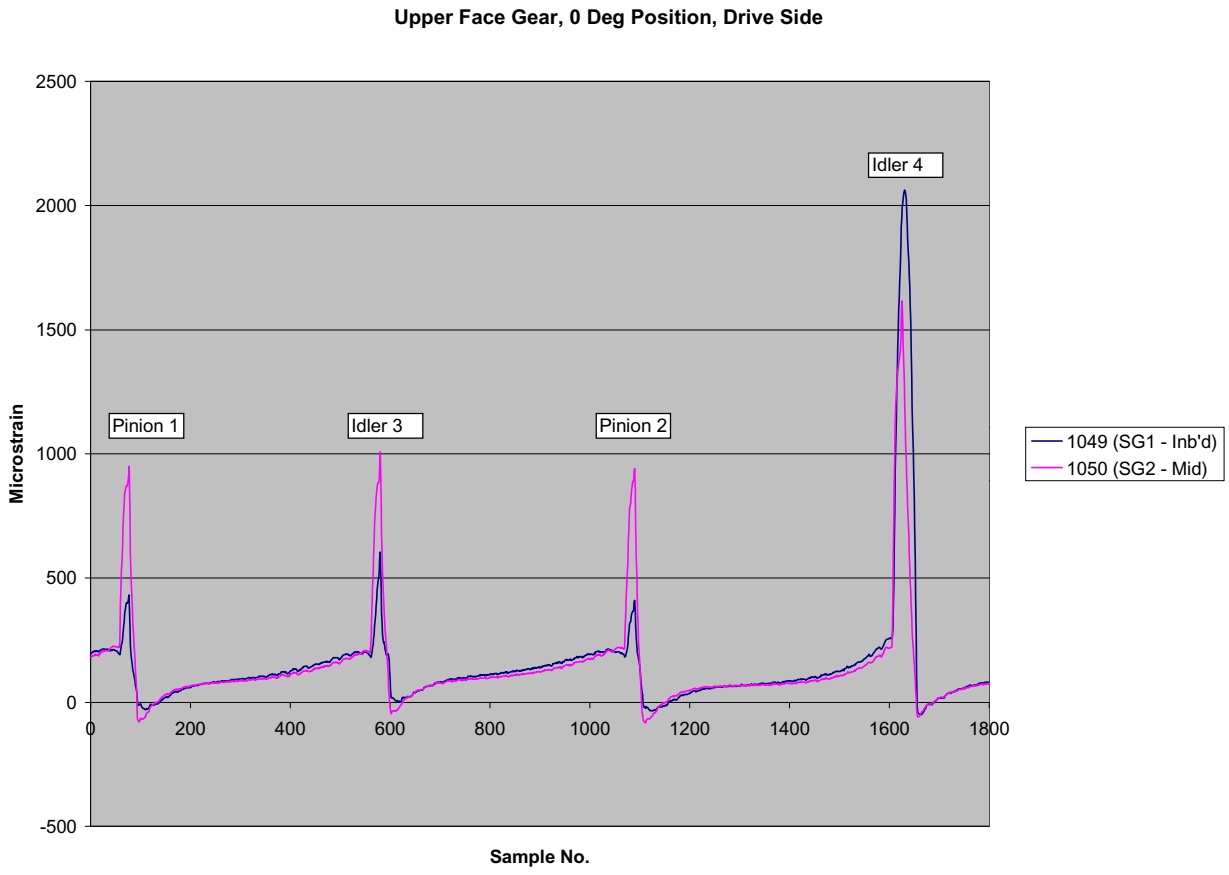

Figure 34. Upper face gear strain output from initial 2 and 2 test run.

It was hoped that the upper face gear strain gages would yield an indication of torque split. Figure 34 shows fairly even strain peaks for all gears except Idler 4 which greatly exceeds the other three gears. To assess whether this strain spike was more a function of the specific

idler or the housing bore at that location, Idlers 3 and 4 were swapped. The resulting upper face gear strains are shown in Figure 35 (Run No.7). The results are nearly identical confirming that any irregularity was a function of the housing bore at the Idler 4 location and not related to Idler 4.

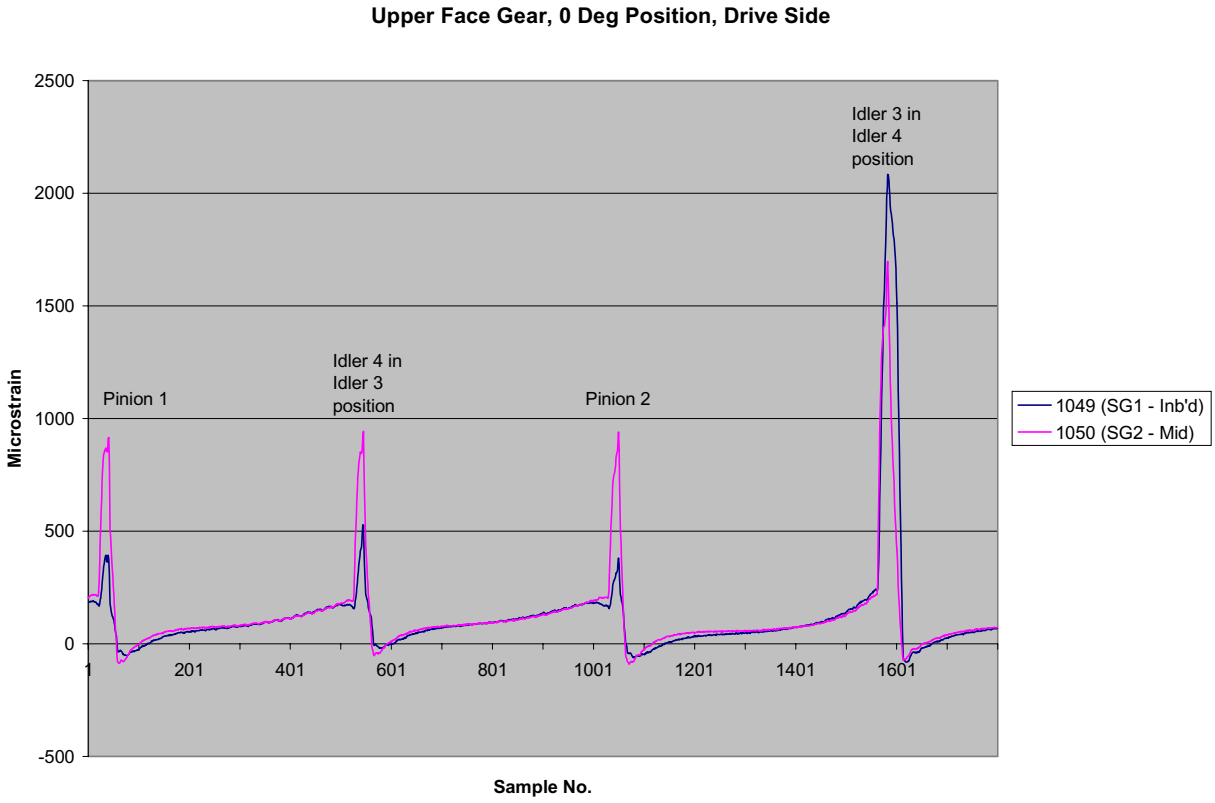

Figure 35. Upper face gear strain output from initial 2 and 2 test run with Idlers 3 and 4 swapped.

Some additional testing was conducted using only Pinion 1 and Idler 3. A decision was made to halt the testing and send the POC gearbox housing for inspection and possible rework of the idler bore. Inspection did reveal misalignment for both idler bores. Plugs were created for the idler bore locations and the bores were re-machined more accurately in accordance with drawing requirements. The re-worked housing was returned to the Structures Test lab and the POC gearbox reassembled. Though still showing high strain for the mesh with Idler 4, Figure 36 shows the upper face gear strain results (Run No.102) were altered due to the re-bore process. Results in Figure 36 indicate more of a separation in the strain plot characteristics between the pinions and idlers. Not only are the strain magnitudes higher for the idler meshes, but the distribution of strain across the upper face gear tooth face varies between the pinions and idlers. The mid strain gage for the pinion meshes registered much higher strain relative to the inboard strain gage. For the idler meshes, strain for both gages was relatively equal. The higher strain magnitude recorded for the idler meshes is likely an indication that the centroid of tooth loading was located more closely to the gage locations

(toe region), whereas, for the pinion meshes, the loading centroid was likely outboard of the gage locations. In order to try and shift the load at the Idler 4 mesh further towards the heel of the UFG tooth, the I4 backlash was decreased. Figure 37 shows the resulting UFG strain output. As I4 backlash decreased, there was no significant change in the UFG strain for the I4 mesh, however, UFG strain at the I3 mesh appeared to decrease slightly. Although it appears that decreasing I4 backlash did little to change the load distribution at the UFG/I4 mesh, it is likely that the reduced backlash caused Idler 4 to carry a greater percentage of lower face gear load, hence, the reduction in strain at the Idler 3 mesh.

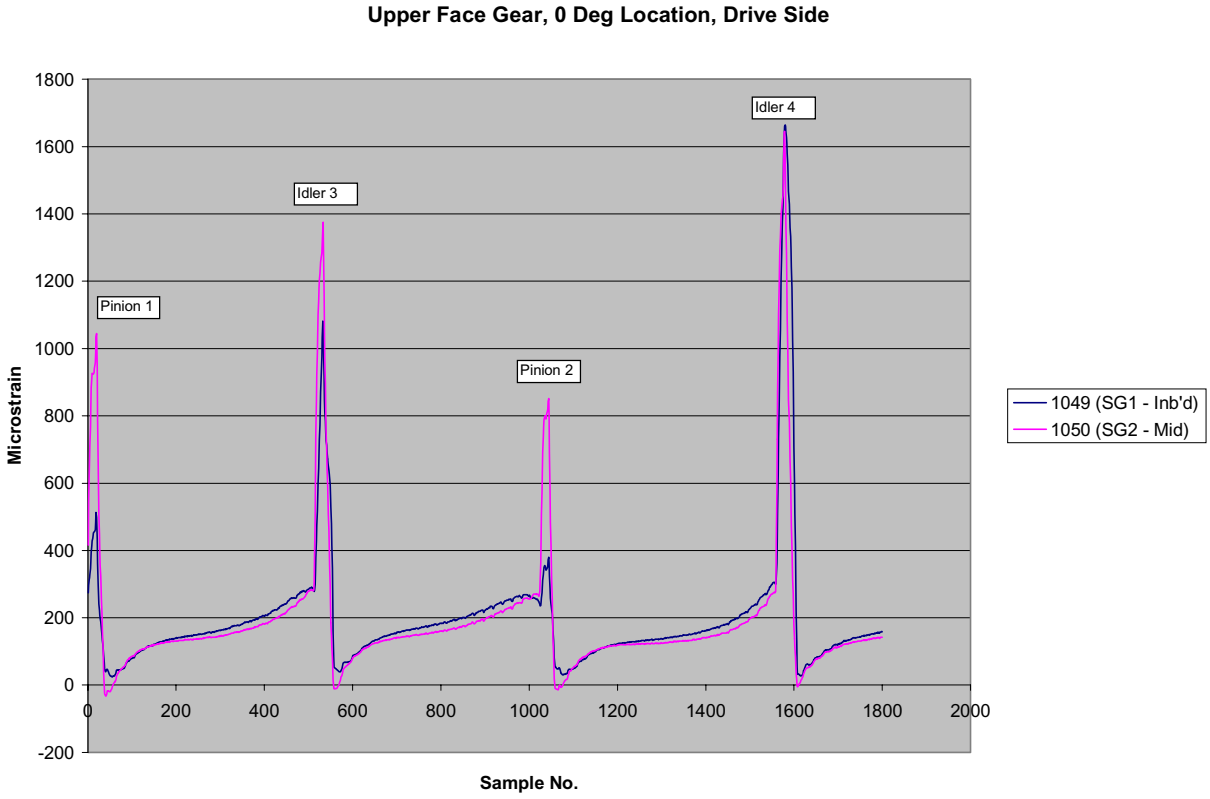

Figure 36. Upper face gear strain output from initial 2 and 2 test run after re-bore of the gearbox housing.

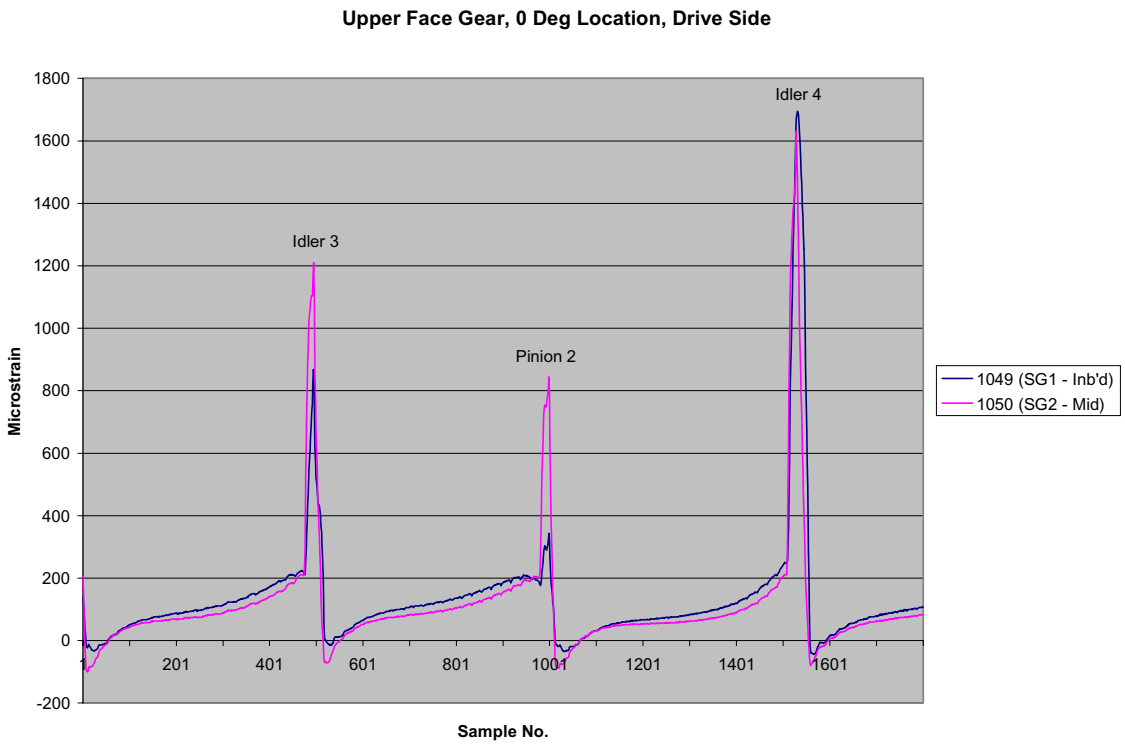

Figure 37. Upper face gear strain output from initial 2 and 2 test run after re-bore of the gearbox housing with reduced I4 backlash.

While understanding that the UFG tooth strain indications were affected both by the location of tooth loading and the magnitude of the tooth load, the relative magnitudes of inboard and middle gage strains for the idler meshes were similar, therefore, it was assumed that the UFG strain peaks for the idler meshes provided a reasonable estimate of the load share between the idlers. Because a decrease in I4 backlash had little noticeable effect on the UFG tooth strain distribution, it was reasoned that the UFG strains for the two idlers could be equalized by increasing Idler 4 backlash. This was done and it had the desired effect. Figure 38 shows the impact of increasing the Idler 4 backlash – a significant decrease in UFG strain at the I4 mesh and an increase in strain at the Idler 3 mesh. Although the mid gage registers a higher peak for the I3 mesh, the inboard gage registers a higher peak for the I4 mesh. The average of the inboard and mid gage peaks is about the same for both meshes.

The conclusion from this exercise was that backlash adjustments could be used to affect the distribution of load between idlers. Idler backlash adjustments seemed to do little to change the distribution of loading on a given tooth. Instead, these changes affected the magnitude of strain. It is believed that this change in strain magnitude corresponded to a change in transmitted load and that the relative load carried by each idler was related to the amount of backlash at the idler mesh.

The load distribution on a tooth for a given mesh is dependent on the alignment between the idlers/pinions and face gears. Alignment is controlled by the housing and underscores the importance of accurately machined bores.

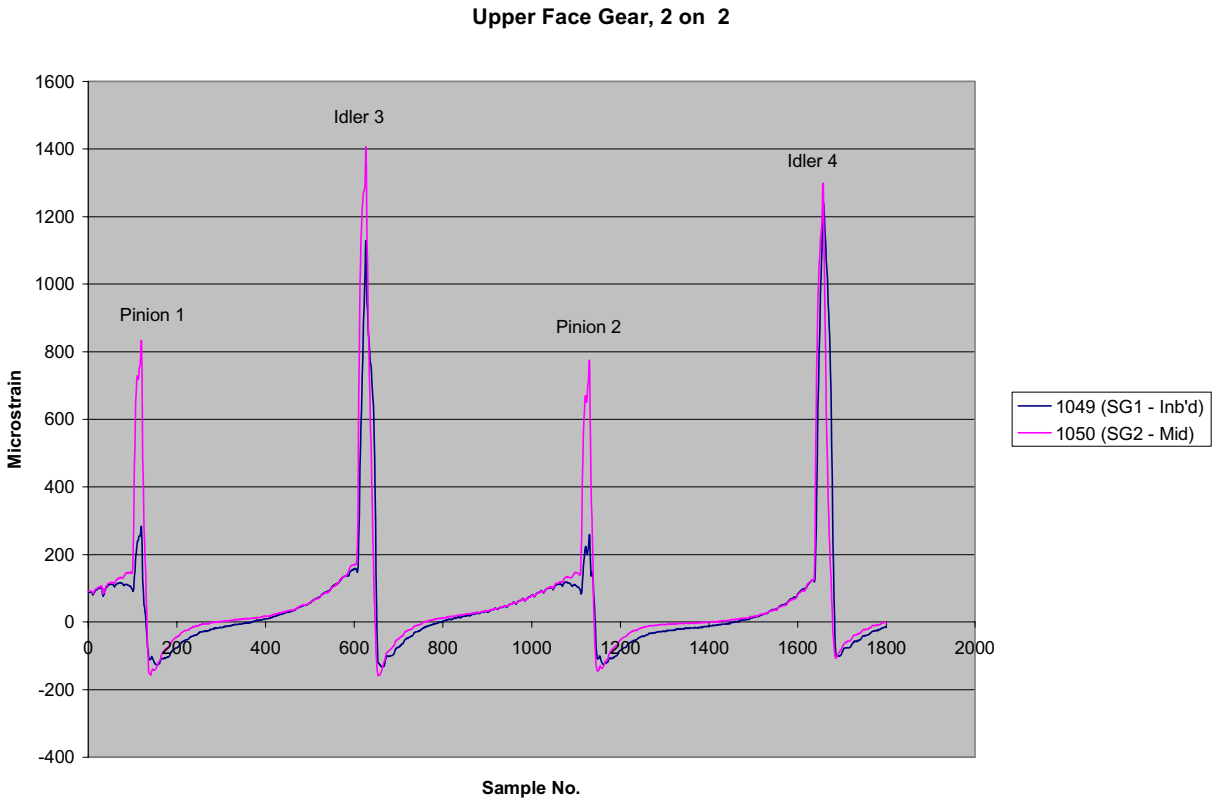

Figure 38. Upper face gear strain output from 2 and 2 test run after re-bore of the housing and with increased Idler 4 backlash.

VII. FORMAL TESTING

As described in the previous section, the two pinion-two idler configuration was tested after the idler re-bore operation. A final gear mounting configuration was arrived at and three slow roll tests – POC Test Runs 140-142 - conducted for that configuration. Table 2 is a summary of all the POC slow roll testing completed after the re-bore operation. Only test runs that satisfied the formal test requirements using the final gearbox setup configuration are shown. Note that there was a requirement in para. 6.1.b of [12] to conduct test runs with a one pinion-two idler configuration. These runs were not conducted due to a reduction in scope required to conclude the testing within budget and schedule constraints. Also, slow roll tests were conducted using rotation in the normal direction, only. The reversed direction runs specified in paragraphs 6.1.a-6.1.c of [12] were not conducted as they were not considered essential.

The test runs were generally conducted in groups of three to insure that consistent runs were being achieved. Comparisons of repeat data show that the data recorded for a given gearbox configuration is very consistent. Figure 39 shows a comparison of repeat runs 140-142 for Pinion 1 Gage No. 1002.

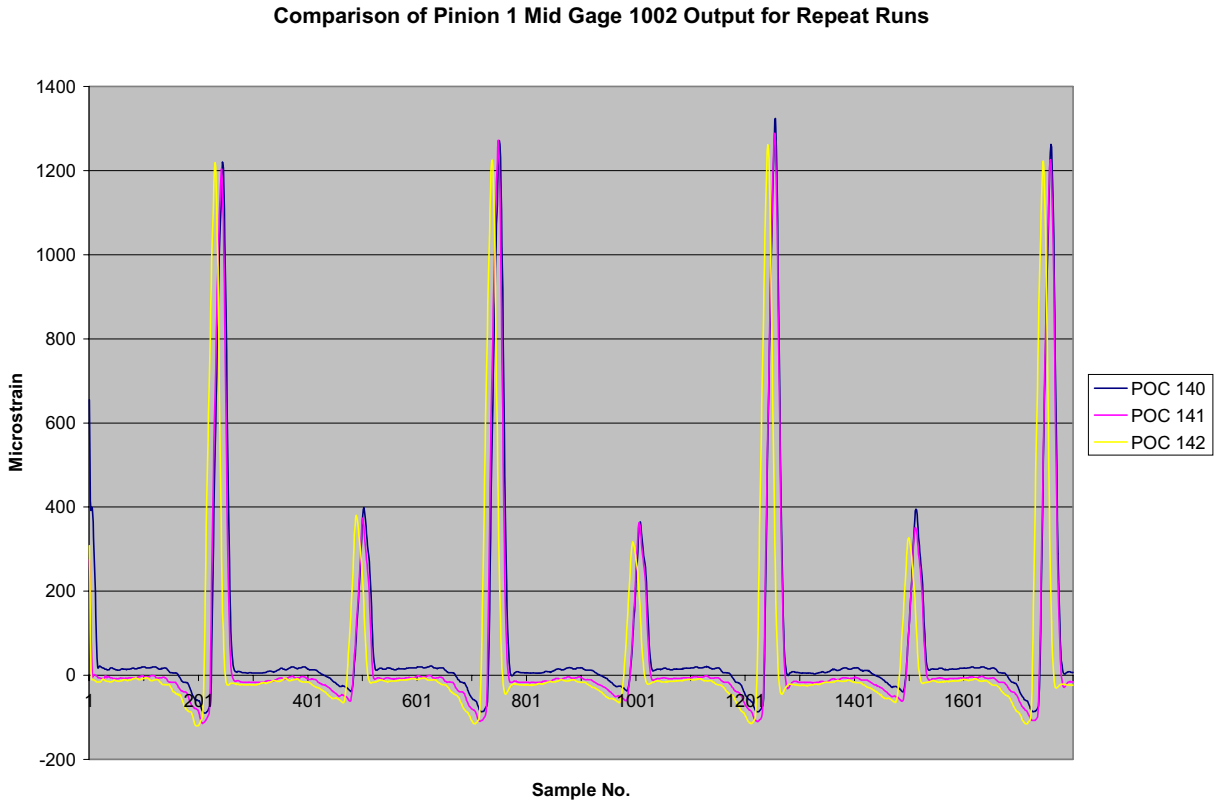

Figure 39. Comparison of repeat runs for Pinion 1 drive side mid gage, No. 1002.

Table 2. POC gearbox test identification table.

Test Description	Test I.D.	Gear Components Included In Test					
		Idler 4	Idler 3	Pinion 2	Pinion 1	UFG	LFG
2 Pinion, 2 Idler Tests	POC 140 POC 141 POC 142	Yes	Yes	Yes	Yes	Yes	Yes
1 Pinion, 1 Idler Tests	POC 210 POC 211 POC 212	Yes	No	No	Yes	Yes	Yes
	POC 300 POC 301 POC 302	No	Yes	Yes	No	Yes	Yes
Single Idler Torque Calibration (idler operates as a pinion)	POC 400 POC 401 POC 402	Yes	No	No	No	Yes	No
	POC 500 POC 501 POC 502	No	Yes	No	No	Yes	No

Test results and trends are discussed below by component.

1. Pinions

i. Pinion 1

Figures 40 and 41 show strain plots from Run No. 141 (2 and 2) for Pinion 1 tooth drive side gages. Figure 40 is for the tooth location that is initially in mesh with the upper face gear, while Figure 41 is for the tooth location that is diametrically opposed (initially in mesh with the lower face gear). The two plots are similar, as they should be. It is apparent that the pinion loading is biased toward the heel for the upper face gear mesh, and toward the toe for the lower face gear mesh. This would be expected based on the offset of the POC face gears – see Figure 27. The major difference between the two plots is the magnitude of the peak output for the heel strain gage – nos. 1003 and 1009. Based on strain gage calibration data, the slope of gage output versus load for Gage 1003 is 1.24 times that for Gage 1009. This appears to explain the fact that the peak strain for Gage 1003 is roughly 26% greater than that for Gage 1009.

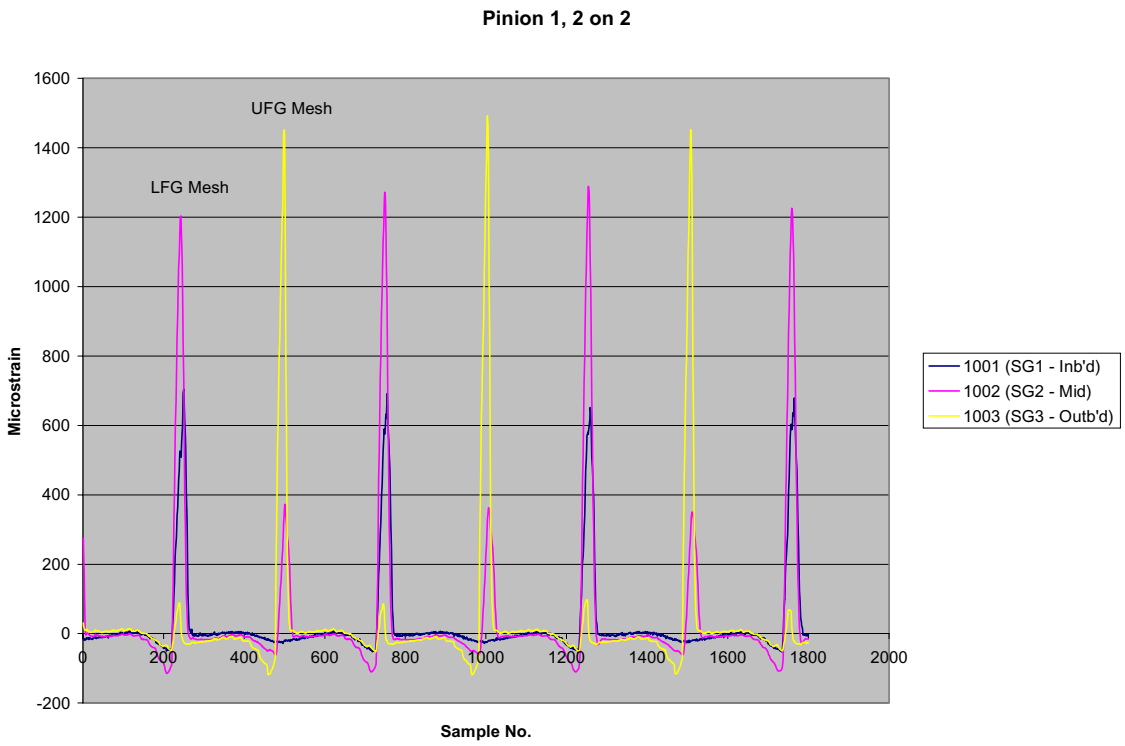

Figure 40. Strain output for Pinion 1, UFG location, Run No. 141.

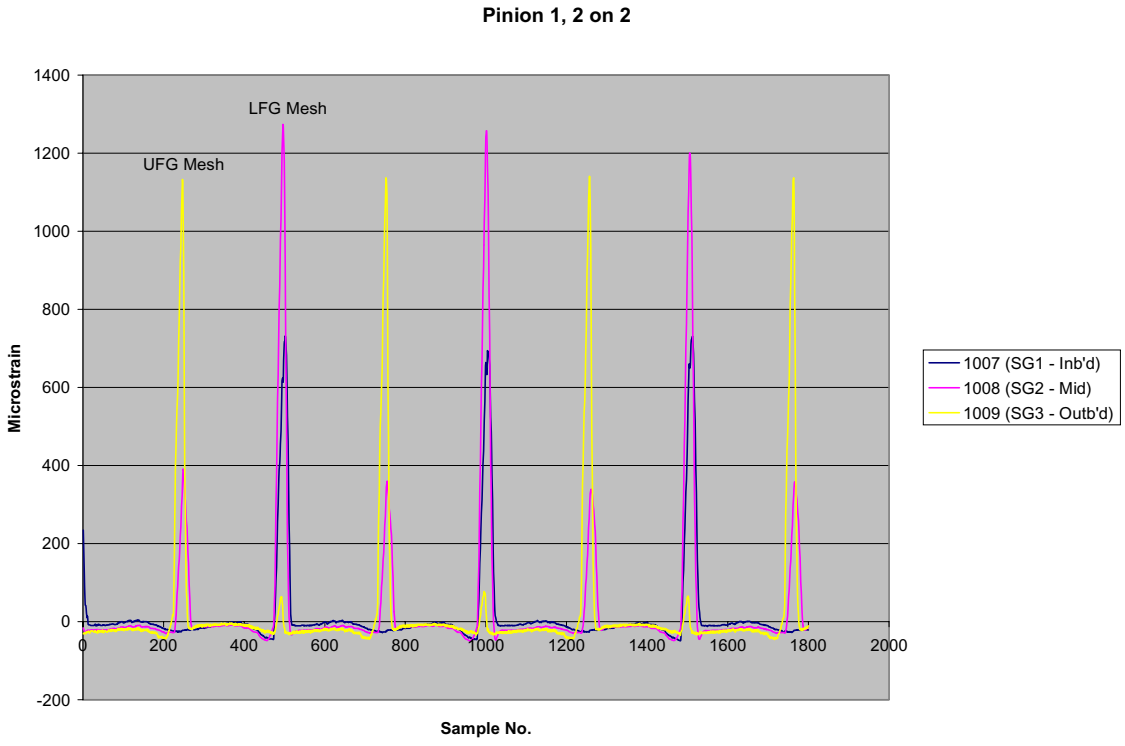

Figure 41. Strain output for Pinion 1, LFG location, Run No. 141.

Figures 42 and 43 show Pinion 1 tooth drive side gage strain data for the one pinion-one idler configuration test – Run No. 211 (Table 2). While there appears to be a very slight increase in peak strain for the UFG mesh and decrease in strain for the LFG mesh in going from 2 and 2 results to 1 and 1 results, this cannot be construed as a reliable indication of a change in torque split. There also appears to be an inboard shift in load for both meshes for both gage locations in going from 2 and 2 to 1 and 1. The reasons for the change in load distribution in going from 2 and 2 to 1 and 1 are not known, however, it may be related to deflections in the overall face gear "ring" due to a significantly different set of loads between the two test configurations.

ii. Pinion 2

Figures 44 and 45 show strain plots from Run No. 141 for Pinion 2 tooth drive side gages for the two pinion-two idler configuration. The results are similar to those shown in Figures 40 and 41 for Pinion 1 as expected. The subtle differences are likely due to a combination of slight differences in the housing pinion bores and the various gage locations. Figures 46 and 47 present strain plots from Run No. 301 for Pinion 2 drive side gages for the one pinion-one idler test configuration. In going from 2 and 2 data to 1 and 1 data, there is a very marked inboard shift in the tooth load. This is further illustrated in the load distribution plots of Figures 48-51 (Figures 48 and 49 are for the 2 and 2 configuration, Figures 50 and 51 are for the 1 and 1 configuration). The reason for this phenomenon is not known but may be partially due to the reasons proposed above for Pinion 1.

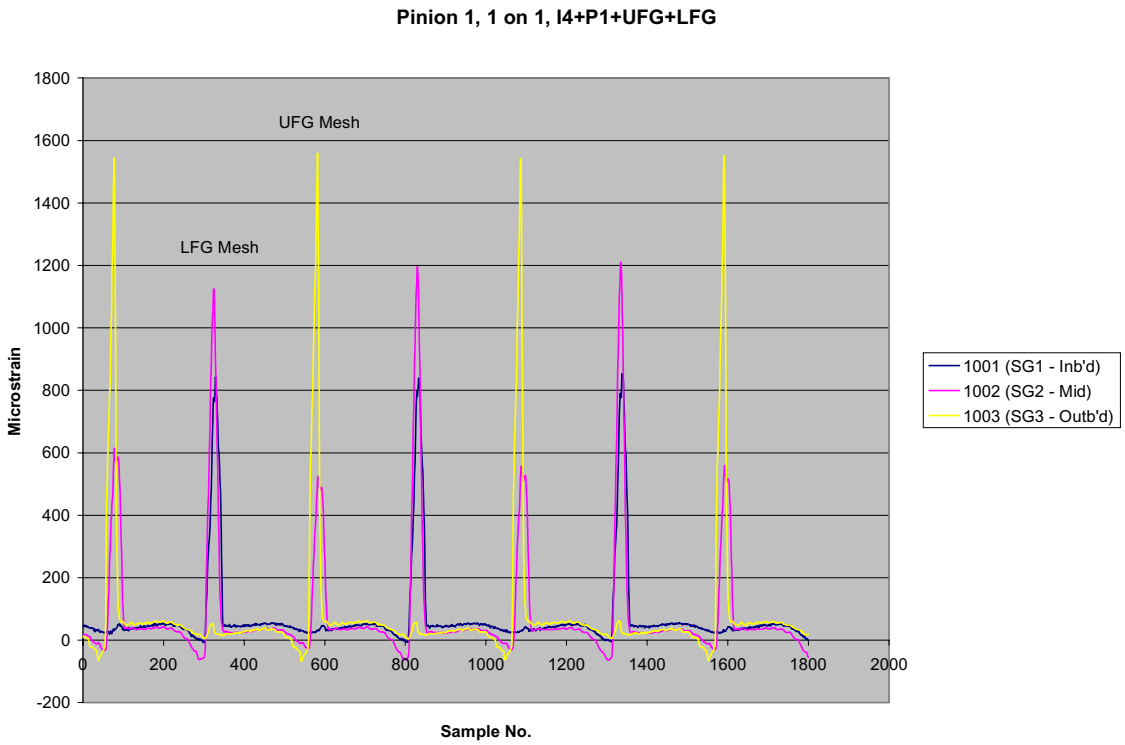

Figure 42. Strain output for Pinion 1, UFG location, Run No. 211.

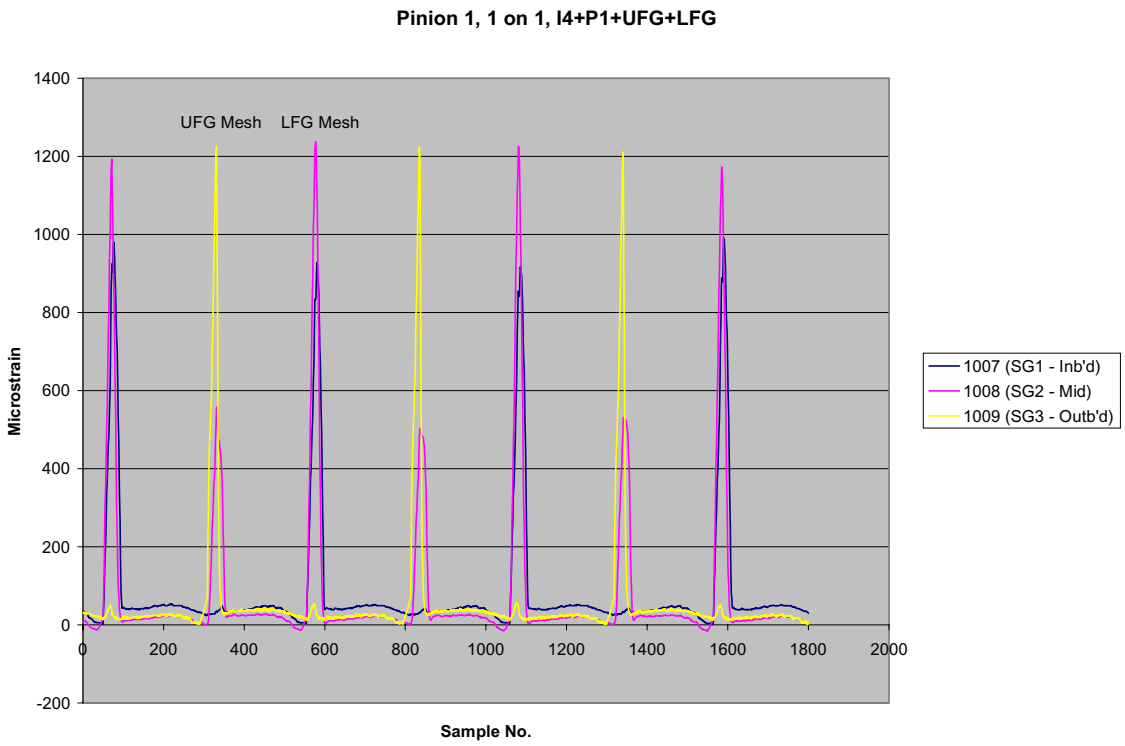

Figure 43. Strain output for Pinion 1, LFG location, Run No. 211.

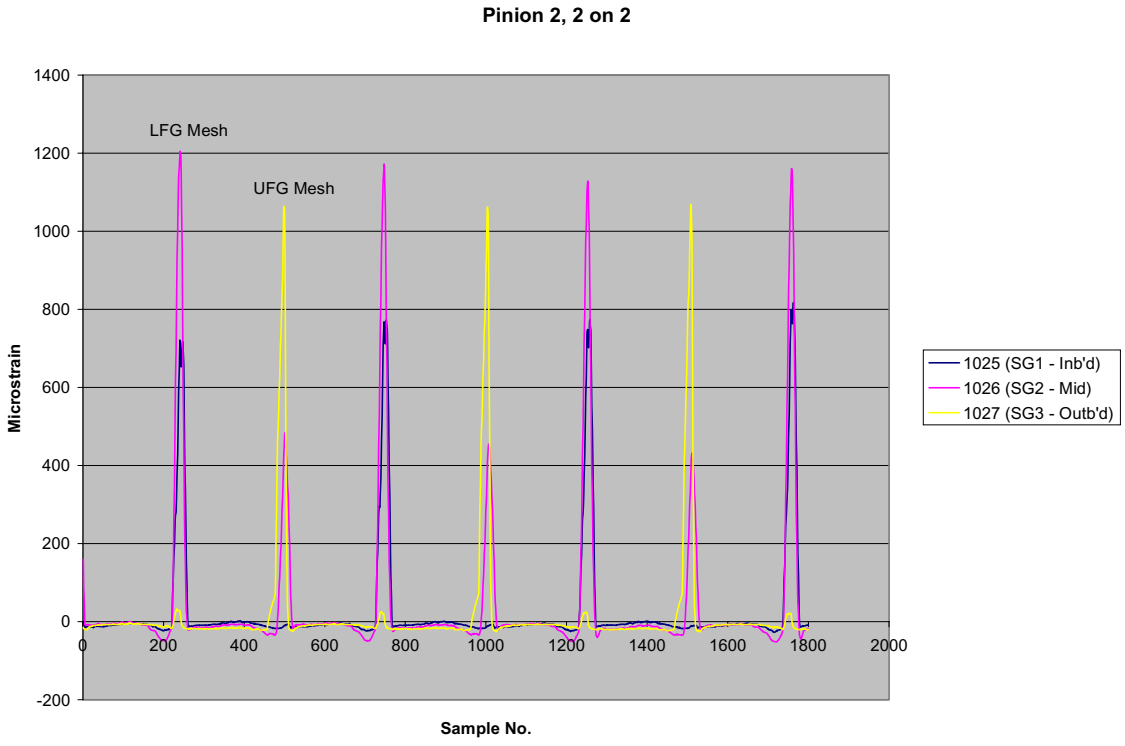

Figure 44. Strain output for Pinion 2, UFG location, Run No. 141.

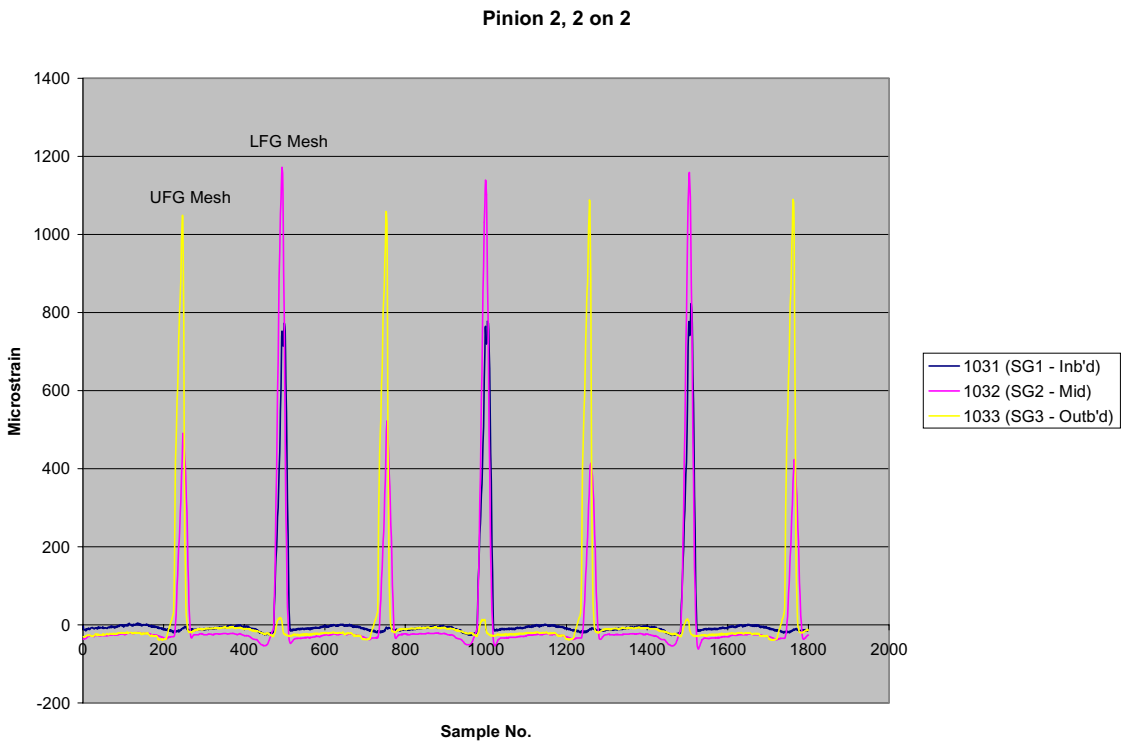

Figure 45. Strain output for Pinion 2, LFG location, Run No. 141.

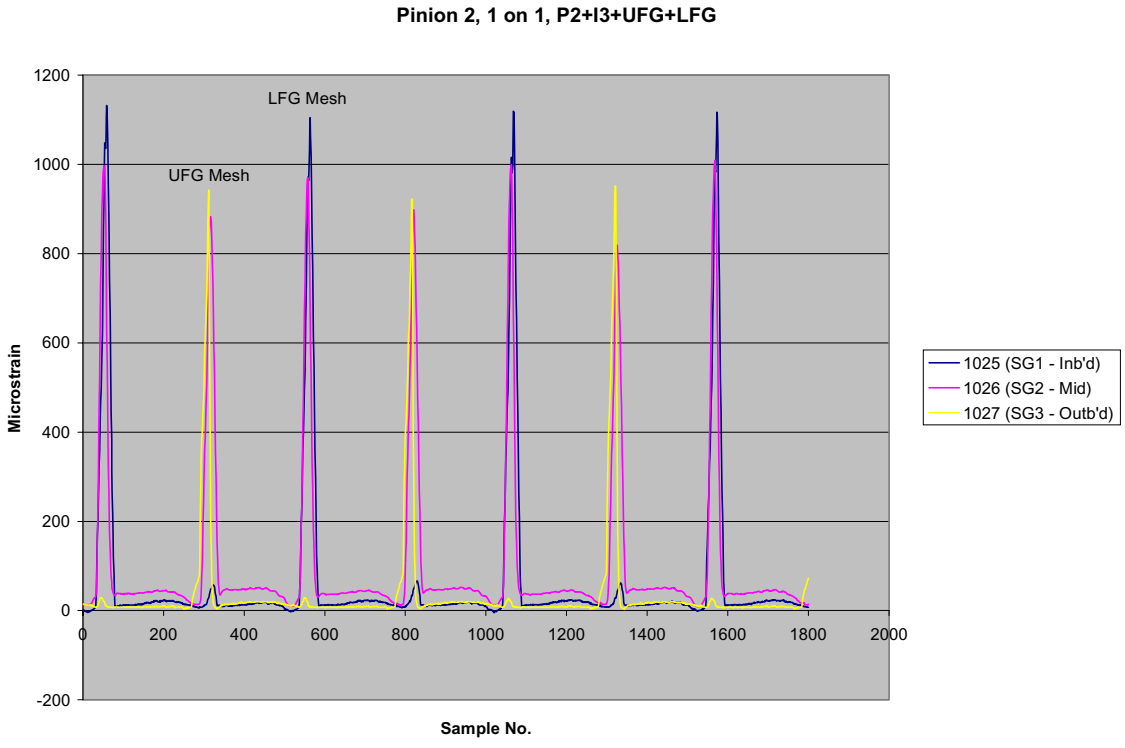

Figure 46. Strain output for Pinion 2, UFG location, Run No. 301.

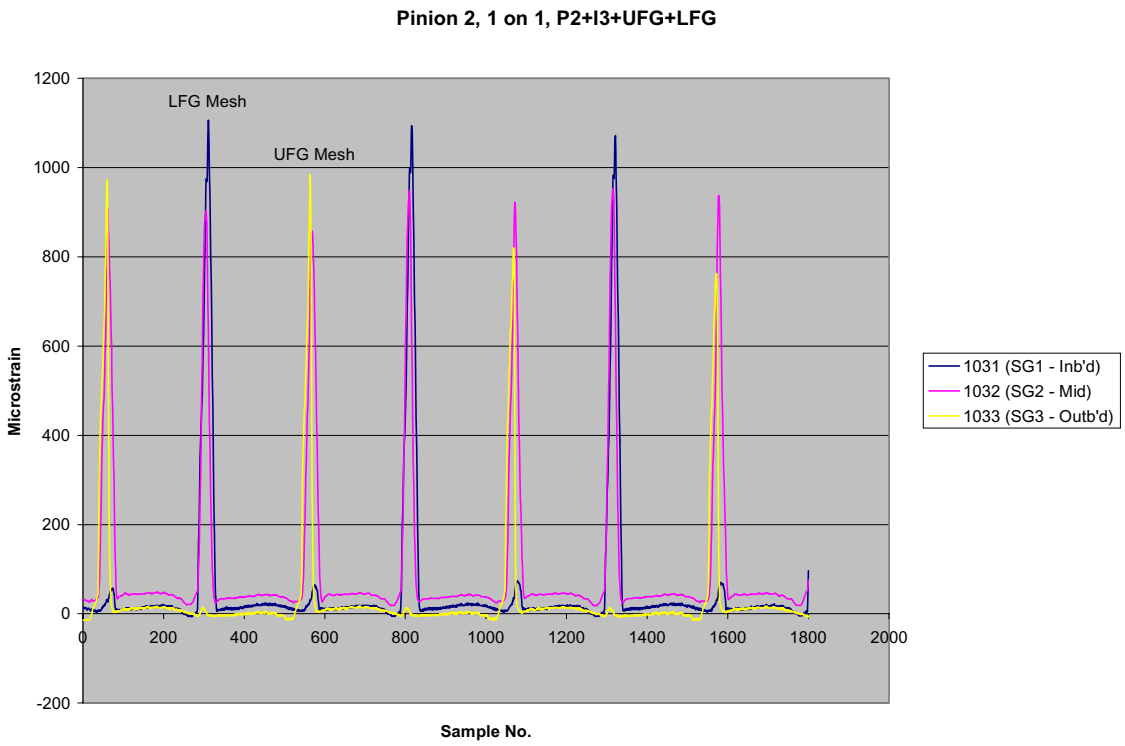

Figure 47. Strain output for Pinion 2, LFG location, Run No. 301.

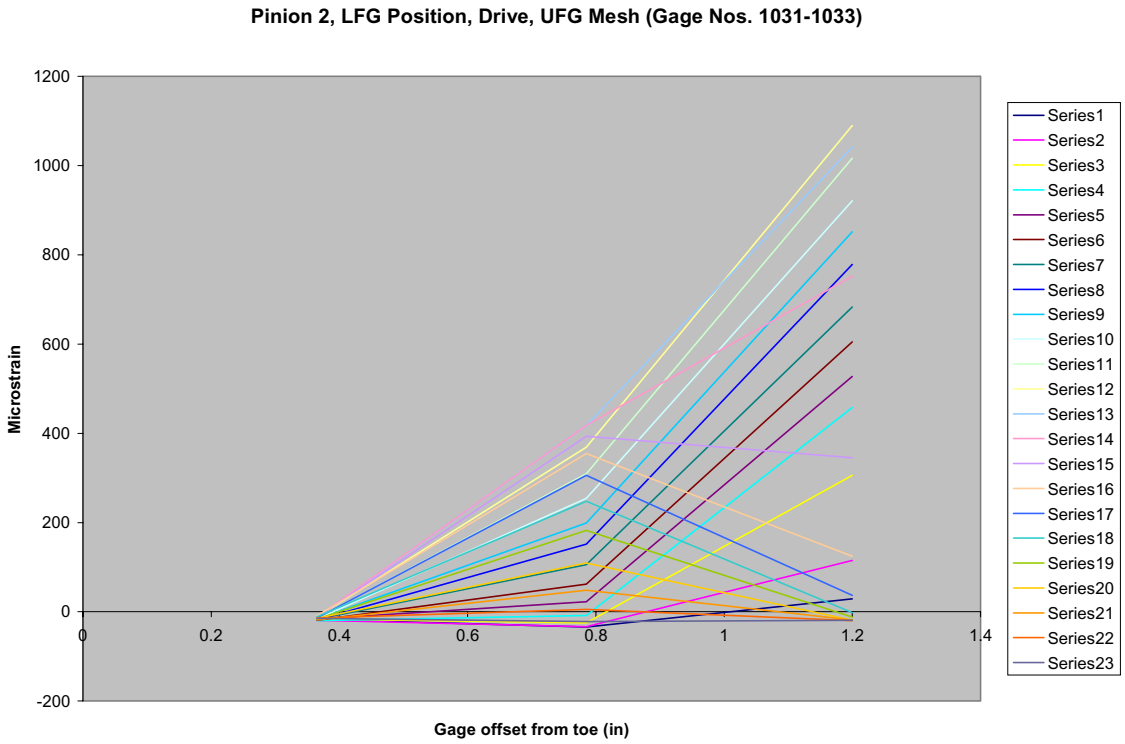

Figure 48. Load distribution plot for P2, LFG location, Run No.141 (2+2), UFG Mesh.

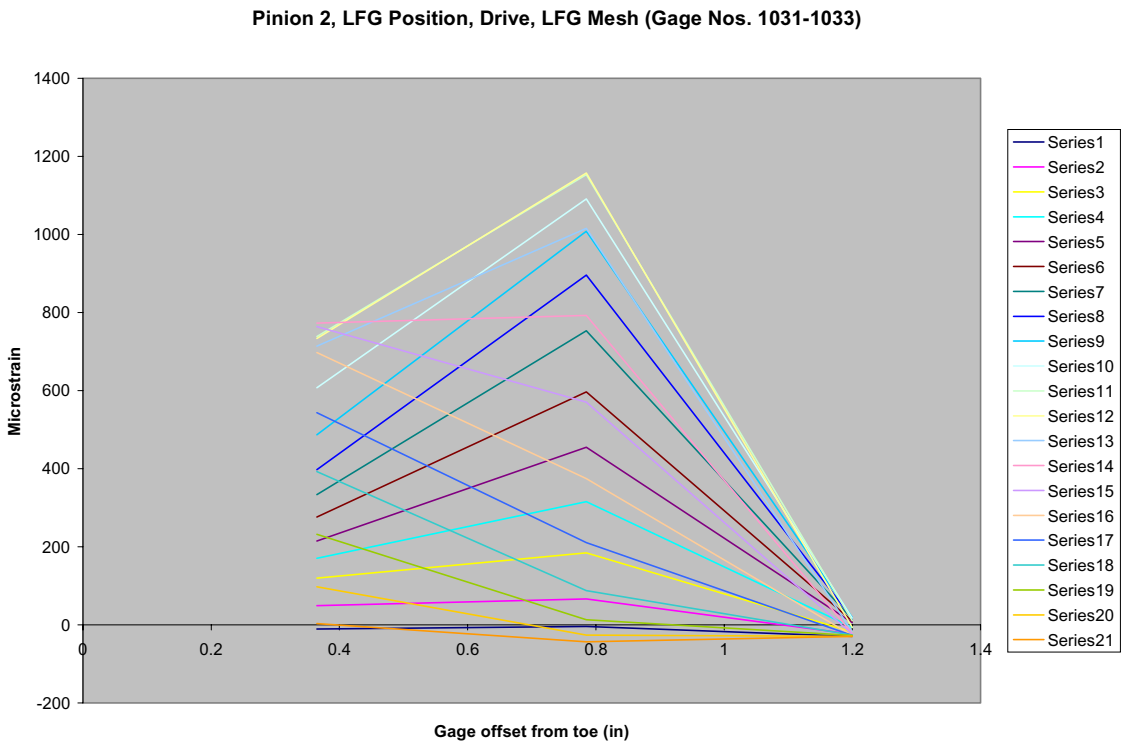

Figure 49. Load distribution plot for P2, LFG location, Run No.141 (2+2), LFG Mesh.

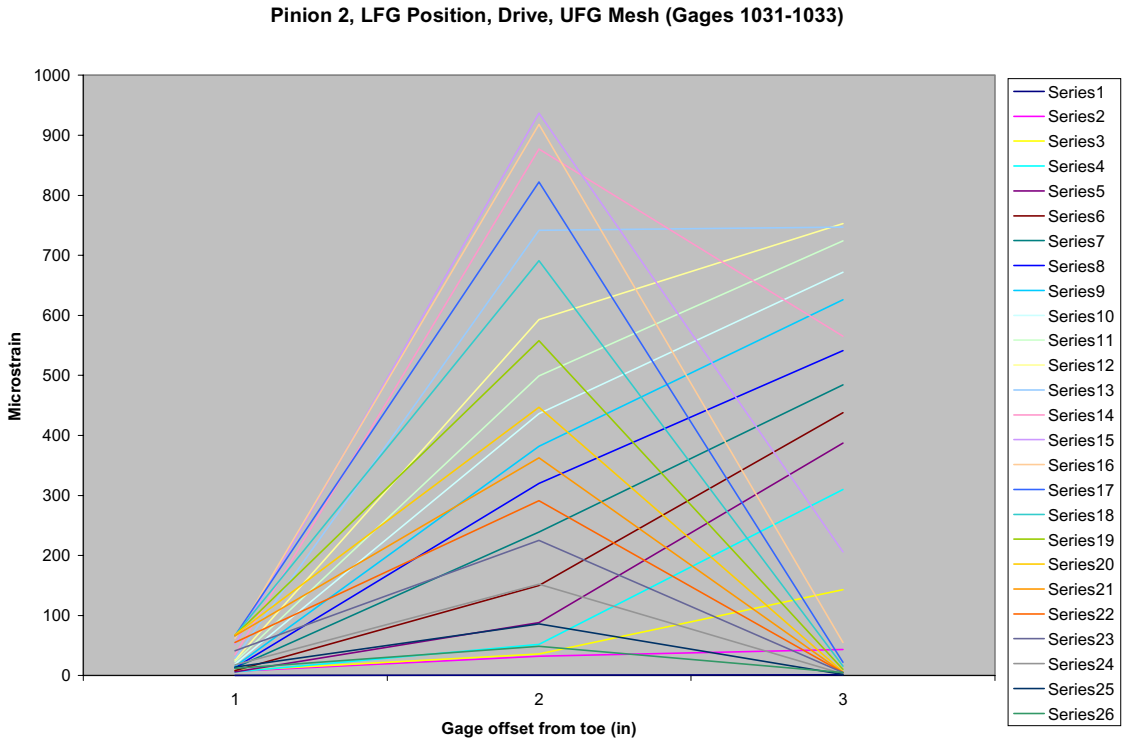

Figure 50. Load distribution plot for P2, LFG location, Run No.301 (1+1), UFG Mesh.

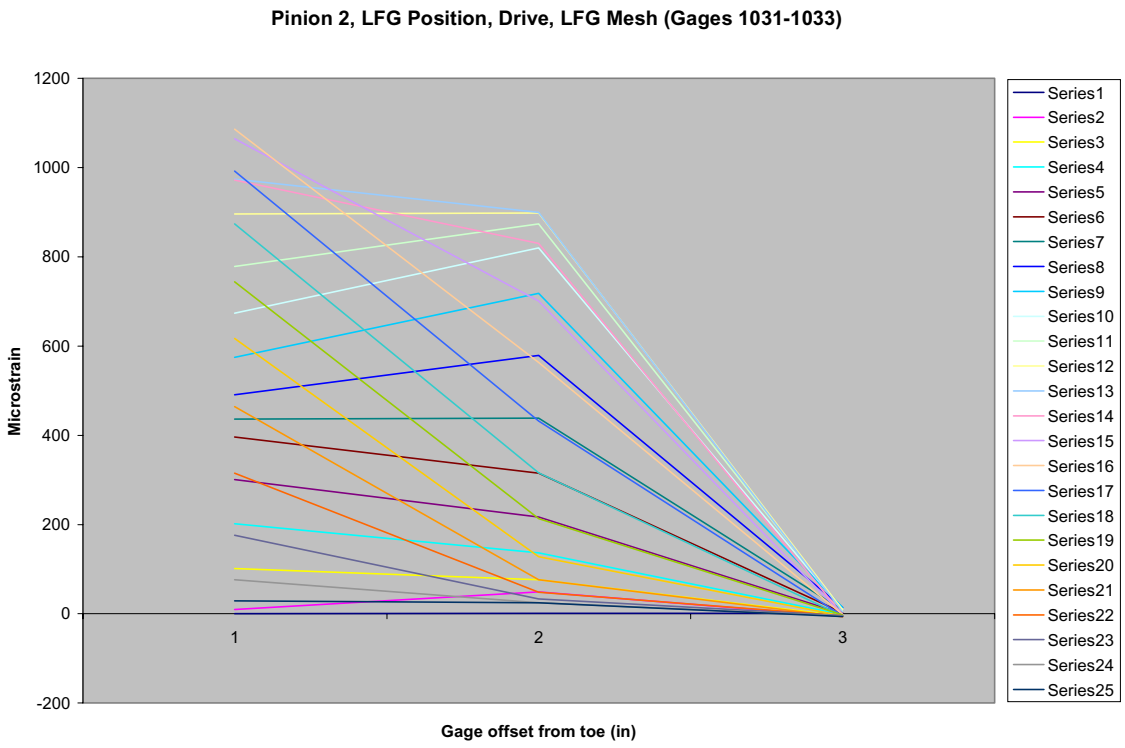

Figure 51. Load distribution plot for P2, LFG location, Run No.301 (1+1), LFG Mesh.

2. Idlers

i. Idler 3

Strain plots for Idler 3 for the 2 and 2 configuration (Run No. 141) are presented in Figures 52 and 53. Note the significant difference as compared to the pinion strain plots in Figures 40 and 41. The pinion is the driving member at both face gear meshes splitting the input torque between the upper and lower face gears. The purpose of the idlers is to transmit torque from the lower face gear to the upper face gear, therefore, the idler is the driven member at the LFG mesh, and the driving member at the UFG mesh. The strain trace for the UFG mesh of Idler 3 shown in Figure 52 is very similar to that measured for the pinion in Figures 40 and 41. That is to be expected because the pinion and idler are designed to transmit the same amount of torque to the upper face gear. The same idler gages that are in tension while driving the upper face gear are in compression when the tooth they are on is being driven by the lower face gear. This is illustrated in Figure 52. The same trend is apparent in Figure 53 although the gages are located such that they experience compression at the UFG mesh and tension at the LFG mesh. Note that Figure 53 is almost a mirror image of Figure 52 about the zero strain line with the exception that compressive stresses are slightly higher than the corresponding tensile stresses for a given mesh. This is due to the fact that compressive strain due to the radial component of tooth load is additive to bending strain produced by the tangential component of tooth load on the coast side of the tooth and subtractive on the drive side of the tooth.

Also notable in Figures 52 and 53 is the fact that while predominantly loading the central portion of the idler tooth, the lower face gear mesh produces negligible strain at the toe gage. This contrasts with the pinion results (Figures 40 and 41). The Idler 3 strain distribution plot for the lower face gear mesh is presented in Figure 54. This shows a predominantly centered loading on the idler tooth. Compare this to Figure 49, which shows a significant shift in load toward the toe during the latter part of the roll through the LFG mesh for the pinion. Based on the position of the lower face gear relative to the idler (Figure 27), and results shown in Figures 52-54, it appears that load remains biased toward the heel of the lower face gear throughout its mesh with the idler.

Strain plots for Idler 3 for the 1 and 1 gearbox assembly configuration (Run No. 301) are shown in Figures 55 and 56. As with the pinions, strains are similar to those for the 2 and 2 configuration except for a slight inboard shift in tooth load which can be detected in going from the 2 and 2 to the 1 and 1 configuration.

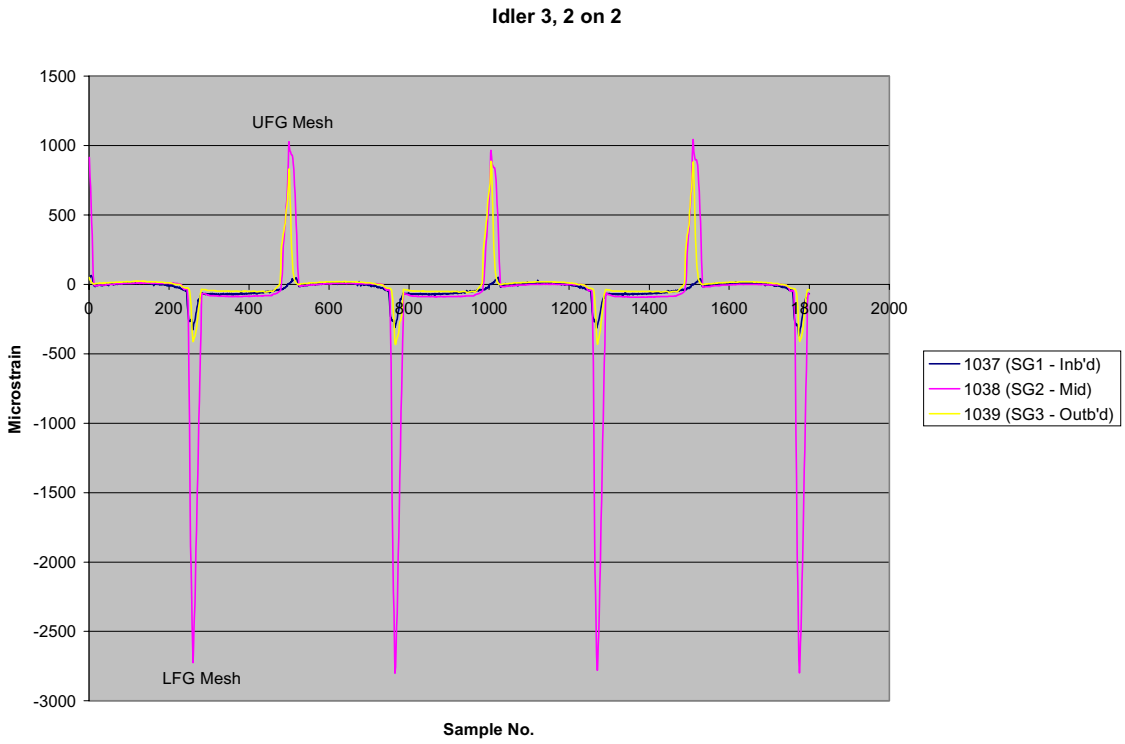

Figure 52. Strain output for Idler 3, UFG location, Run No. 141.

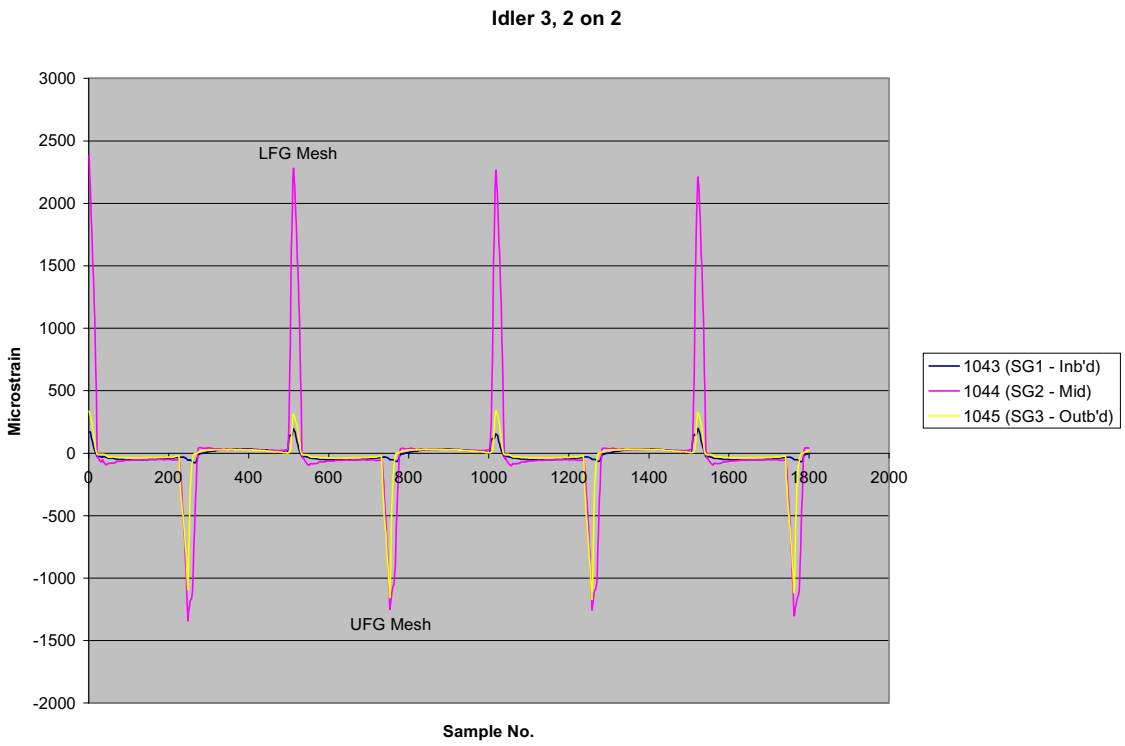

Figure 53. Strain output for Idler 3, LFG location, Run No. 141.

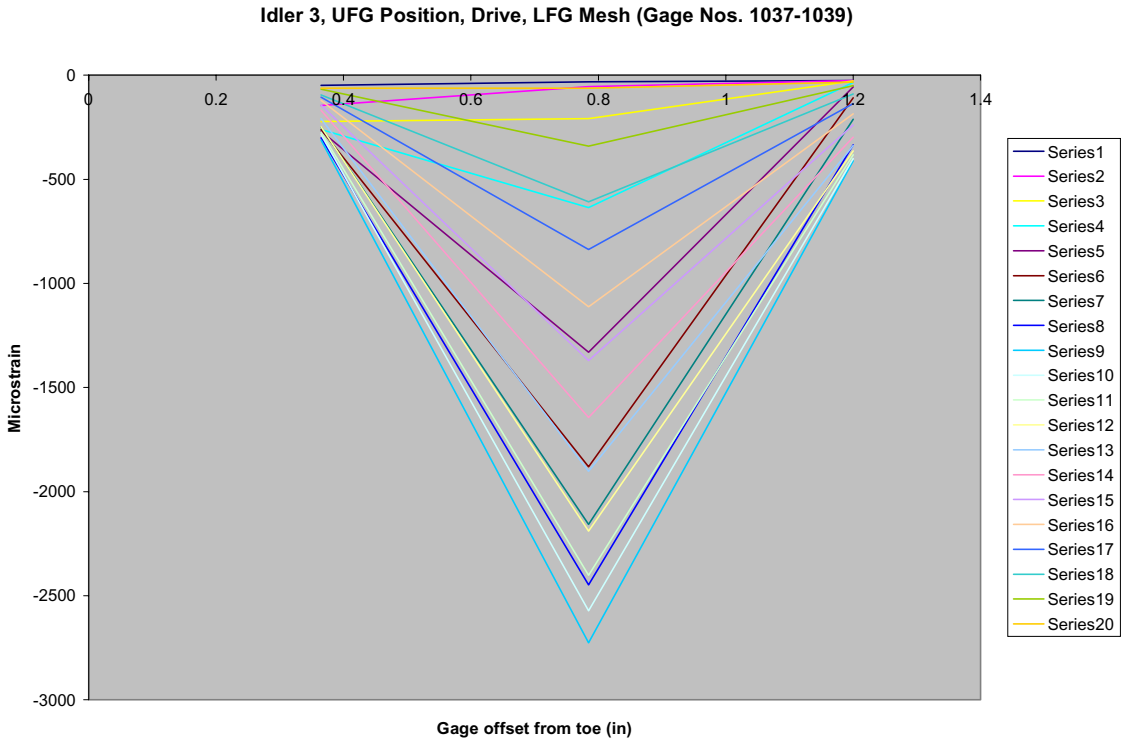

Figure 54. Strain distribution plot for I3, UFG location, Run No. 141 (2+2), LFG mesh.

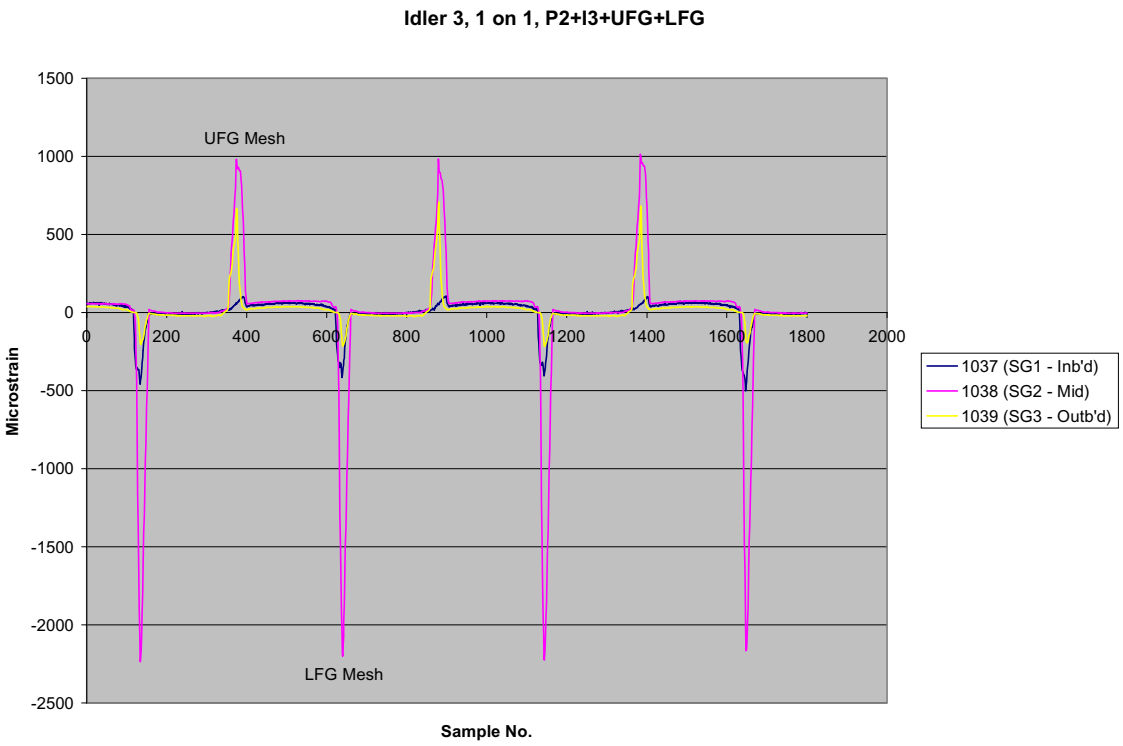

Figure 55. Strain output for Idler 3, UFG location, Run No. 301.

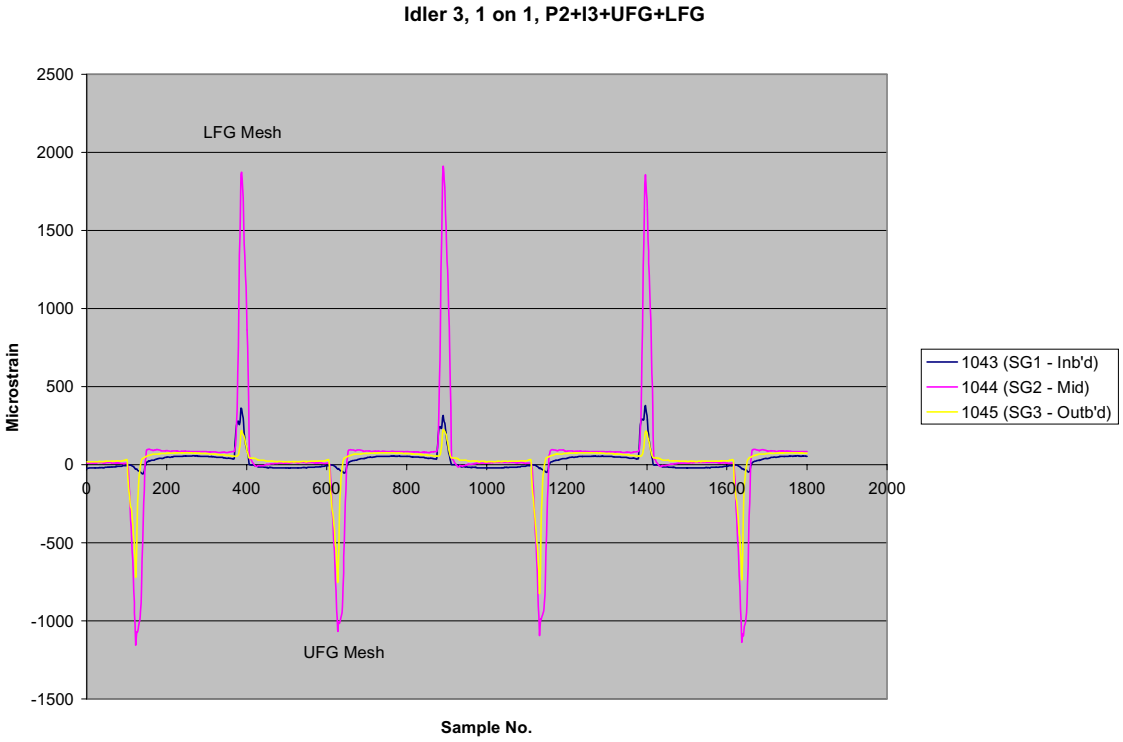

Figure 56. Strain output for Idler 3, LFG location, Run No. 301.

ii. Idler 4

Strain plots for Idler 4 for the 2 and 2 configuration (Run No. 141) are presented in Figures 57 and 58. When comparing Idler 4 strain traces with those for Idler 3, there are some notable differences. The Idler 4 lower face gear mesh shows significant strain at the inboard gage. This is similar to the strain patterns exhibited by the pinions for the lower face gear mesh, but much different from the Idler 3 strain patterns which show very little strain at the inboard gage.

For the upper face gear mesh, Idler 4 shows very little strain for the outboard gage, whereas, Idler 3 shows very significant strain for this gage. The indication is that the upper face gear tooth is loaded fairly evenly across its width for the Idler 3 mesh, but for the Idler 4 mesh, the loading appears to be heavily biased toward the toe. This is in contrast to the pinions for which the outboard strain is predominant for the upper face gear mesh. The upper face gear tooth patterns shown in Figures 59-61 support this finding. Note the dark area of heaviest wear in Figure 59, Pinion 1 mesh, is at the heel end of the tooth. In Figure 60, Idler 3 mesh, the area of heaviest wear appears to be more centralized although towards the heel end. In Figure 61, Idler 4 mesh, the heaviest wear appears to be at the toe end.

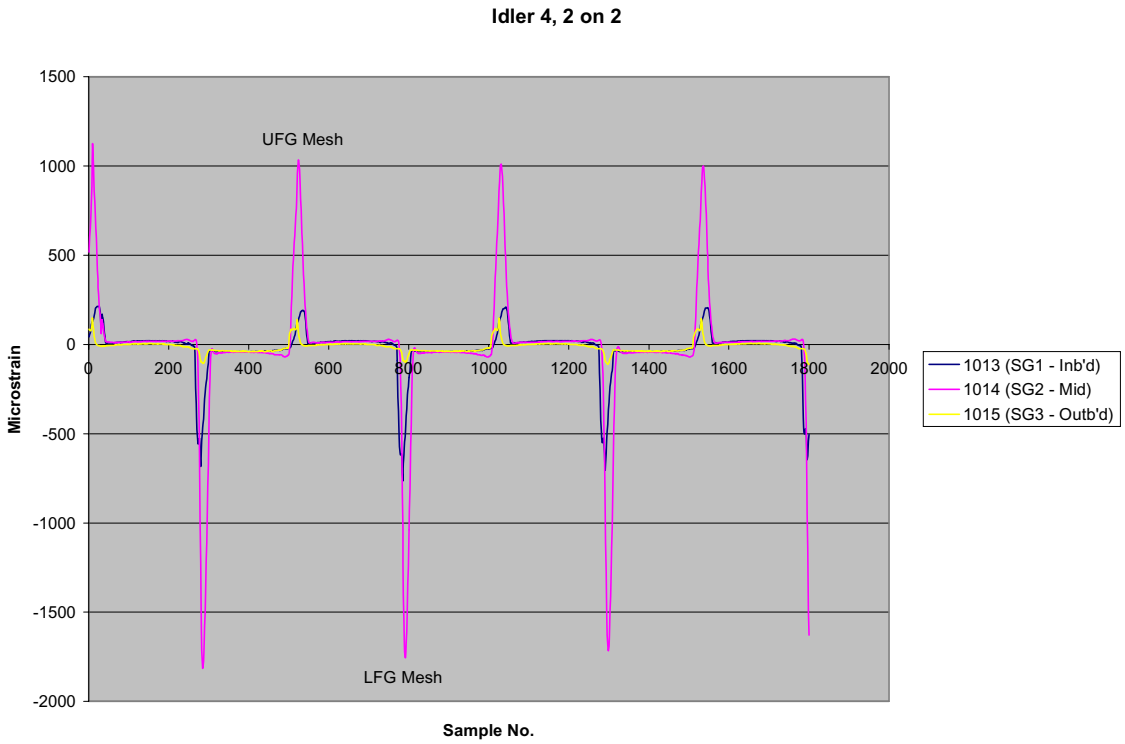

Figure 57. Strain output for Idler 4, UFG location, Run No. 141.

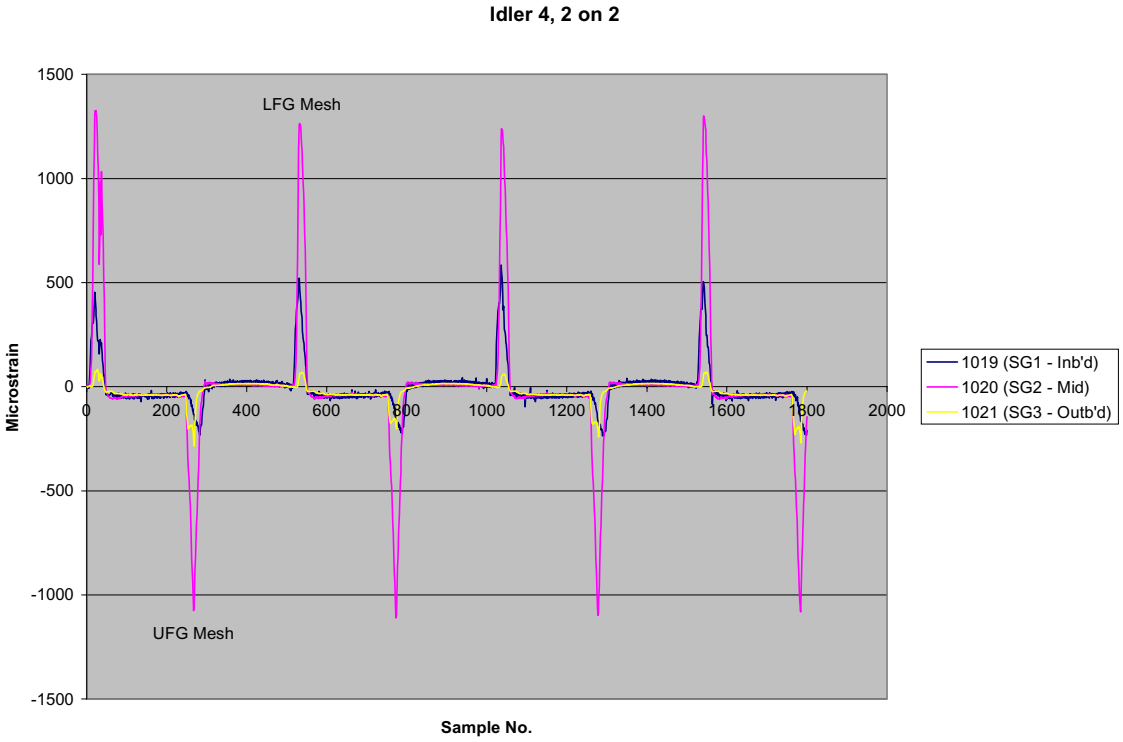

Figure 58. Strain output for Idler 4, LFG location, Run No. 141.

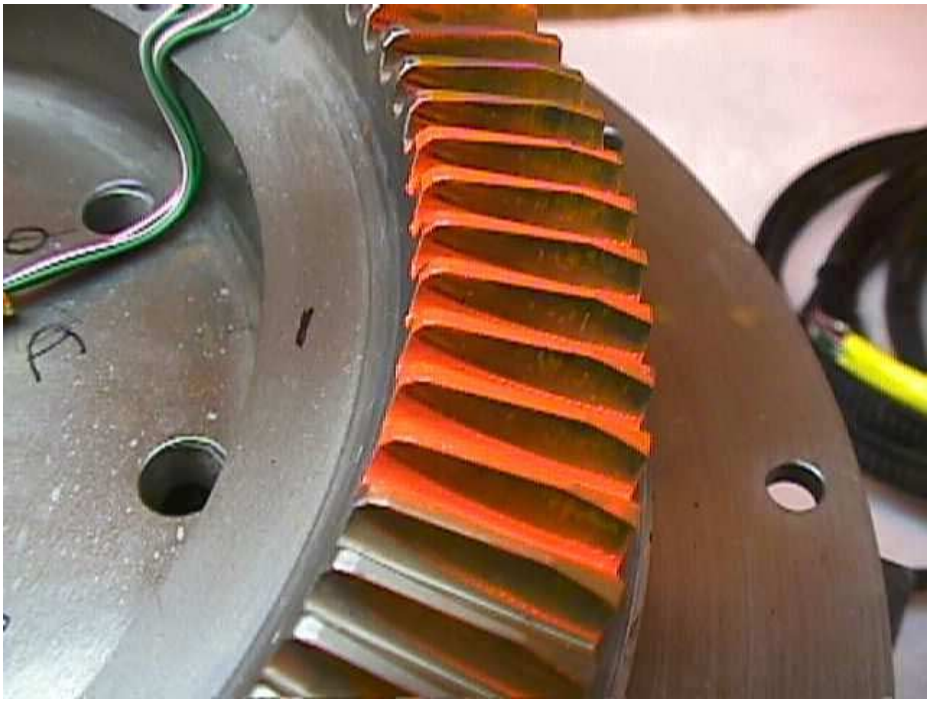

Figure 59. Upper face gear tooth patterns for Pinion 1 mesh.

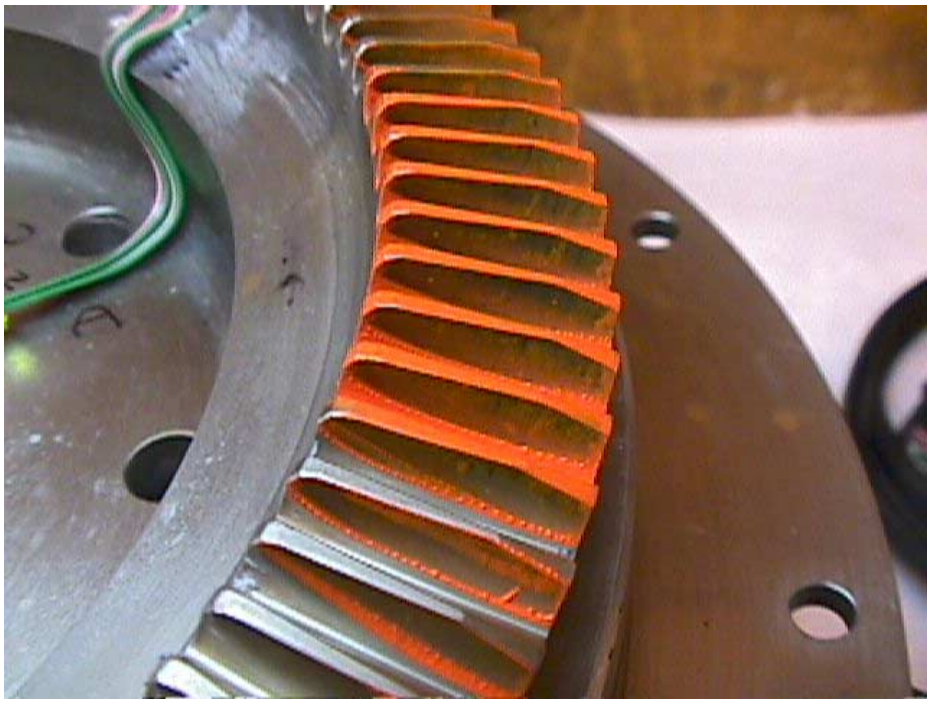

Figure 60. Upper face gear tooth patterns for Idler 3 mesh.

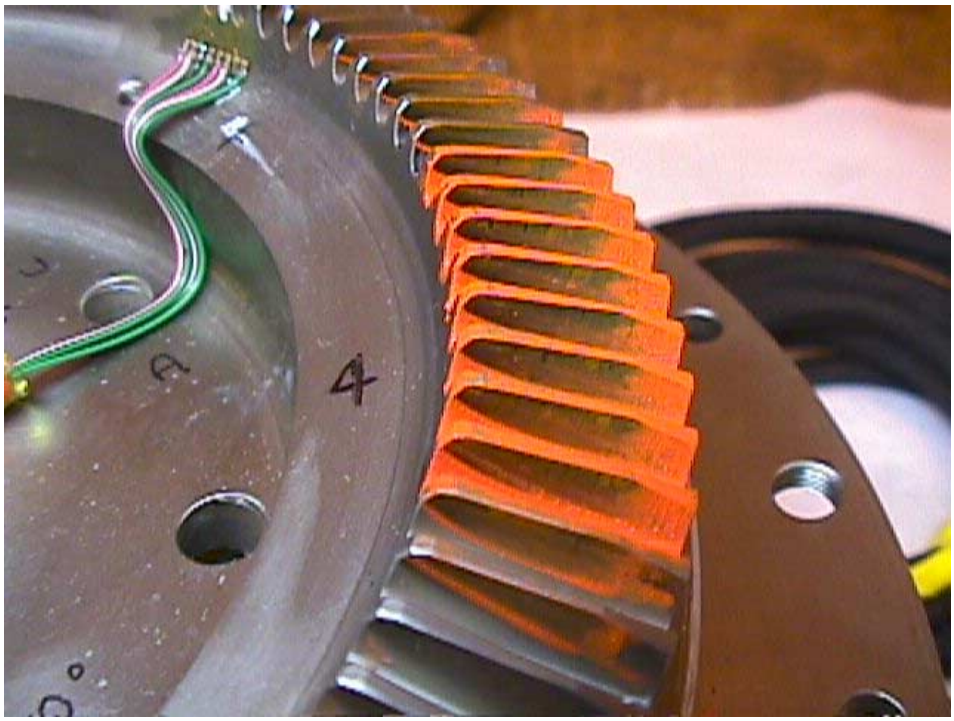

Figure 61. Upper face gear tooth patterns for Idler 4 mesh.

Load distribution plots for the Idler 4 upper face gear mesh and the upper face gear Idler 4 mesh are shown in Figures 62 and 63. These figures should be viewed while referencing Figure 27 which shows gage locations, i.e., both upper face gear gages are near the toe end of the UFG tooth and the middle idler gage is near the toe end of the UFG. Figures 62 and 63 support the conclusion that Idler 4 appears to be loading the upper face gear tooth at the toe end.

Strain plots for Idler 4 for the 1 and 1 gearbox assembly configuration (Run No. 211) are shown in Figures 64 and 65. As with Idler 3, strains are similar to those for the 2 and 2 configuration. There appears to be an inboard shift in tooth loading in going from the 2 and 2 configuration to the 1 and 1 configuration. Additionally, strain registered by the middle gage for the UFG mesh increased significantly for the 1 and 1 setup relative to the 2 and 2 arrangement.

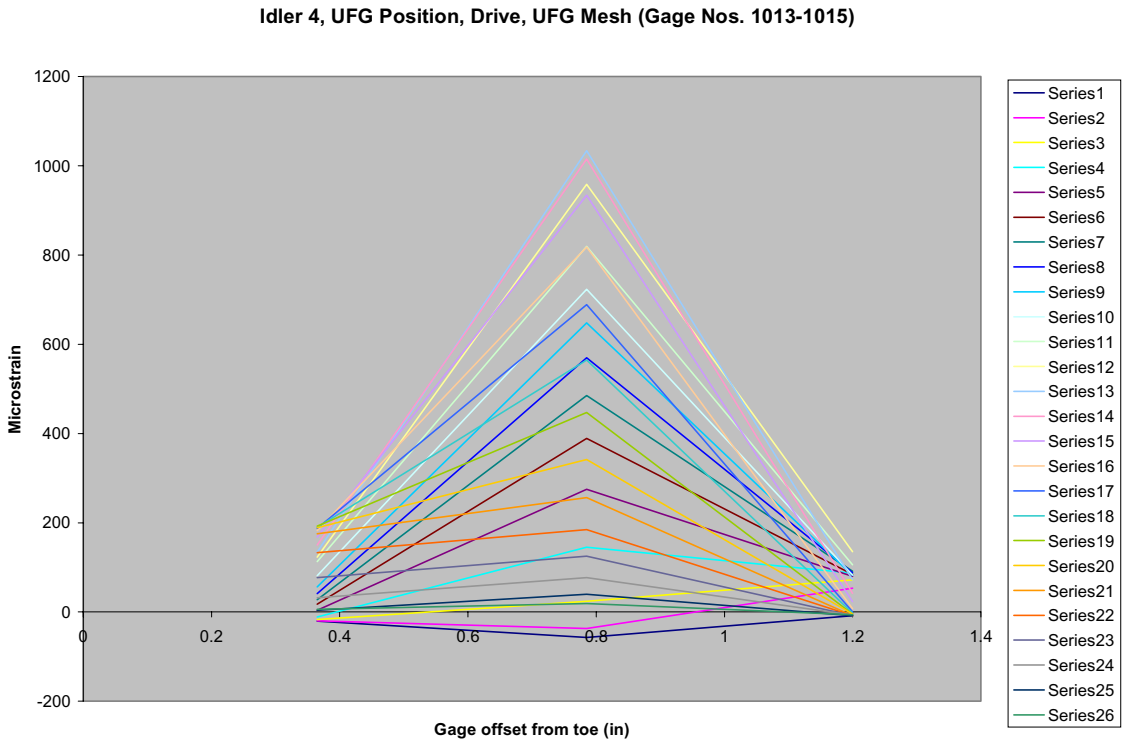

Figure 62. Strain distribution plot for I4, UFG location, Run No. 141 (2+2), UFG mesh.

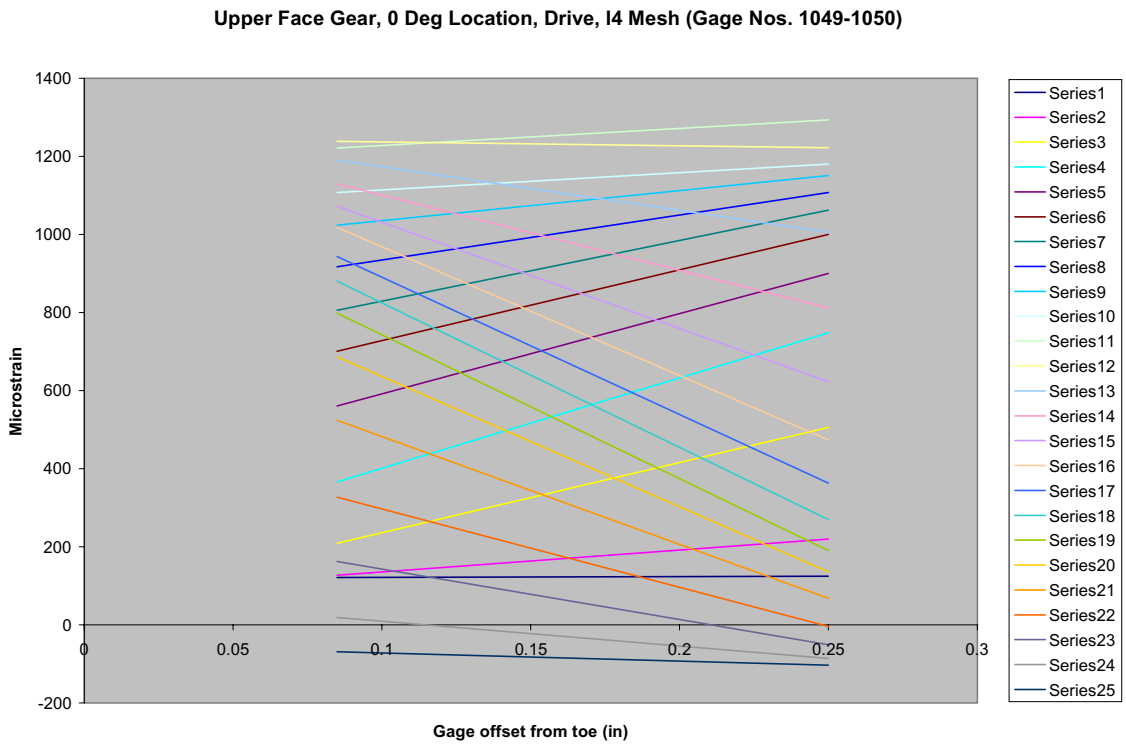

Figure 63. Strain distribution plot for UFG, 0 deg location, Run No. 141 (2+2), I4 mesh.

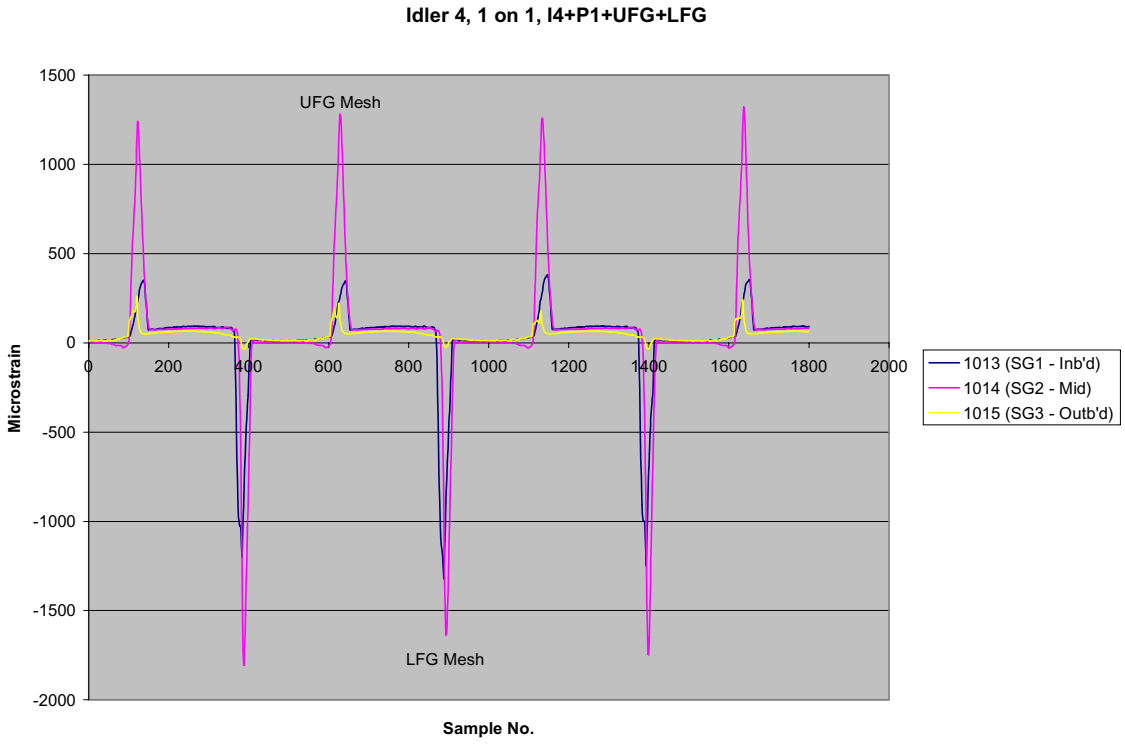

Figure 64. Strain output for Idler 4, UFG location, Run No. 211.

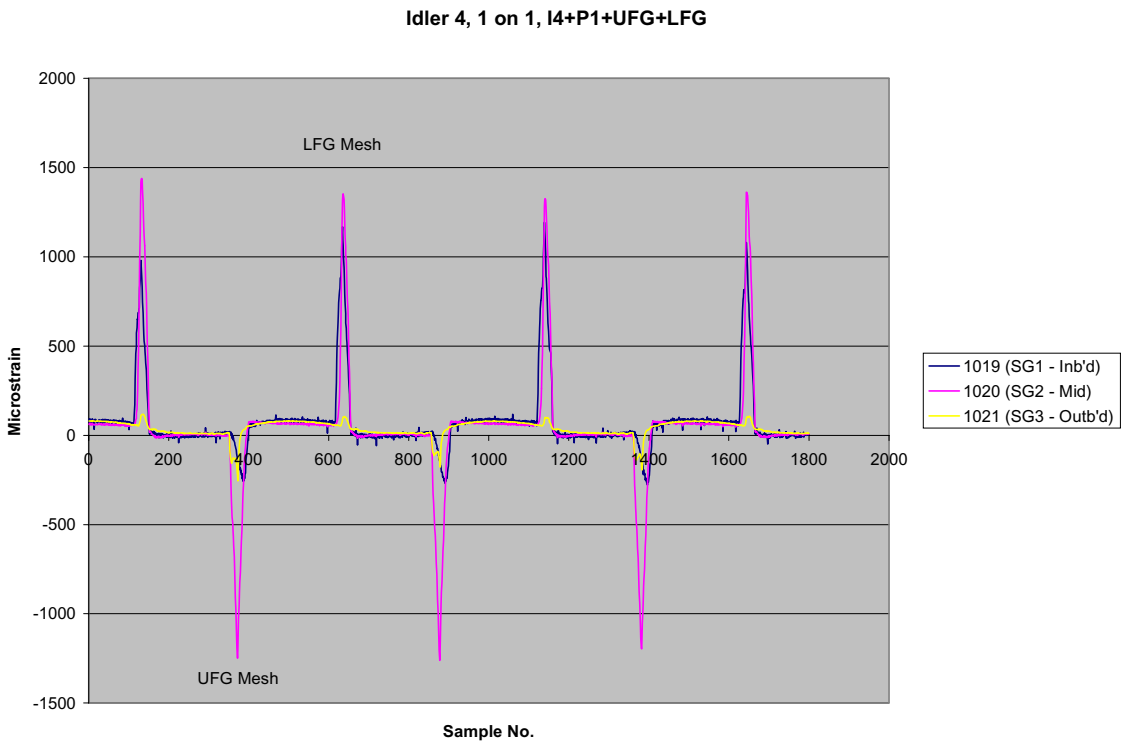

Figure 65. Strain output for Idler 4, LFG location, Run No. 211.

3. Face Gears

i. Upper Face Gear

Strain plots for the upper face gear for the two pinion-two idler configuration (Run No. 141) are shown in Figures 66 and 67 for the tooth drive side gages at the 0 degree and 180 degree locations, respectively.

The plots for the two different UFG tooth gage locations are quite similar as expected. The inboard and mid strain gages appear to be loaded fairly evenly at the idler meshes. For the pinion meshes, the mid gage is loaded significantly more than the inboard gage indicating tooth loading is farther outboard at the pinion meshes relative to the idler meshes. Of the two idler meshes, load for the Idler 4 mesh appears to be further inboard. All these observations are consistent with the observations noted for the pinions and idlers in the previous sections. Refer to the UFG tooth patterns in Figures 59-61 showing an apparent inboard shift in tooth load going from Pinion 1 to Idler 3 to Idler 4.

There is an obvious difference in strain magnitude between the pinion and idler meshes. Strain magnitude is a function of tooth load proximity to the gage location as well as a function of load magnitude. It is believed that the differences in the UFG strains at the different meshes (pinions versus idlers) are more a function of tooth load proximity to the UFG gages. Based on the results shown in Figures 66 and 67, the pinions appear to load the UFG teeth farther toward the heel than the idlers. See the “Initial Testing” section for further discussion of the UFG 2 and 2 results.

Results for both 1 and 1 configurations are shown in Figures 68 and 69. As with the pinions and idlers, there appears to be a general slight shift of the tooth load toward the toe. The magnitude of strains for all meshes increased, with the exception of the Idler 3 mesh. It is believed this increase is primarily due to the inboard shift of load – closer to the gage locations. The likely reason that Idler 3 mesh strains decreased is due to the large backlash at the Idler 4 mesh. As discussed in the "Initial Testing" section, the backlash at Idler 4 was increased considerably in order to equalize the magnitude of the strain peaks as measured by the upper face gear 0 degree location drive side gages. The effect of the increased Idler 4 backlash was to force Idler 3 to transmit a larger share of the LFG load to the UFG. Based on the results of the torque calibration and torque split determination, all carried out after the formal testing was completed, it is believed that the idlers were splitting torque fairly evenly prior to the backlash adjustment (the higher peak at the Idler 4 mesh was due to proximity of the tooth load to the UFG tooth gages). The backlash adjustment apparently caused Idler 3 to carry much more than 50% of the LFG load. For the 1 and 1 test, during which there was only 50% of the 2 and 2 load in the LFG, Idler 3 actually experienced a decrease in load.

ii. Lower Face Gear

The lower face gear acts as a type of idler in that it transmits load from pinion to idler but does not transmit torque. Similar to the idlers, the lower face gear teeth are both driven and driving. At the pinion mesh, the lower face gear is driven; at the idler mesh, the LFG drives the idler, which in turn drives the upper face gear. The plots shown in Figures 70 and 71 show output for the LFG drive side gages at the 0 degree and 90 degree tooth locations.

In Figure 70, drive side gages at the 0 degree location are in tension for the pinion meshes. As shown in Figure 26, these gages are on the tension side of the tooth when being driven by a pinion. At the idler meshes, where the lower face gear drives the idlers, it can be seen that the 0 degree location "drive side" gages are now on the compression side of the tooth. From Figure 26, it can be seen that for the 90 degree and 270 degree LFG locations, drive side gages are on the opposite side of the tooth compared to the drive side gages at the 0 and 180 degree locations. Therefore, Figure 71 shows that strains at the drive side gages at the 90 degree location are roughly a mirror image of those at the 0 degree location. As mentioned in the "Idlers" section, strain gages on the compressive side of a tooth will record higher magnitude output than gages on the tension side of the tooth due to the compressive radial component of the applied load. This effect can be seen when comparing Figures 70 and 71. Apparently, there was some noise in the instrumentation channel for Gage 1069 – Figure 71.

Figure 72 shows the strain data for the lower face gear drive side gages at the 180 degree location. Ideally, these results would match those for the 0 degree location. The results are similar, however, middle gage strains appear higher at the 0 degree location compared to the 180 degree location. This could be related to the fact that the middle gage at the 180 deg location, No. 1074, from the strain gage calibration, demonstrated the lowest sensitivity and highest correction factor of all LFG strain gages.

In Figure 72, Gage No. 1073 shows significant strain even when the tooth is not in mesh (strain spikes correspond to the tooth in mesh). Strain variation outside the mesh is apparent in all the plots but is more pronounced in this case. It is not understood why, Gage 1073 stands out in this regard. The overall shape of the strain plot outside the mesh can be explained by the fact that in its capacity as an idler, the lower face gear is subject to opposing loads every 90 degrees about the azimuth. In one quadrant, these loads would tend to produce tension at the upper surface of the gear "rim" near the inner diameter due to both in-plane bending of the gear ring and out-of-plane bending from the tooth loads applied above the section neutral axis. In the adjacent quadrant, the opposite would be true and both effects would tend to produce compression.

Another observation gleaned from the lower face gear plots is that the idler mesh consistently produces less strain than the pinion mesh. The load on the lower face gear tooth for the idler mesh is biased toward the heel of the face gear tooth, more so than for the pinion mesh, and so produces lesser strain output for the LFG gages which are in the toe region. This conclusion is supported by the fact that the middle gage strain is much greater than the inboard gage strain when the LFG tooth is in mesh with the idler; see Figures 70-72 and also the strain distribution plot in Figure 73. These findings are consistent with those in the "Pinions" and "Idlers" sections.

Figures 74 and 75 show the LFG 0 degree location drive side strain results for both 1 and 1 tests. The strain peak magnitudes for both gages at all meshes are higher for the 1 and 1 test relative to the 2 and 2 test results. For some of the meshes, there appears to be a shift of the tooth load toward the toe, however, this is not the case for the Pinion 1 mesh. In fact, at the Pinion 1 mesh, there appears to a slight shift toward the heel. Additionally, strains for the Idler 3 mesh are actually of higher magnitude for the 1 and 1 configurations. This is opposite to the trend observed for the UFG and appears to invalidate the explanation proposed to explain the decrease in UFG strain for the Idler 3 mesh in going from the 2 and 2 to the 1 and 1 configuration. In the "Torque Split" section that follows, it is concluded that Idler 3 did carry significantly more load than Idler 4 for the 2 and 2 configuration. While there is not high confidence in the torque split numbers, the significant difference between the two idlers suggests there was a real bias towards Idler 3. Why the LFG strains for the Idler 3 mesh actually increase for the 1 and 1 configuration cannot be adequately explained, however, the LFG strains at the Idler 4 mesh increased to a much greater degree in going from 2 and 2 to 1 and 1.

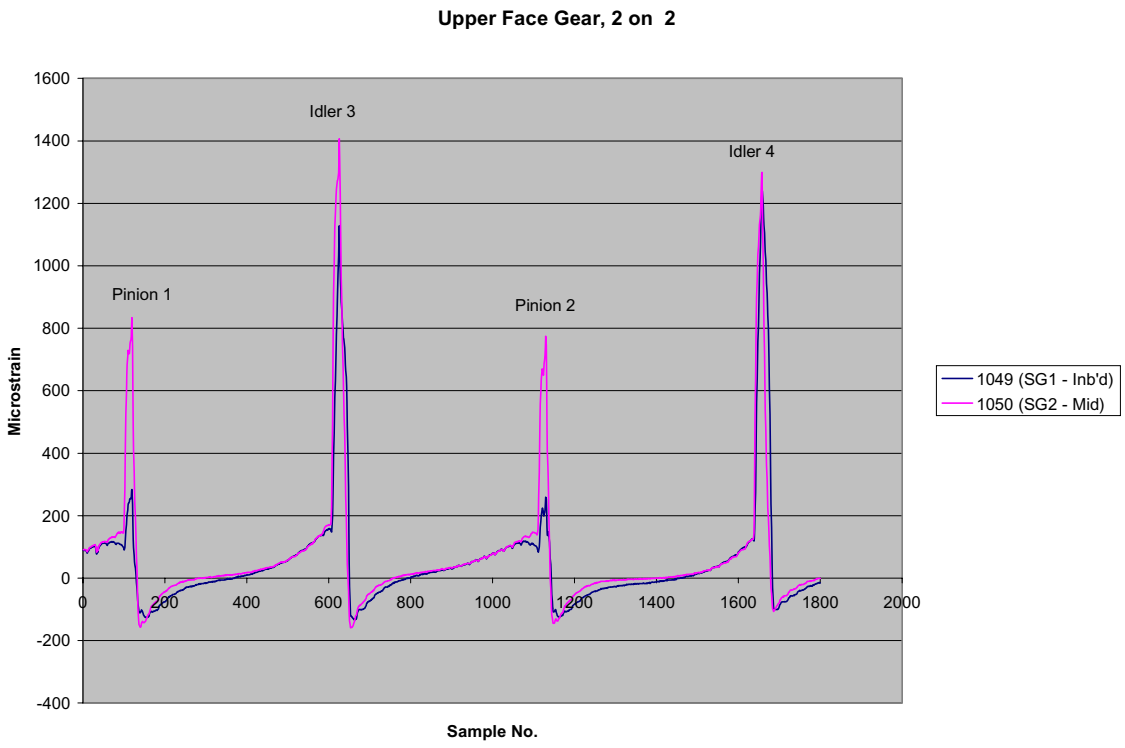

Figure 66. Strain output for UFG, 0 degree location, Run No. 141.

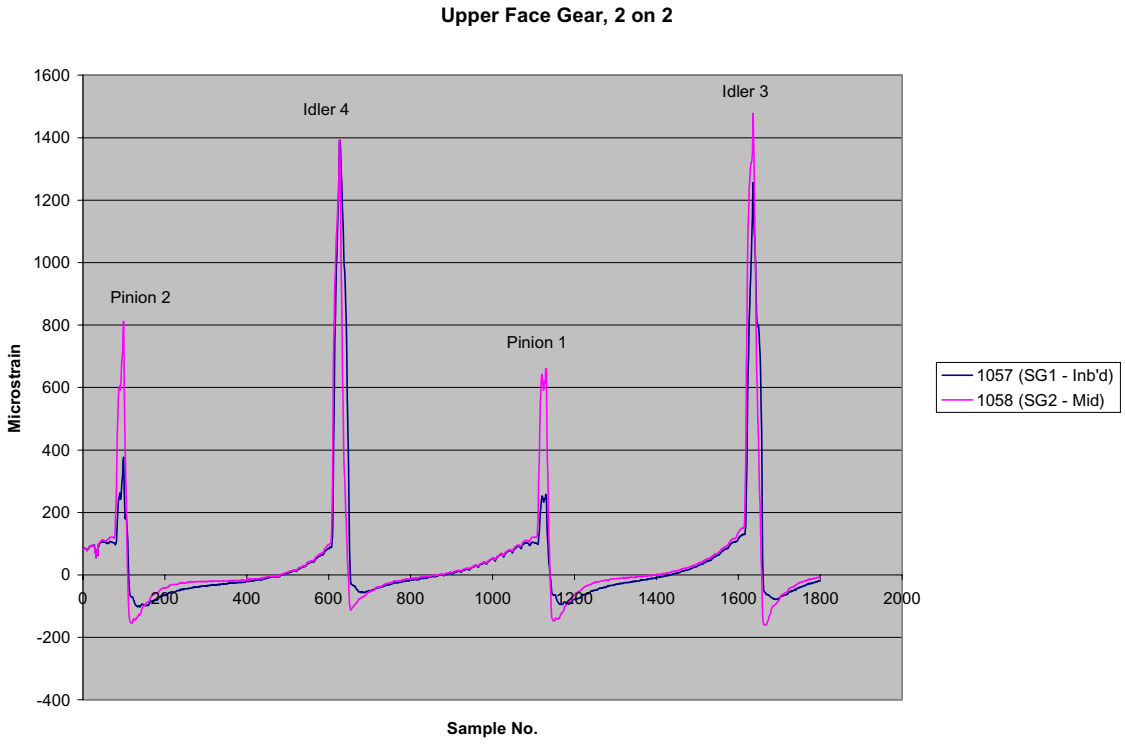

Figure 67. Strain output for UFG, 180 degree location, Run No. 141.

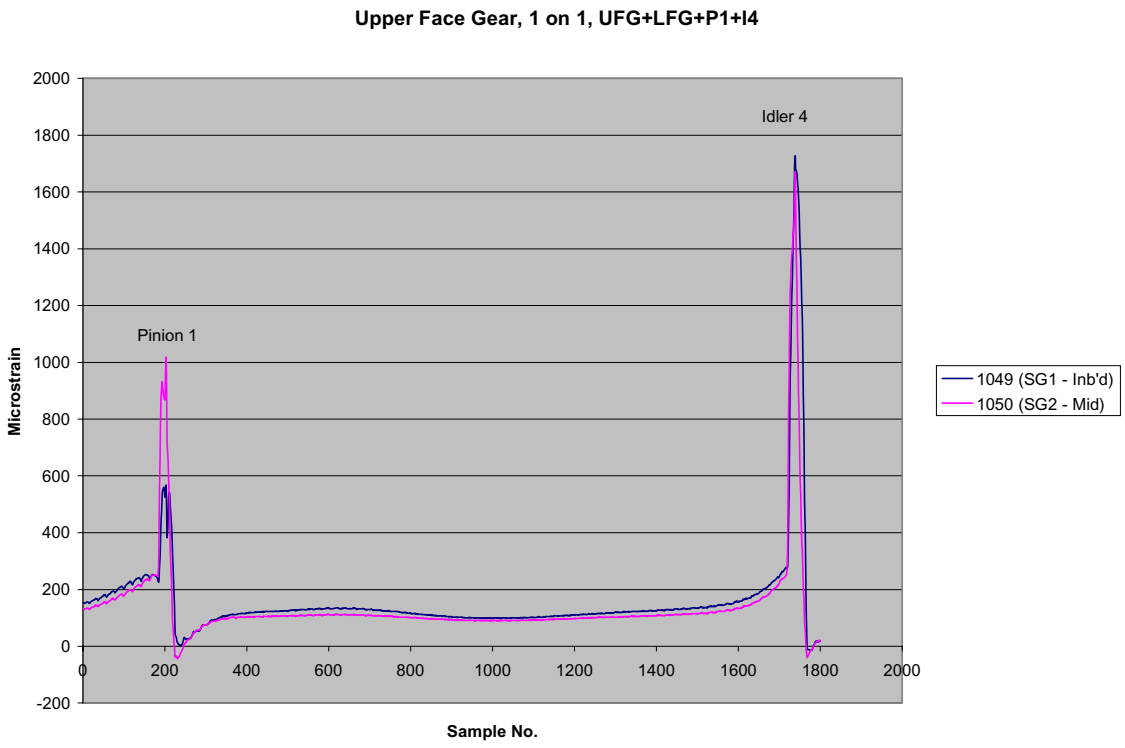

Figure 68. Strain output for UFG, 0 degree location, Run No. 211 (1+1).

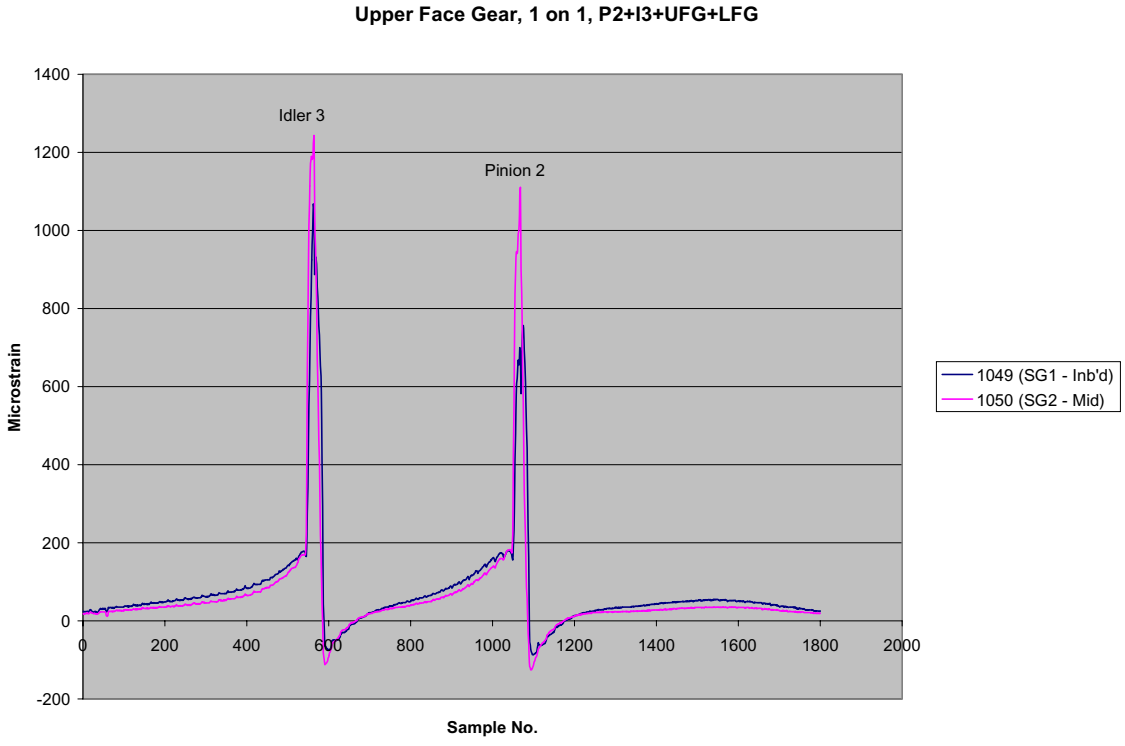

Figure 69. Strain output for UFG, 0 degree location, Run No. 301 (1+1).

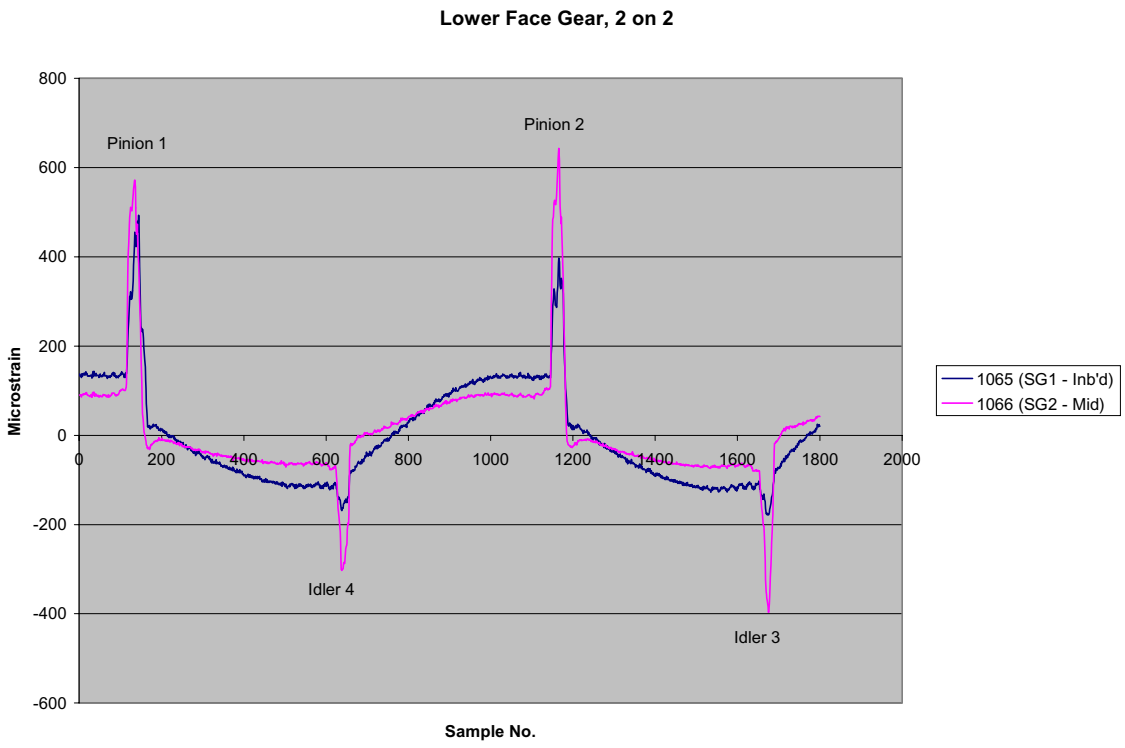

Figure 70. Strain output for LFG, 0 degree location, Run No. 141.

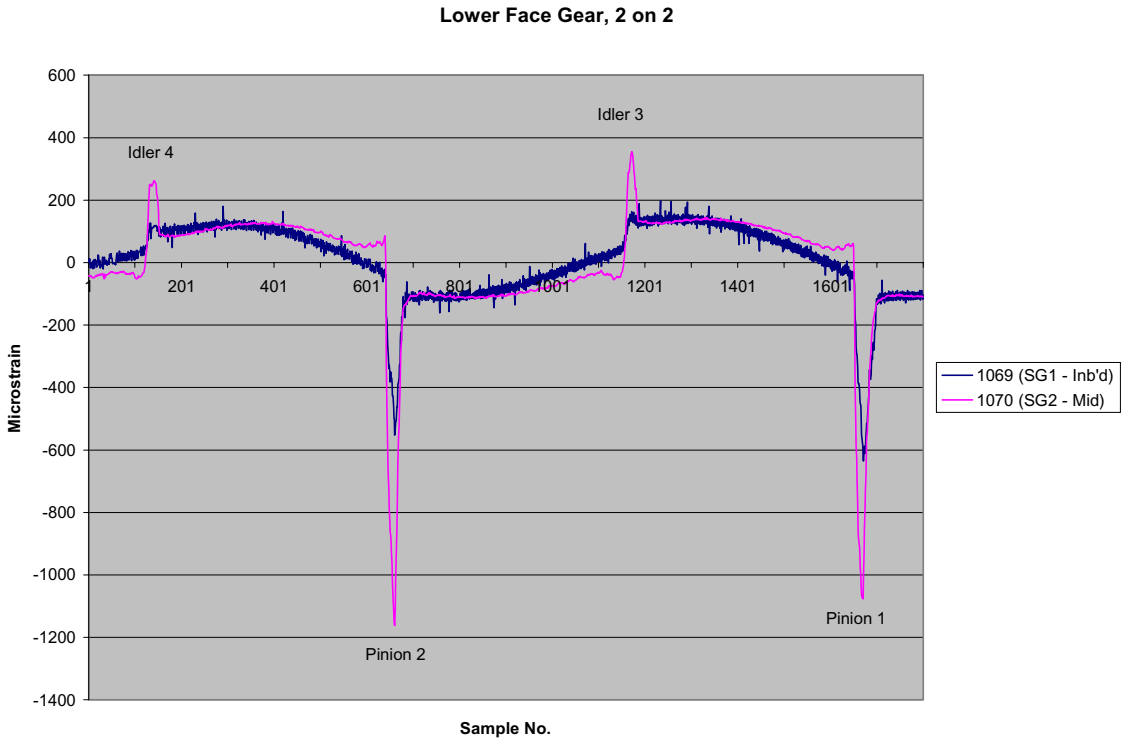

Figure 71. Strain output for LFG, 90 degree location, Run No. 141.

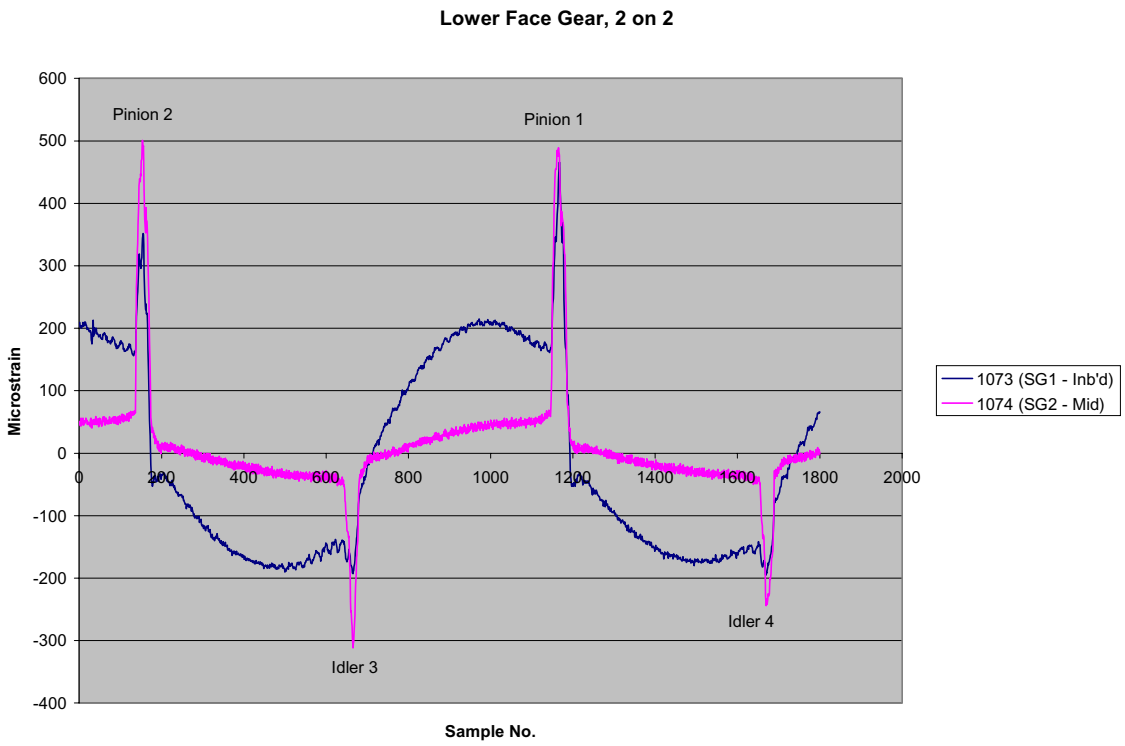

Figure 72. Strain output for LFG, 180 degree location, Run No. 141.

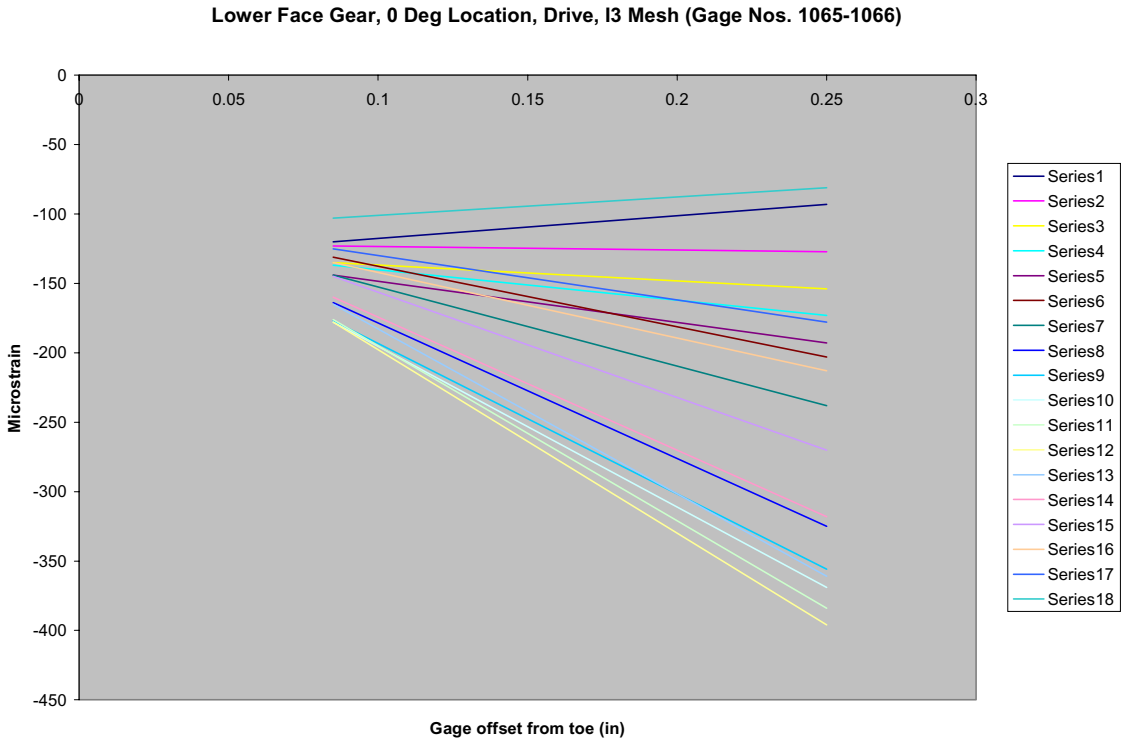

Figure 73. Strain distribution plot for LFG, 0 deg location, Run No. 141 (2+2), I3 mesh.

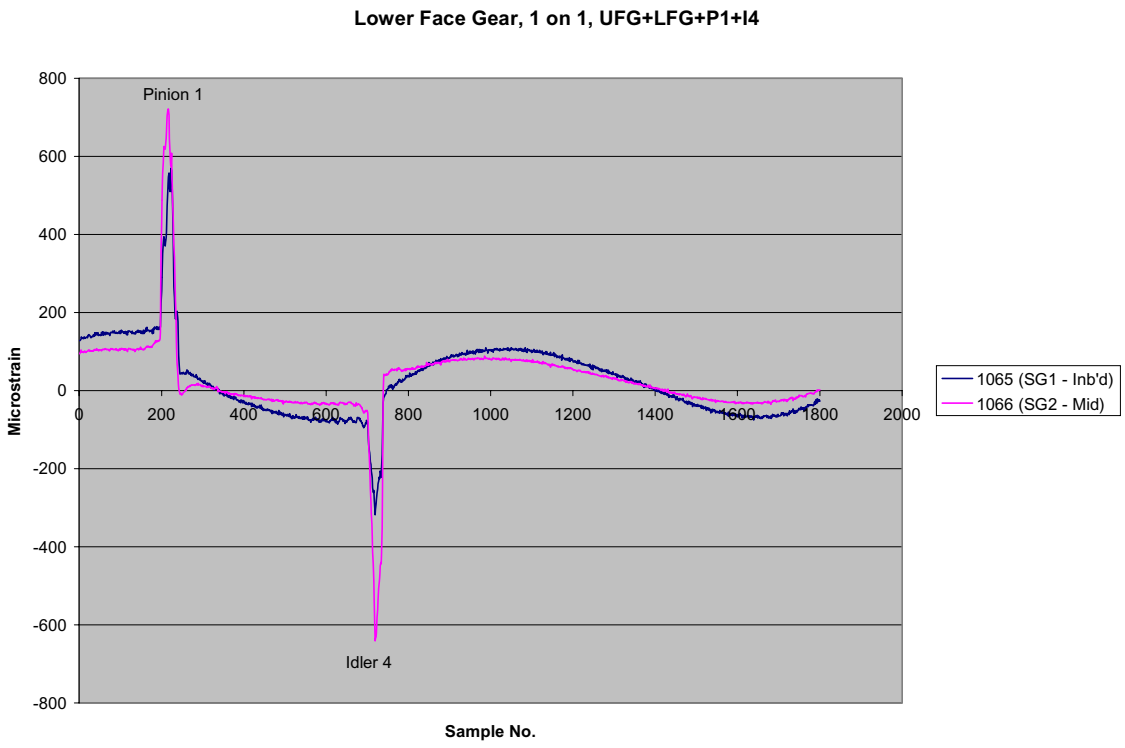

Figure 74. Strain output for LFG, 0 degree location, Run No. 211 (1+1).

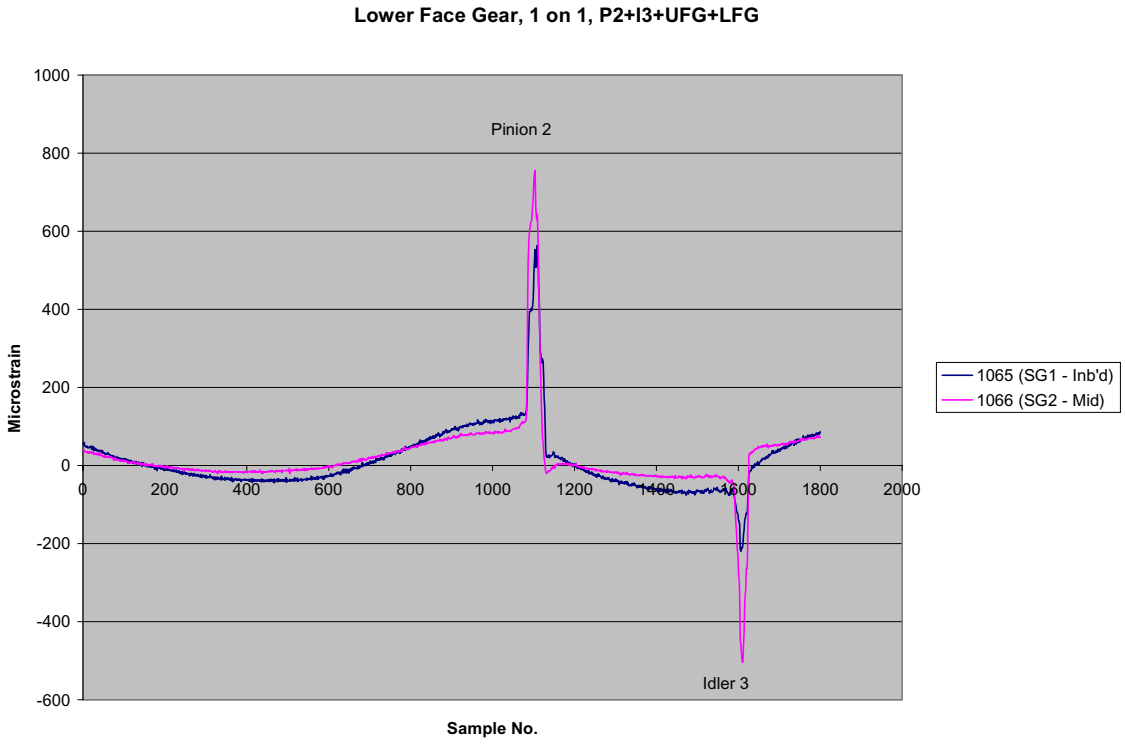

Figure 75. Strain output for LFG, 0 degree location, Run No. 301 (1+1).

VIII. TORQUE SPLIT DETERMINATION

1. Background

One of the primary objectives of this POC test program was to determine and optimize, if necessary, the torque split between the upper and lower face gears. The means intended for this purpose were the gear tooth root strain gages. It was assumed that measured bending strain would be proportional to load transmitted at the mesh.

The tapered configuration and offset between the upper and lower face gear (Figure 27) made use of the pinion gages undesirable for the purpose of torque split determination. It was hoped that the upper face gear would yield the torque split information as the geometry of the contact between the upper face gear and both the pinions and idlers was the same. Load transmitted by the idlers to the upper face gear (UFG) is the portion of input torque transmitted from the pinion to the lower face gear and then to the idlers. A cursory review of the results for UFG drive side gages shown in Figures 66 and 67 would seem to indicate that much more load was split to the lower face gear than the upper.

Closer scrutiny showed that the distribution of load across the face gear tooth differs between the pinion and idler meshes. For the pinion meshes, strain registered at the middle gage is much greater than that measured at the inboard gage. For the idler meshes, inboard and middle gages measure roughly the same strain. Furthermore, it is difficult to make an accurate load comparison based on two gages near one end of the tooth. As testing progressed, it became apparent that directly measured tooth bending strains would not be sufficient to determine torque split. Torque loading transmitted through a given mesh cannot be directly related to output from a gage or even group of gages as configured for this test.

2. Torque Calibration

i. Introduction

To ascertain the torque split between the pinion upper and lower face gear meshes, it was decided to conduct a “torque calibration.” The torque calibration is used to develop a relationship between pinion torque and gear tooth strain for the purpose of torque split determination. There are many factors that make this difficult to do analytically – e.g., high contact ratio, asymmetric face gear configuration and offset contact between the upper and lower face gear relative to the pinion. As such, these relationships were developed experimentally using the POC gearbox test stand.

ii. Procedure

For the initial calibration, only the upper face gear and a single modified idler, No.4, were used. The lower face gear was in its normal position, but with no standard idler installed, it was “free-wheeling” offering no torsional resistance. Idler 4 was temporarily modified by the attachment of a “hub” such that torque could be applied to the idler as if it were a pinion. A modified idler was used in lieu of a pinion as the idler design includes bearing support both inboard and outboard of the face gear meshes which was necessary for this calibration step that effectively included only the single modified idler and upper face gear.

Torque was applied to the modified idler and reacted through the upper face gear to the output coupling. While under torque, the assembly was slowly rolled through nearly one revolution of the upper face gear (approximately four revolutions of the modified idler). This procedure was conducted at the modified idler torque level of 883.5 in-lbs (50% torque level). The modified idler was rotated counterclockwise; output for all modified idler and upper face gear strain gages was recorded for this test.

After completing this slow roll test using Idler 4 in the modified configuration, it was repeated using only Idler 3 in the modified configuration.

For the second calibration step, the configuration was the same as for the initial step, with the exception that one modified idler and one standard idler were used. The test was then conducted using the same procedure described above except that a modified idler torque level of 1767 in-lbs (100% torque level) was applied. Output for both idler and upper and lower face gear strain gages was recorded. This second step was conducted using Idler 3 as the modified idler and Idler 4 as the standard idler. Data from this test run was reviewed. Based on this review, it was decided not to proceed with testing Idler 4 in the modified configuration and Idler 3 in the standard configuration.

For all the torque calibration tests, the idlers were installed in their own bores with the same mounting distances used for the formal POC test program.

3. Torque Split Method

i. Initial Method

The torque calibration yielded, for each of the idlers in the modified configuration, the relationship between the tangential load at the modified idler/upper face gear mesh, and the strain measured at the root of the modified idler gear tooth. Because it was feared that the idler deflection, load distribution and strain distribution would differ between the torque carrying modified idler, and the standard idler that only transmits load from one point to another about its circumference, the second, “dual idler,” torque calibration step was added. By using a test setup consisting of one modified idler and one standard idler, it should have been possible to use the sensitivity of the modified idler strain to tangential load at the upper mesh, calculated from the first torque calibration step, to determine the tangential load transmitted at the standard idler upper mesh. Once the transmitted load was known, the sensitivity of the standard idler strain gages to tangential load transmitted at the upper mesh could be determined.

ii. Revised Method

Unfortunately, for the first dual idler calibration, with Idler 3 in the modified configuration and Idler 4 in the standard idler configuration, virtually no load was transmitted by the modified idler to the lower face gear. This finding is borne out by Figures 76 and 77. Figure 76 is the strain plot (Run No. 600) for the Modified Idler 3, LFG location, drive side gages. Contrast this with Figure 53 and it is obvious that load is only being transmitted at the UFG mesh. Figure 77 shows the strain plot for the UFG, 180 degree location, drive side gages. The

small blip near the beginning of the trace represents the Idler 4 mesh; the large spike is due to load transmitted at the Modified Idler 3 mesh (compare with Figure 67).

It is believed the reasons Modified Idler 3 transmitted negligible load to the LFG are related to the fixed nature of the idlers (versus the floating pinions). The amount of load transmitted to the LFG mesh by the modified idler is likely very sensitive to the amount of backlash between the idlers and face gears.

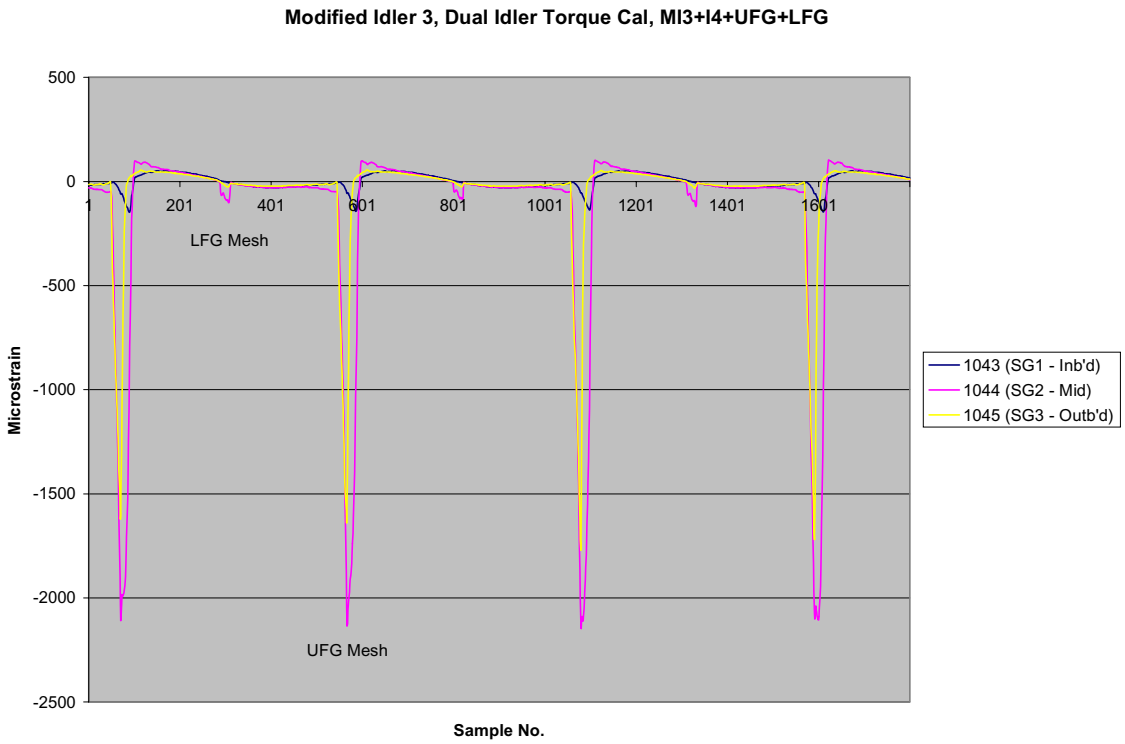

Figure 76. Strain output for Modified Idler 3, LFG location, Run No. 600.

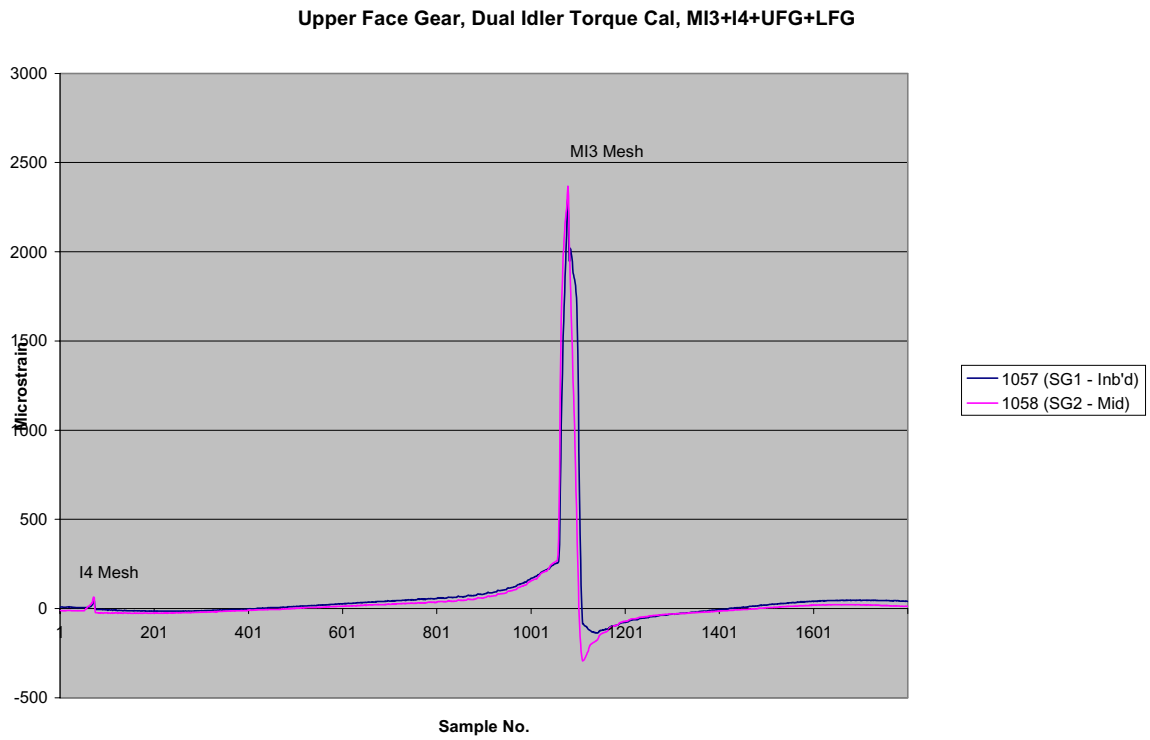

Figure 77. Strain output for UFG, 180 degree location, Run No. 600.

While demonstrating the necessity of having a floating pinion, the initial dual idler torque calibration also obviated the need for the other dual idler torque calibration using a modified Idler 4 and standard Idler 3. The failure of this second calibration step required a revision to the method for determining torque split. The revised method assumes that the sensitivities between transmitted tangential load and strain developed for the modified idler gages during the initial torque calibration step, are the same as the sensitivities for the idler gages when the idler is operating in its standard fashion. This assumption is not always true. Comparing strain output from the Idler 3 torque calibration (Figure 78) to the 1 and 1 test results (Figure 79) shows that the strain distribution changes significantly. Nevertheless, this revised method is used to estimate the torque split results.

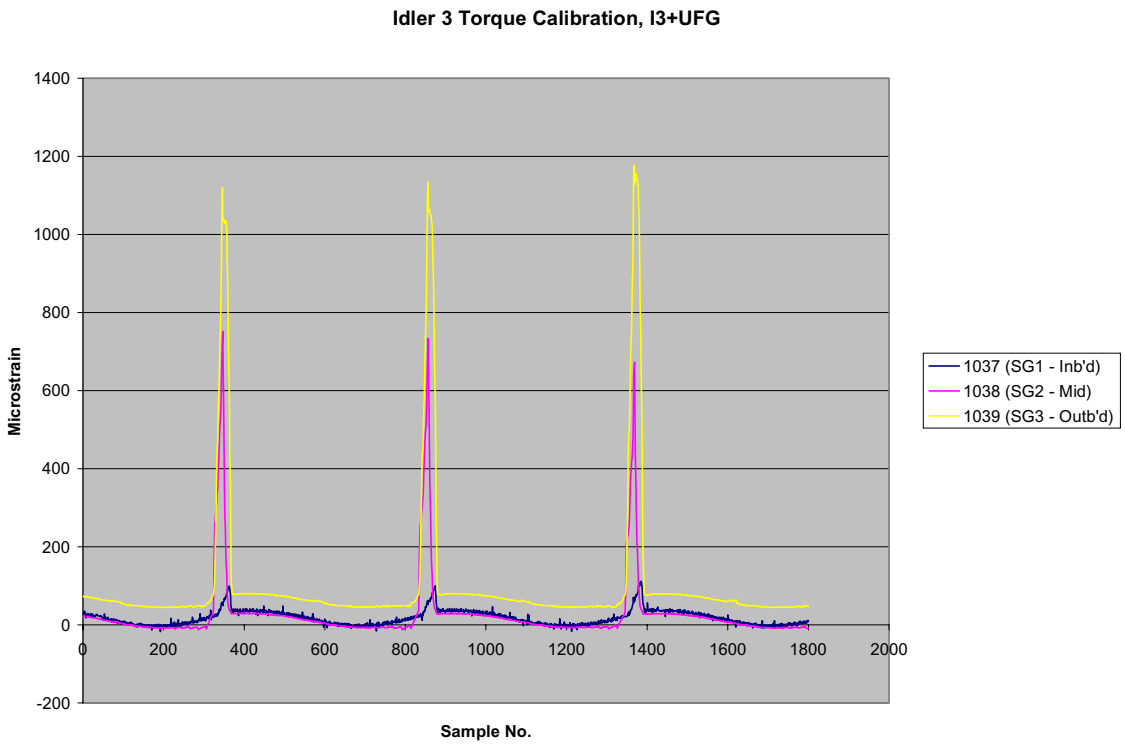

Figure 78. Strain output for Idler 3, UFG location, Run No. 501.

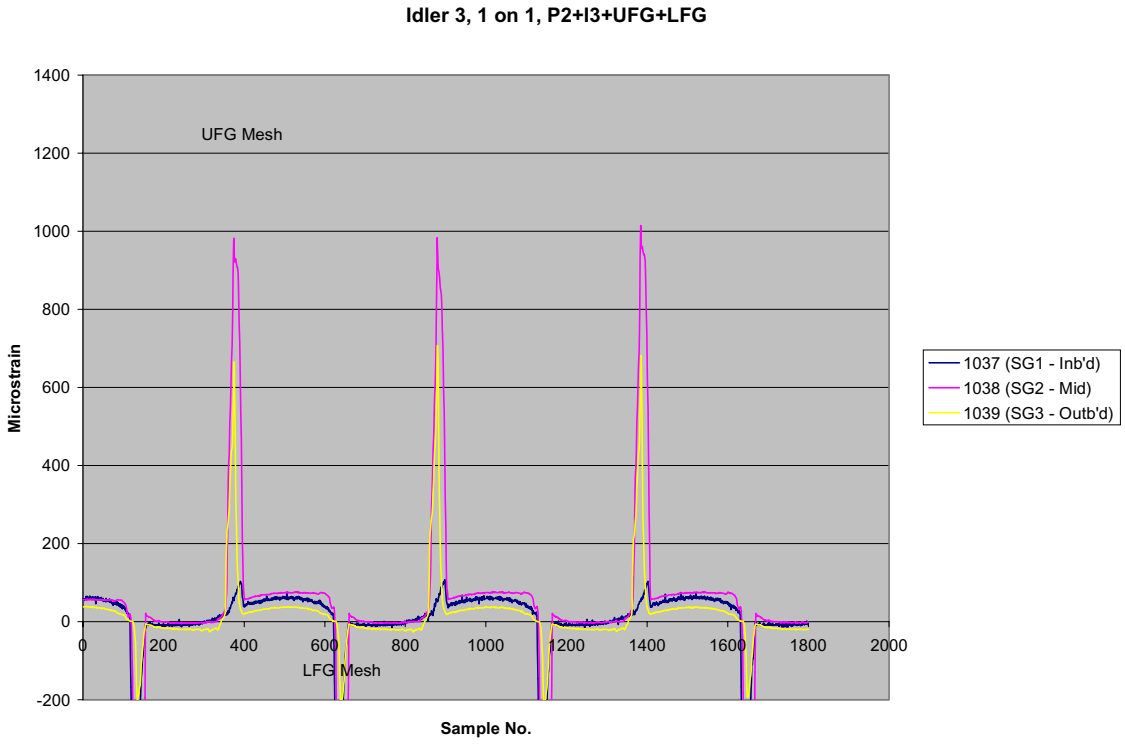

Figure 79. Strain output for Idler 3, UFG location, Run No. 301.

iii. Derivation of Revised Torque Split Method

For the one pinion-one idler configuration:

R_U = pinion/idler pitch radius at the center of the upper face gear tooth
R_L = pinion/idler pitch radius at the center of the lower face gear tooth
W_{TPU} = tangential load transmitted at pinion/upper face gear mesh
W_{TPL} = tangential load transmitted at pinion/lower face gear mesh
W_{TIU} = tangential load transmitted at idler/upper face gear mesh
W_{TIL} = tangential load transmitted at idler/lower face gear mesh
T_P = pinion input torque

$T_P = W_{TPU}*R_U + W_{TPL}*R_L$ (Torque split at pinion between upper and lower meshes)

$W_{TIU}*R_U = W_{TIL}*R_L$ (Idlers transmit no torque.)

$W_{TPL} = W_{TIL}$ (The lower face gear transmits no torque.)

$W_{TIU}*R_U = W_{TPL}*R_L$

$T_P = W_{TPU}*R_U + W_{TIU}*R_U$

$W_{TPU} = (T_P - W_{TIU}*R_U)/R_U = T_P/R_U - W_{TIU}$

T_P = 1767 in-lbs (from [12])
R_U = 0.967 inch (from drawing geometry)

W_{TIU} is determined from the torque calibration. Torque is applied to the idler which has been modified by attaching a hub. In the torque cal, W_{TIU} is known and assumed equal to $W_{TIU} = T/R_U$ where T is the torque applied to the idler.

T = 883.5 in-lbs (see "Procedure" section under "Torque Calibration")
W_{TIU} = 883.5 / 0.967 = 913.7 lbs

During this calibration, the bending gage strains were recorded. Ratios of $K_{IU} = W_{TIU}$/strain were calculated using the maximum or minimum strain, as appropriate, recorded during the complete roll. During the one-and-one test, from measured idler strain and using K_{IU}, W_{TIU} was determined. W_{TPU} was then calculated.

From the equations above, the fraction of torque transmitted at the upper pinion mesh is

Upper Torque Split = $W_{TPU}/(W_{TPU} + W_{TIU})$

Lower Torque Split = 1 – Upper Torque Split

Ratios of $K_{PU} = W_{TPU}$/strain were calculated from the results of the one and one test.

This process was carried out for the combinations of the Modified Idler 4 torque calibration (Run No.401) and Pinion 1/Idler 4 one and one test (Run No.211), as well as, the Modified Idler 3 torque calibration (Run No.501) and Pinion 2/Idler 3 one and one test (Run No.301). K values were then available for both pinions and both idlers. These K values were used with the 2 and 2 test results in terms of strain to arrive at the overall upper/lower torque split at the pinions and the idler load-sharing split.

Because of the known inaccuracy in this method for determining torque split, K values for each gage of a given component were calculated and used to determine several values of W (tangential load) which were then averaged. W values based on K values for gages with known low output for a given mesh were not used to arrive at the average for W.

In order to provide an even broader sample from which to calculate average values for W, K values were developed for upper face gear gages as well. The only difference in the process described above for the pinion and idler gages was that the maximum or minimum strain value (as appropriate) was not calculated for the entire slow roll run, but only from the data samples encompassing the UFG mesh of interest. For example, to determine the tangential load for an idler/UFG mesh for the 1 and 1 test using a UFG drive side gage, only the maximum value for the portion of the UFG strain trace that encompassed the spike representing the idler/UFG mesh would be obtained. This maximum would then be multiplied by the appropriate K value to arrive at the tangential load, W.

4. Torque Split Results

Using the process described above, the results of the torque split determination are shown in Tables 3-5, below. The overall trend is that the torque splits fairly evenly. The idler load-sharing results indicate that Idler 3 transmitted significantly more LFG load than Idler 4. This is likely due to the fact that the Idler 4 backlash was increased significantly as mentioned previously.

Table 3. Estimated Torque Split Results from 1 and 1 Test – Pinion 1 and Idler 4.

Description	I4 Mid Gage Average	Upper Face Gear Average	Combined Average
Average W_{TI4U}	867	968	917
W_{TP1U}	961	859	910
Upper Torque Split	52.6%	47.0%	49.8%
Lower Torque Split	47.4%	53.0%	50.2%

Table 4. Estimated Torque Split Results from 1 and 1 Test – Pinion 2 and Idler 3.

Description	I3 Mid Gage Average	Upper Face Gear Average	Combined Average
Average Wti3u	906	862	884
Wtp2u	921	965	943
Upper Torque Split	50.4%	52.8%	51.6%
Lower Torque Split	49.6%	47.2%	48.4%

Table 5. Estimated Torque Split Results from 2 and 2 Test.

Description	Pinion/Idler Average	Upper Face Gear Average	Combined Average
Wtp1u (lbs)	900	807	853
Wti4u (lbs)	741	768	755
Wtp2u (lbs)	843	684	764
Wti3u (lbs)	1058	941	1000
Target sum = 3655	3542	3201	3372
Upper torque split	49.2%	46.6%	48.0%
Lower torque split	50.8%	53.4%	52.0%
Idler 3 split	58.8%	55.1%	57.0%
Idler 4 split	41.2%	44.9%	43.0%

IX. STRENGTH SUMMARY

Maximum tensile stresses, calculated from strains measured during POC Run No. 141 - the full-up two pinion-two idler test - are shown, by gear, in the row labeled “maximum measured” in Table 6, below. The input pinion torques for this test run were 1767 in-lbs, equivalent to a 100% or maximum continuous torque level.

Table 6. Tooth bending fatigue strength (POC Run 141, 2 on 2).

Description	Gear Tooth Bending Stress (PSI)					
	Pinion 1	Idler 4	Pinion 2	Idler 3	UFG	LFG
Maximum Measured (100% MCP)	43268	48053	34945	69020	44341	25520
Predicted Spur Pinion (100% MCP)	32500	32500	32500	32500	<32500	<32500
Predicted Face Gear Pinion (100% MCP)	23723	23723	23723	23723	<23723	<23723
Allowable Bending Stress (Carburized and Hardened)	75000	52500	75000	52500	75000	52500

The row labeled “predicted spur pinion” presents stresses calculated using the bending stress formula in [13] (AGMA standard) for a spur gear. For all predicted stresses, an even torque split is assumed.

The AGMA formulas for spur gears are intended for a spur pinion meshing with a spur gear. In this application of a tapered spur pinion meshing with a conical face gear, some adjustment is necessary to arrive at bending stress for the “face gear” pinion. This adjustment involves a factor used in conjunction with the results for the straight spur gear. Adjusted stresses are shown in the row of Table 6 labeled “predicted face gear pinion.” Lines of contact for a face gear mesh are at an angle to the pitch plane and the contact ratio for a face gear set is typically higher than that for a spur gear set (see [7] and [14]). These factors should lead to increased tooth surface to carry the load and, subsequently, lower stresses. Therefore, the stresses predicted for a face gear pinion are lower than those predicted for a straight spur pinion. The predicted spur gear stress formula assumes a nearly uniform distribution of load along the full face width of the face gear tooth.

The allowable bending stresses shown in Table 6 for carburized and hardened steel gears, the production heat treat condition, are taken from Table 6 of [13]. A reduction factor of 0.70 is applicable for the idlers and lower face gear that see reversed bending – Sec. 16.2 of [13].

The predicted face gear pinion stresses are all below the actual maximum measured stresses. The measured stresses for the pinions are fairly close to what was predicted for a straight spur gear. The lower face gear stress is lower than either the pinion or idler stresses. The upper face gear stress, however, is higher than the pinion stresses but lower than the idler stresses. The face gear teeth are similar to those of a rack with a relatively wide base at the root. Because of this geometry, it was expected that the pinion/idler tooth bending stresses would be more critical than those of the face gears. This was not completely borne out by the test results. The face gear gages are near the toe of the face gear teeth which is the region where the tooth root is thinnest and higher stresses would be expected. Additionally, the Idler 4/UFG mesh appears to be heavily biased toward the toe of the UFG tooth which leads to more localized, higher stresses in the UFG toe (see the "Idler 4" section). Figure 80 shows the UFG strain plot that captures the highest measured UFG strain. Note the maximum strain occurs for an inboard gage during the I4 mesh further supporting the case of toe end loading by Idler 4.

An unexpected result from Table 6 is the high stresses recorded for the idlers, particularly Idler 3. Of all the gears, and specifically the idlers, Idler 3 experiences the highest tensile bending strain. It was expected that the idler stresses would be comparable with those of the pinion. As shown above, the maximum measured idler stress is almost 60% greater than the maximum measured pinion stress. The highest idler tooth bending stress was measured by an Idler 3 middle strain gage for the I3/LFG mesh – see Figure 53. As stated in the Idler 3 and Lower Face Gear sections above, for the idler/lower face gear mesh, the load appears to be concentrated near the middle of the idler tooth and correspondingly near the heel end of the lower face gear tooth. As with the I4/UFG mesh, the load is apparently concentrated to an excessive degree producing high loading on a very local region of the idler tooth leading to root bending stress much higher than was expected.

For the full-scale face gear main transmission design, three idlers have been proposed instead of the two used for the full-up configuration of the POC gearbox. The intent is to reduce the bending stresses by using more idlers to transmit the load. Even if they were the same as the pinion stresses, it would be necessary to reduce the idler teeth bending stresses to a lower level than that for the pinions because the idlers experience reversed bending and are subject to a lower fatigue strength allowable.

Further study is necessary to determine, in general, why measured stresses are higher than predicted and, in particular, why the idler stress is much higher than the pinion stress. Based on results reported in [15], a NASA evaluation of high-contact-ratio spur gears, it was shown that, for straight spur gears, the stress calculated with the AGMA tooth bending stress formula matched the measured stress very well. One possible reason why predicted and measured stresses for this test do not match well is misalignment in the face gear transmission assembly. The transmission housing is undergoing a post-test inspection to try to ascertain the level of accuracy in the housing bores. Misalignment can lead to uneven tooth loading and high, localized stresses. Another possible explanation for the mismatch between predicted and measured stresses is that the spur gear formula, even with the adjustment currently used, does not adequately predict stress for a face gear pinion. Both of these aspects are likely contributors to the higher measured strains.

Some preliminary finite element analysis of the pinion gear tooth has been done. Although the pinion was modeled, it was used to investigate the end loading that is apparent at the I3/LFG mesh. The pinion and idler have the same geometry and this model does not take into account the mounting stiffness of the pinion, therefore, it is more accurately used to represent the idler. A Unigraphics model of the POC assembly was used to develop contact surfaces between the pinion and face gears. The contact surface developed for the pinion/LFG mesh was used to define a bounded surface within the finite element model (FEM). To simulate end loading, a pressure load was applied over the contact surface that varied linearly from a maximum at the outboard end to near zero at the inboard end. Results are shown in Figure 81. The magnitude of the pressure load applied is somewhat arbitrary; therefore, the magnitudes of the maximum principal stresses shown in Figure 81 are not significant. What is significant is that the model stress distribution appears to match the strain distribution observed in the test. Simulated end loading in the model produced very high stresses near the center of the "idler" with relatively low stresses toward both ends of the tooth root. This is exactly what was noted for Idler 3 – see Figures 52-54. Figure 82 shows FEM results for the case of a uniform LFG pressure load. Note that although the highly strained area extends further along the face width, it is still fairly concentrated and the maximum principal stress is approximately the same as for the simulated end-loading case. There are many factors that affect the stress/strain distribution and these include variation in the tooth profile along the gear axis, the skewed nature of the tooth contact and the shape of the contact surface. Further finite element analysis should be conducted to better understand the results of this test and the nature of stress distribution in the teeth of the tapered face gear components.

It is of some concern that high strains/stresses have been measured using strain gages that cover only limited points on the gear teeth. For future slow roll testing, at least some of the teeth should be more extensively strain gaged to better define the strain distribution along the tooth such that the maximum strain value can be interpolated. Where possible, gages should cover the length of the face width in even increments. Due to the relatively fine pitch and profile variation of the face gear teeth along the gear axis, there was insufficient "space" to apply root bending gages toward the heel of the POC face gear teeth for this test.

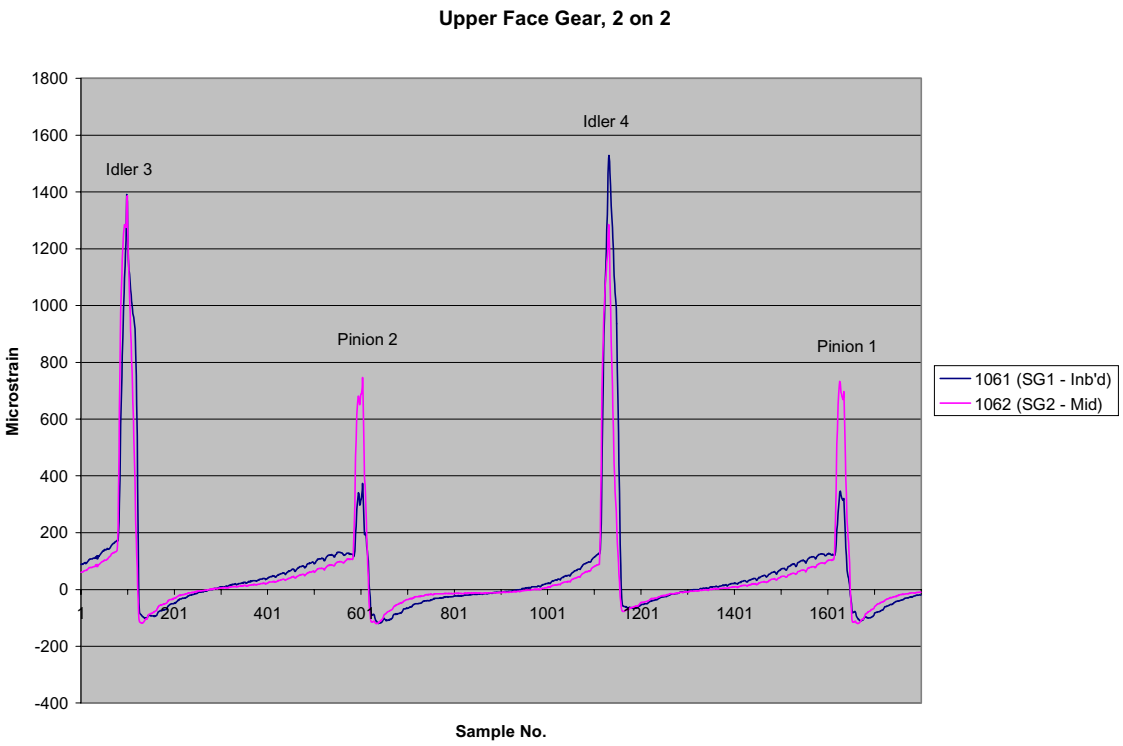

Figure 80. Strain output for UFG, 270 degree location, Run No. 141.

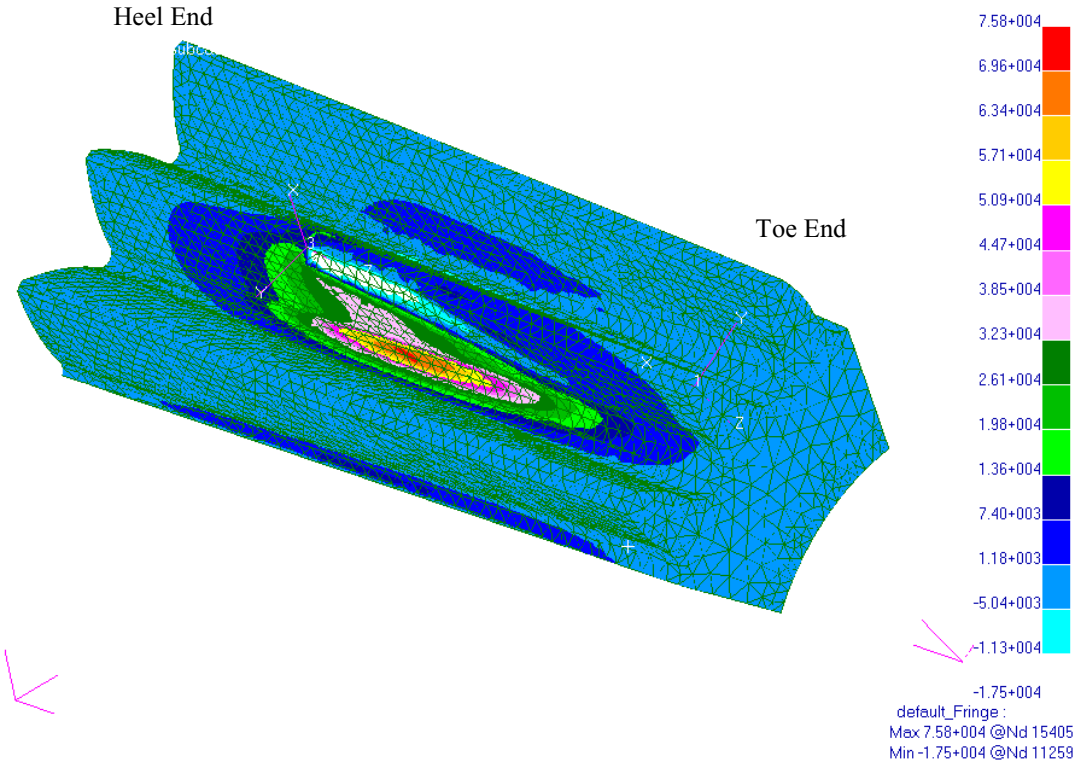

Figure 81. Finite element analysis showing pinion model with heel-biased LFG load.

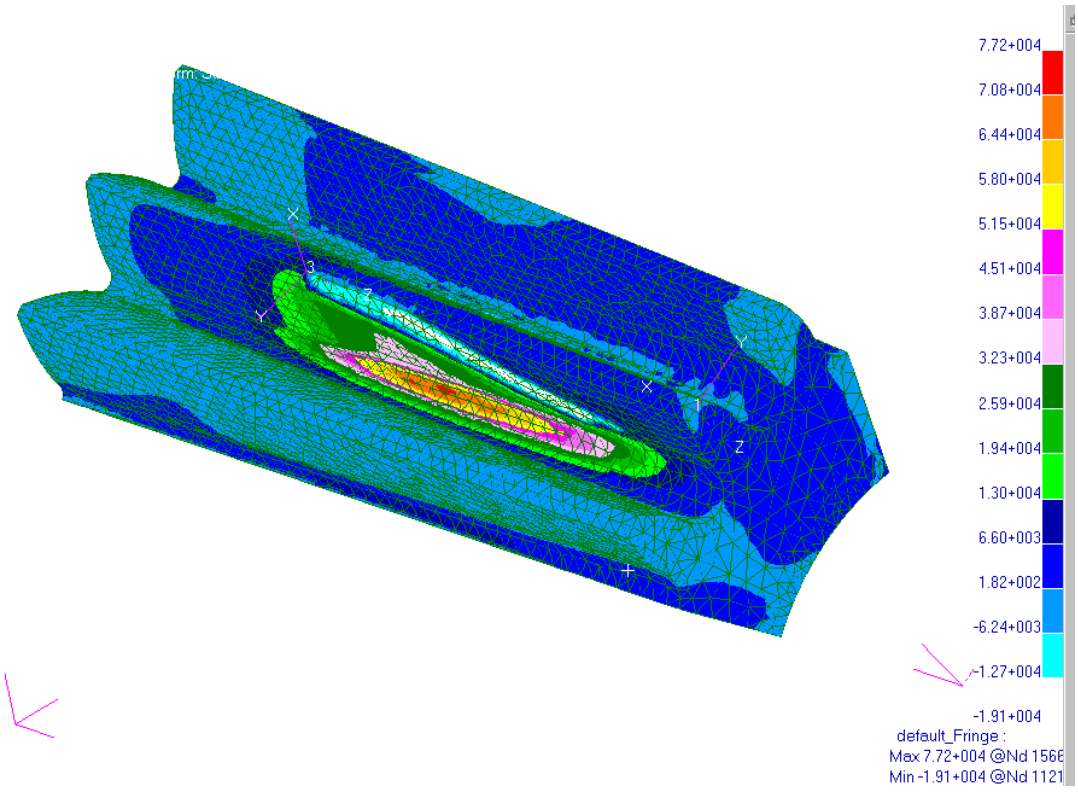

Figure 82. Finite element analysis showing pinion model with uniform LFG load.

X. CONCLUSIONS

The primary objective of this test program was to determine the torque split for a tapered, off-90-degree face gear transmission. All indications point to a nearly even torque split at the input pinions - 48% to the upper face gear mesh and 52% to the lower face gear mesh. The load sharing between idlers was not equal - 57% for Idler 3 and 43% for Idler 4 - but the testing demonstrated that the load sharing between idlers could be adjusted by changing relative amounts of backlash. It was only after all formal testing was completed that the torque calibration was conducted and pinion torque splits and idler load sharing could be determined. It is believed that the idler backlash could be adjusted to arrive at approximately equal load sharing.

Strain was not a reliable indicator of load transmitted at a given mesh as the distribution of tooth bending strain varied between similar components (pinions and idlers) and different meshes on the same component, i.e., the upper face gear. A torque calibration was performed in an effort to develop a relationship between load transmitted at a given mesh and measured strain. It was discovered that even these load/strain relationships changed depending on the assembly configuration and the magnitude of load. The torque calibration results were averaged over several strain gages to try and offset error, however, there may be some inaccuracy associated with these test results.

Maximum measured bending strain levels were higher than expected for all components. This was particularly true for the idlers. It is believed that some of the highest strains are contributed to by end loading which is apparent based on the tooth strain patterns. This type of loading was particularly evident at the toe end of the UFG in its mesh with Idler 4 and at the heel end of the LFG in its mesh with Idler 3. The situation of apparent end loading emphasizes the sensitivity of the face gear assembly to proper alignment. Initial testing indicated possible misalignment in the Idler 4 bore resulting in inspection and re-machining of both idler bores prior to conducting the formal test. The re-boring operation did affect the tooth strain distributions.

The effectiveness of the floating pinion was demonstrated in an indirect way. During the dual idler torque calibration, one idler was modified by the addition of a hub such that it could be used to apply torque. As such, the modified idler acted as a fixed pinion. The assembly was configured to use the modified idler along with the standard idler with both face gears. Nearly all load from the modified idler was transmitted to the upper face gear. It is believed that with a fixed pinion, the torque split is very sensitive to relative backlash values.

Significant effort was invested in trying to calibrate the pinion, idler and face gear strain gages. Due to friction in the calibration setup and dimpling of the tooth surface by the calibration ball, the gage calibrations were not repeatable and, therefore, not necessarily accurate. Although an improved calibration process was developed, due to the apparent accuracy of the installations, for future tests, such a calibration may not be warranted.

New methods have been developed for face gear grinding, grinding wheel dressing and coordinate measurement. Unique features of this DARPA-related work include the use of a simple geometric feature (a plane) as the basic member, the decomposition of the two-parameter dressing motion into simple linear motion with constant normal velocity plus stepped angular adjustment, the adaptation of the method of continuous generation by synchronous rotations in grinding and, above all, the true conjugate action between the pinion, the dressing tool, the grinding wheel and the face gear. A tooth undercutting problem that was encountered in the early stages of development has been successfully solved by a new dressing method. One-to-one correspondence between the dressing tool position and a point on the grinding wheel, the face gear and the pinion has been mathematically established. A result of this is that special tooth profile design modifications can be applied to the face gear through the use of CNC technology in the dressing process. Computer-aided tooth contact analysis is performed to predict the contact pattern and transmission errors. Pattern rolling on ground face gears with mating pinion confirms TCA results. A new in-line coordinate measurement method utilizing touch-trigger probes to inspect face gears right on the grinding machine shows promising results for a closed-loop system. Prototype developments have demonstrated the capabilities of finishing face gears to required case hardness, profile accuracy and surface finish for aerospace applications. A custom-built face gear grinding machine is under development at Derlan Aerospace Canada for production.

XI. RECOMMENDATIONS

As a result of the observations made during this POC test program, several recommendations can be made.

A reliable approach for the determination of torque and idler split for future face gear assembly testing must be defined for development purposes. A robust method is required that is independent of gear mounting locations. Ideally, this would be a fairly simple method that would yield rapid feedback in response to configuration changes.

If possible, gages should be added along the entire length of the instrumented gear teeth for the pinions, idlers and face gears. This will give a better picture of the strain distribution and is more likely to capture the maximum strain. High strains were measured during this test, and it is likely that the highest strains were not captured. Also, to aid in tooth contact ratio determination, one sector of four teeth in a row should be instrumented on each gear.

Additional finite element analysis (FEA) should be conducted to better understand tooth loading and stress distribution. Results of the POC test should be used to validate the FEA.

Means of eliminating the apparent end loading must be pursued. Changes in tooth geometry, particularly crowning/end relief, should be considered. Care should be given to the manufacture and inspection of the transmission housing to insure accurate bores. More uniform tooth load distribution will result in a lower maximum bending strains and surface contact stresses.

For future testing, calibrations of the tooth bending gages are not recommended. Eliminating this step will save considerable test time and associated cost.

The use of repeat runs can be minimized. Testing showed the strain results for a given configuration to be very repeatable.

Finally, it is recommended to perform subsystem component bending fatigue tests and 140% (of maximum continuous power) dynamic bending fatigue tests to complete primary evaluations of the split torque face gear configuration.

XII. REFERENCES

1. Heath, G.F., Gilbert, R.E., Tan, J., and Doubts, T.L., "Face Gear Split Torque Transmission Development," American Helicopter Society 55th Annual Forum, Montreal, Canada, May 1999.
2. Lewicki, D.G., Handschuh, R.F., Heath, G.F., and Sheth, V., "Evaluation of Carburized and Ground Face Gears," American Helicopter Society 55th Annual Forum, Montreal, Canada, May 1999.
3. Handschuh, R.F., Lewicki, D.G., Heath, G.F., and Bossler, R.B., "Experimental Evaluation of Face Gears for Aerospace Drive System Applications," 7th International Power Transmission and Gearing Conference, San Diego, CA, October 1996, pp. 581–588.
4. Handschuh, R.F., Lewicki, D.G., and Bossler, R., "Experimental Testing of Prototype Face Gears for Helicopter Transmissions," Journal of Aerospace Engineering, Proceedings of the Institute of Mechanical Engineers, Vol. 208, (G2), October 1994, pp. 129–135.
5. Heath, G.F., and Bossler, R.B., "Advanced Rotorcraft Transmission (ART) Program - Final Report," NASA CR–191057, Army Research Laboratory ARL–CR–14, January 1993.
6. Litvin, F.L., et al., "Application of Face-Gear Drives in Helicopter Transmissions," ASME Journal of Mechanical Design, Vol. 116, (3), September 1994, pp. 672–676.
7. Litvin, F.L., et al., "Design and Geometry of Face-Gear Drives," ASME Journal of Mechanical Design, Vol. 114, (4), December 1992, pp. 642–647.
8. Bloomfield, B., "Face Gear Design," Machine Design, Vol. 19, 1947, pp. 129–134.
9. Buckingham, E., "Analytical Mechanics of Gears," Dover Publications Inc., New York, NY, 1949.
10. Litvin, F.L., Chen, Y.D., Heath, G.F., Sheth, V., and Chen, N., "Apparatus for Precision Grinding Face Gears," U.S. Patent Number 6,146,253, November 2000.
11. Tan, J., "Apparatus and Method for Improved Precision Grinding of Face Gears," U.S. Patent No. 5,823,857, October 1998.
12. Engineering Test Request 97–53, Split Torque Proof of Concept Gearbox Tests, 26 October 2000.
13. ANSI/AGMA 2001–C95, Fundamental Rating Factors and Calculation Methods for Involute Spur and Helical Gear Teeth.
14. Chen, Y.D., and Bossler, R.B., "Design, Analysis, and Testing Methods for a Split-Torque Face-Gear Transmission," AIAA Technical Paper 95–3051, July 1995.
15. NASA Technical Paper 1458, Evaluation of High-Contact-Ratio Spur Gears With Profile Modification, 1979.

REPORT DOCUMENTATION PAGE

Form Approved
OMB No. 0704-0188

1. AGENCY USE ONLY (*Leave blank*)	2. REPORT DATE	3. REPORT TYPE AND DATES COVERED
	May 2002	Final Contractor Report

4. TITLE AND SUBTITLE

Development of Face Gear Technology for Industrial and Aerospace Power Transmission

5. FUNDING NUMBERS

WU–708–90–13–00
NCC3–356
1L162211A47A

6. AUTHOR(S)

Gregory F. Heath, Robert R. Filler, and Jie Tan

7. PERFORMING ORGANIZATION NAME(S) AND ADDRESS(ES)

The Boeing Company
5000 E. McDowell Road
Mesa, Arizona 85215–9797

8. PERFORMING ORGANIZATION REPORT NUMBER

E–13131

9. SPONSORING/MONITORING AGENCY NAME(S) AND ADDRESS(ES)

National Aeronautics and Space Administration
Washington, DC 20546–0001
and
U.S. Army Research Laboratory
Adelphi, Maryland 20783–1145

10. SPONSORING/MONITORING AGENCY REPORT NUMBER

NASA CR—2002-211320
ARL–CR–0485
1L18211–FR–01001

11. SUPPLEMENTARY NOTES

Project Manager, David G. Lewicki, Structures and Acoustics Division, NASA Glenn Research Center, organization code 5950, 216–433–3970.

12a. DISTRIBUTION/AVAILABILITY STATEMENT

Unclassified - Unlimited
Subject Category: 37 Distribution: Nonstandard

Available electronically at http://gltrs.grc.nasa.gov/GLTRS

This publication is available from the NASA Center for AeroSpace Information, 301–621–0390.

12b. DISTRIBUTION CODE

13. ABSTRACT ***(Maximum 200 words)***

Tests of a 250 horsepower proof-of-concept (POC) split torque face gear transmission were completed by The Boeing Company in Mesa, Arizona, while working under a Defense Advanced Research Projects Agency (DARPA) Technology Reinvestment Program (TRP). This report provides a summary of these cooperative tests, which were jointly funded by Boeing and DARPA. Design, manufacture and testing of the scaled-power TRP split torque gearbox followed preliminary evaluations of the concept performed early in the program. The testing demonstrated the theory of operation for the concentric, tapered face gear assembly. The results showed that the use of floating pinions in a concentric face gear arrangement produces a nearly even torque split. The POC split torque tests determined that, with some improvements, face gears can be applied effectively in a split torque configuration which yields significant weight, cost and reliability improvements over conventional designs.

14. SUBJECT TERMS	15. NUMBER OF PAGES
Gears; Transmission (machine elements); Load distribution; Grinding; Strain gages	96
	16. PRICE CODE

17. SECURITY CLASSIFICATION OF REPORT	18. SECURITY CLASSIFICATION OF THIS PAGE	19. SECURITY CLASSIFICATION OF ABSTRACT	20. LIMITATION OF ABSTRACT
Unclassified	Unclassified	Unclassified	